

Electromagnetic compatibility in high-voltage engineering

Citation for published version (APA):

Houten, van, M. A. (1990). *Electromagnetic compatibility in high-voltage engineering*. [Phd Thesis 1 (Research TU/e / Graduation TU/e), Electrical Engineering]. Technische Universiteit Eindhoven.
<https://doi.org/10.6100/IR336248>

DOI:

[10.6100/IR336248](https://doi.org/10.6100/IR336248)

Document status and date:

Published: 01/01/1990

Document Version:

Publisher's PDF, also known as Version of Record (includes final page, issue and volume numbers)

Please check the document version of this publication:

- A submitted manuscript is the version of the article upon submission and before peer-review. There can be important differences between the submitted version and the official published version of record. People interested in the research are advised to contact the author for the final version of the publication, or visit the DOI to the publisher's website.
- The final author version and the galley proof are versions of the publication after peer review.
- The final published version features the final layout of the paper including the volume, issue and page numbers.

[Link to publication](#)

General rights

Copyright and moral rights for the publications made accessible in the public portal are retained by the authors and/or other copyright owners and it is a condition of accessing publications that users recognise and abide by the legal requirements associated with these rights.

- Users may download and print one copy of any publication from the public portal for the purpose of private study or research.
- You may not further distribute the material or use it for any profit-making activity or commercial gain
- You may freely distribute the URL identifying the publication in the public portal.

If the publication is distributed under the terms of Article 25fa of the Dutch Copyright Act, indicated by the "Taverne" license above, please follow below link for the End User Agreement:

www.tue.nl/taverne

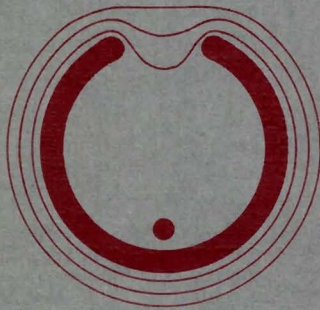
Take down policy

If you believe that this document breaches copyright please contact us at:

openaccess@tue.nl

providing details and we will investigate your claim.

ELECTROMAGNETIC COMPATIBILITY
in
HIGH-VOLTAGE ENGINEERING



M.A. VAN HOUTEN

ELECTROMAGNETIC COMPATIBILITY
in
HIGH-VOLTAGE ENGINEERING

PROEFSCHRIFT

ter verkrijging van de graad van doctor
aan de Technische Universiteit Eindhoven,
op gezag van de Rector Magnificus,
prof. ir. M. Tels, voor een commissie aan-
gewezen door het College van Dekanen
in het openbaar te verdedigen op
dinsdag 23 oktober 1990 om 14.00 uur

door

Marinus Albertus van Houten

geboren te Breda

**ELECTROMAGNETIC COMPATIBILITY
IN
HIGH-VOLTAGE ENGINEERING**

CIP-GEGEVENS KONINKLIJKE BIBLIOTHEEK, DEN HAAG

Houten, Marinus Albertus van

Electromagnetic compatibility in high-voltage engineering/

Marinus Albertus van Houten. -[S.l.:S.n.]- Fig., tab.

Proefschrift Eindhoven. Met lit. opg, reg.

ISBN 90-9002929-X

SISO 661.55 UDC 621.311.4.027.8.013.79.08(043.3)NUGI 832

**Trefw.: hoogspanningsinstallaties; elektromagnetische
interferentie.**

Dit proefschrift is goedgekeurd door de promotoren:

prof.dr.ir. P.C.T. van der Laan

en

prof.dr. M.P.H. Weenink

aan broer DIRK

CONTENTS

SUMMARY	6
INTRODUCTION	9
- High-Voltage Engineering and Electromagnetic Compatibility	
- A basic problem	
- Aim of the present work	
- Outline of the thesis	
ELECTROMAGNETIC COMPATIBILITY AND GROUNDING	13
2.1 Grounding	14
2.2 Criticism on standard definitions of "ground"	15
- Ground, a perfect sink or source ?	
- Ground, a point of equal potentials ?	
2.3 Misconceptions due to an incorrect philosophy	19
- Jumping potentials	
- Single point grounding	
- Multiple grounding systems	
- The so-called "clean earth"	
- Ground loops	
2.4 Distributed inductance and grounding	24
2.5 Design rules for grounding	27
2.6 Protected regions formed by grounding structures	31
2.6.1 Protected region for leads	33
2.6.2 Protected region for instruments	36
2.7 Applications	41
- Lightning protection system	
- Open substation	
THE TRANSFER IMPEDANCE OF GROUNDING STRUCTURES	44
3.1 The transfer impedance concept	44
3.2 The transfer impedance of GS's for leads	48
3.2.1 Ideal GS, a tube	48
3.2.2 Practical GS's, plates or conduits <i>(model, the shape factor, Z_{tr}-measurements, setup, experimental results and discussion)</i>	49
3.2.3 An almost ideal GS: covered conduits	59
3.3 The transfer impedance of grounding structures for the protection of instruments	65
- An ideal GS for an instrument	
- Real GS's for instruments	
- Transfer impedance measurements <i>(setup, experimental results and discussion)</i>	

ELECTROMAGNETIC COMPATIBILITY AND SIGNAL HANDLING ASPECTS OF A DIFFERENTIATING/INTEGRATING MEASURING SYSTEM	79
4.1 High-Voltage dividers	79
4.2 D/I-system for fast rising voltage transients	82
- Principle	
- High frequency problems	
- Input circuit	
- Sensor electrode	
- Coaxial cable	
- Fifty-ohm termination resistor	
- Fast passive integrator	
- Step response of the measuring system	
4.3 EMC-aspects of a D/I-measuring system	94
ELECTROMAGNETIC COMPATIBILITY IN GIS-SUBSTATIONS	97
5.0 INTRODUCTION	97
5.1 GIS-INSTALLATION AS A HF-INTERFERENCE SOURCE	99
5.1.1 Unnecessary interruptions in a GIS-enclosure	100
- Insulated enclosures	
- Continuous enclosures	
- Comparison of dissipation in enclosures	
<i>GIS-enclosures</i>	
<i>HV-cables with a lead sheath</i>	
<i>Insulated-phase bussystems</i>	
5.1.2 Necessary interruptions in a GIS-enclosure	108
- GIS/HV-line transition	
- GIS/HV-cable transition; cathodic protection	
- GIS/HV-cable transition; current-transformer arrangement (<i>setup, experimental results and discussion</i>)	
CONCLUSIONS	126
REFERENCES	128
SAMENVATTING	133
DANKWOORD	135
CURRICULUM VITAE	136

SUMMARY

Electromagnetic Compatibility, within the field of Electrical Engineering, is the ability of electronic and electrical apparatus to function correctly in each others vicinity. This thesis describes new EMC-concepts for an efficient and consistent approach to practical interference problems. Analysis should lead to methods to eliminate and preferably prevent interference early in the design phase. In this thesis the concepts developed are mainly used in high-voltage installations. The integration of modern electronics within this type of installations poses high EMC-demands. Electromagnetic Compatibility is obtained here by the use of correct layout, and by the installation of leads and additional metal at strategic places. The concepts developed can however be used -in appropriate form- within the whole field of Electrical Engineering.

The thesis starts with a critical analysis of "Grounding", a subject of fundamental importance within EMC. Due to an incorrect understanding about what a grounding system is supposed to do, the noun "ground" causes much confusion in practice. This incorrect understanding is related to two basic elements of the generally accepted definition of "ground":

- a ground can absorb or supply current without any change in voltage;
- a ground is an equipotential point or plane which serves as a reference for the circuit considered.

By ignoring the concept of potential and by concentrating ourselves on the physically meaningful currents, on the circuits which carry these currents, and on the magnetic fluxes, we developed a general protection philosophy. The central concept within this philosophy is the "transfer impedance" of "Grounding Structures (GS's)". By using GS's we create protected regions in which the sensitive electronic equipment can operate without any problems. We distinguish between GS's for leads and GS's for apparatus.

In this sense, the outer conductor of a coaxial cable is already a simple GS, which creates a protected region. An "EMC-cabinet" is an essential part of the GS for the protection of sensitive equipment.

The significance of the transfer impedance concept is that it gives a meaningful criterion for the quality of GS's (including the "layout" of the complete "network"). The transfer impedance of complex GS's, which can generally not be calculated, can always be measured with so called "current injection test methods". Models as well as measurements of the transfer impedance of GS's for leads as well as GS's for equipment are discussed.

An EMC attractive solution for signal transport in high-voltage measuring techniques is the use of differentiated signals. The differentiated signal should be integrated again at the input of the electronic equipment. The components of the first part of the integrator can be of normal size as used in electronics and passive. With a correct design of the integrator, interference is suppressed before it reaches the vulnerable active electronics. The EMC-cabinet plays an important role here. It has to protect the measuring equipment as well as the integrated signal. The design of a "Differentiated/Integrated (D/I)"-system to measure fast voltage transients is described. The D/I-system has among others been used for transient voltage measurements in the 150/10 kV "Gas Insulated Switchgear (GIS)"-substation Eindhoven-West.

A GIS-installation is an intense source of high-frequency interference. Measurements of steep transient voltages across interruptions in a GIS-installation, due to switching actions, are presented. Means to reduce the influence of this interference source on the measuring equipment are available, and are discussed.

CHAPTER 1

INTRODUCTION

High-voltage engineering and EMC

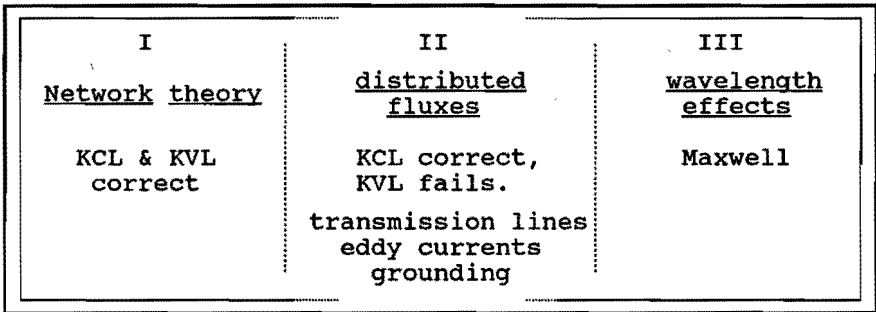
In high-voltage installations of electrical utilities, or in HV-experiments or in testing, much capacitive energy is present. During switching actions in HV-substations, or during experiments, with intentional or inadvertent breakdowns, this energy is partially converted into high power electromagnetic waves. Due to the resulting intense EM-interference, modern electronics -increasingly used for measurement and control- may not function properly in HV-installations, or may even be destroyed. Therefore "Electromagnetic Compatibility (EMC)", the ability of electronics or electrical apparatus to function correctly in each others vicinity, is of crucial importance to high-voltage engineering. We on purpose give a definition different from the IEC definition: "The ability of a device, equipment or system to function satisfactorily in its electromagnetic environment without introducing intolerable electromagnetic disturbances to anything in that environment". It will become clear later that the term EM-environment, although fashionable, can better be avoided.

A basic problem

Electromagnetic compatibility between highly sensitive electronic systems and HV-installations is in addition endangered by the large geometric dimensions of the HV-installation. A basic EMC-problem is then that the complex three-dimensional circuitry cannot be correctly represented by the familiar network theory models (see Sec.2.4). The discrepancy between network model and reality shows up first of all, at fairly low frequencies already, when significant time-varying magnetic fluxes are distributed in space. Kirchhoff's voltage law (KVL) is then not obeyed, which causes a considerable amount of confusion.

If electrical engineering is schematically represented by

the large rectangle in Fig.1 we may distinguish three regions, from left to right, that is with increasing frequency. At low frequency, in region I, network theory can be used, whereas at high frequency where wave length effects are important, the full Maxwell description is required, to describe for instance antennas and wave guides region III). Distributed fluxes are often already



$\omega \rightarrow$

Fig. 1: Regions within electrical engineering where different descriptions are required; network theory at the left, the full Maxwell equations at the right. Grounding often falls in the difficult middle region. KVL and KCL stands for Kirchhoff's voltage law and Kirchhoff's current law, respectively.

important at intermediate frequencies (region II), for instance in transmission lines, in eddy currents and grounding. In transmission lines the problem is usually avoided by the introduction of an equivalent network in which only the voltage in the perpendicular cross-section is considered, after which a "lumping" of the the inductance is permissible. Eddy currents are clearly the result of non-conservative E-fields, and are important enough to make thin laminations necessary in 50-Hz transformers. In the equivalent circuit of the transformer the resulting losses are simulated by a resistor. In grounding, a central problem for EMC, the leads are often long and have an irregular structure. Since also large currents may flow we have to deal with appreciable distributed fluxes. Evidently we are then not any more in region I and cannot use the standard network theory. As a

consequence of the failure of the KVL extended leads no longer "transport" potentials as they do in network diagrams. The description should then concentrate on the flow of currents and on the fluxes associated with the currents for a given layout.

Aim of the present work

The purpose of the present work is to develop concepts for the protection of electronics or electrical apparatus which have to function correctly in each others vicinity. To achieve correct operation of the equipment, it is necessary both to understand and to resolve practical electromagnetic interference problems. A good understanding hopefully leads to modifications early in the design phase of a setup, an apparatus or a large installation. This is cheaper and more efficient than modifications introduced in a later stage. The concepts described here are mainly applied to sensitive digital registration equipment which is used in high-voltage research. Because of the severe interference -often coinciding with the fast phenomena that are to be observed- we have used much metal to obtain an adequate EMC-protection. The concepts developed are however basic and general; they can be easily adapted to other fields of electrical engineering.

Outline of the thesis

The present work discusses first of all EMC-problems and concepts in general and then describes practical EMC-problems in HV-engineering in particular.

Chapter 2 gives an EMC-analysis for high-frequency grounding, such as required for the protection of electronic systems and large scale electrical installations. It starts with a critical analysis of "grounding", and discusses misconceptions around the noun "ground" and related to that the validity of Kirchhoff's laws. Design rules for the activity "grounding" are given and explained. Grounding Structures (GS's) for the protection of leads and instruments are introduced. Special attention is given to conduits made out of iron and to

"EMC-cabinets" for instruments.

In Chapter 3 the transfer impedance concept for GS's is introduced. This concept is used for a quantitative comparison of GS's, both by calculations as well as by measurements. By means of current injection tests we have measured the transfer impedance of GS's for leads as well as the transfer impedance of simple GS's for instruments.

Chapter 4 deals with a D/I measuring system for very fast high-voltage transients. Due attention is paid to the design of this measuring system and to its EMC-aspects.

Chapter 5 -EMC in a GIS substation- considers a Gas Insulated Switchgear (GIS) installation as an intense and concentrated source of HF-interference. Proposals to improve the EMC behavior of the GIS-installation, which still satisfy the other design criteria, are discussed. Measurements on very fast high-voltage pulses are presented.

Chapter 6 gives the main conclusions.

CHAPTER 2

ELECTROMAGNETIC COMPATIBILITY AND GROUNDING

For the design and production of electrical equipment much fundamental and technical expertise exists within the various fields of electrical engineering. To ensure correct operation of pieces of equipment originating from these various fields when they are combined, requires serious ElectroMagnetic Compatibility design (EMC-design) efforts. If no systematic EMC-approach is available -preferably to be used already in the design phase- we may expect EMC-problems to become more and more serious with the growing use of complex electronic systems and the corresponding increase of different power levels. Unfortunately no clear theory for these situations seems to exist and EMC-problems have in fact been solved by experiments or sometimes simply by trial and error. The search for a clear theory which can provide practical guide lines for EMC-correct design remains therefore very important.

Of all the resulting EMC-problems it is recognized [Mer 76] that the design of "correct grounding" is one of the most important aspects of EMC-design of electrical systems. Therefore we start in this thesis with an analysis of "Grounding".

Positive results of this critical analysis will turn out to be:

- We can specify more clearly what a grounding system is supposed to do. The question whether ground wires faithfully transport zero "potentials" becomes meaningless.
- The activity "grounding" is seen as the design and construction of the low voltage sides of all current loops.
- Very often we have to deal with complicated existing electrical systems. In these cases it is difficult or

impossible to control the entire grounding system. However, by using metal "Grounding Structures" (GS), suitably sized for "our" special purposes, we can locally solve all our grounding problems.

-This analysis leads to the development of general, linear and basic methods for protection of electronics and to a design of grounding systems which protect (large) interconnected electrical systems against interference: the main aim of EMC-design.

Note that this approach does not rely on the improvement of the overall "EM-environment" but instead, provides an excellent local "climate", where it is needed.

Elements of this grounding analysis have appeared in earlier publications [Laa 78], [Ott 79], [Jon 83], [Laa 86] [Laa 87] and [Hou 89].

2.1 GROUNDING

Grounding is interpreted in this chapter as all design and actual construction work on the low voltage side of electrical circuits. This makes grounding a very broad subject essential for widely different fields such as lightning protection, power engineering and micro-electronics. We may nevertheless formulate a simple and general objective of grounding: "Grounding should reduce dangerous voltage differences between critical points to safe values".

By grounding correctly we want to achieve the following:

- a) Interference voltage differences across sensitive inputs or across other critical terminals of our circuits should remain low, so that correct operation of the circuit is not affected.
- b) The safety of people must be guaranteed.
- c) In the case of high currents (e.g. lightning) we avoid dissipation in a "poor conductor" by installing a metal grounding conductor parallel to it.

The voltage differences which play a role in a) and b) are equal to $\int_1^2 E \cdot dl$, usually taken along the shortest

connection line. Note that it is this voltage difference that is responsible for the risk to electronics, to people or for breakdown.

Historically the objectives b) and c) were recognized first in grounding practice. As systems became bigger and more complex and with the growing use of electronics the typical EMC objective a) received more and more attention [Pea 62], [Den 73]. Since often only very low interference voltages can be tolerated in micro-electronics a) poses difficult engineering challenges.

The available technical expertise on grounding inside an apparatus (the internal grounding) may seem impressive, but is more a product of art than of science, whereas the expertise on grounding seldom includes the protection against external interference, the EMC grounding. To develop a more scientific description of grounding we have to point out that the generally accepted definition of "ground" is incorrect.

2.2 CRITICISM ON STANDARD DEFINITIONS OF "GROUND".

Most standard definitions of "ground" contain two elements:

1. A ground can absorb or supply current without any change in voltage ; in other words the ground should be a perfect sink or source for currents.
2. A ground is an equipotential point or plane which serves as a reference for the circuit considered.

GROUND, A PERFECT SINK OR SOURCE ?

A ground can only act as a sink or source for current when charges can accumulate, in other words when a capacitor with sufficient capacity is present. This also follows from the continuity equation for charges

$$\operatorname{div} j + \partial \rho / \partial t = 0 \quad (2.1)$$

When the current density j is absorbed or supplied $\operatorname{div} j$ differs from zero and consequently the charge density, ρ , must change.

In the search for the capacitor which collects this charge we have two candidates (See Fig.2.1):

1. The Earth, considered as an isolated sphere with an average radius of 6367 km, has a capacitance of 708 μF (Fig.2.1a).
2. The capacitance between the Earth and the lower layers of the ionosphere at for instance 50 km height, turns out to be 91 mF (Fig.2.1b). This large capacitor is present, and on a world wide scale the thunderstorms charge this capacitor [Vol 82] to several hundreds of kiloVolts. This charge causes the so-called fair-weather-field.

Both capacitors cannot play a role in our grounding because our local engineering activities do not influence the total E-field around our Earth. Between our charged objects and the Earth only a small capacitor is present (Fig.2.1c).

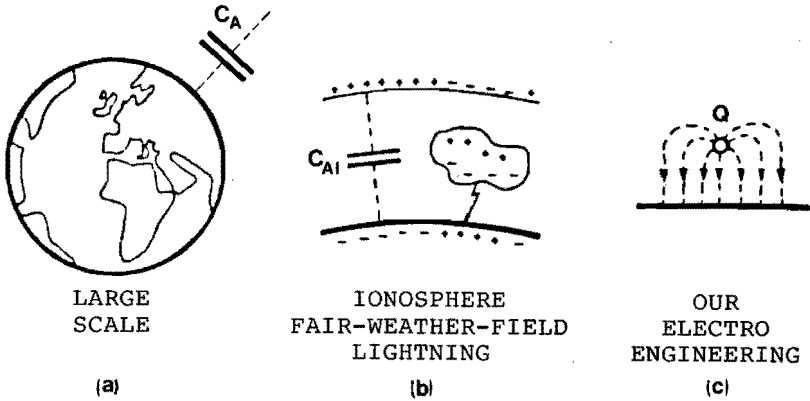


Fig.2.1: Electric fields on different scales. For our electrical engineering we use only a minute part of the Earth.

To arrive at a correct picture we rewrite Eq.2.1 with Gauss' law

$$\text{div} (\mathbf{j} + \partial\mathbf{D}/\partial t) = 0 \quad (2.2)$$

The combined quantity, $\mathbf{j} + \partial\mathbf{D}/\partial t$ is divergence free and has therefore no sink or source. This leads to the correct statement that any current -where we have to include the capacitive current- must flow in a closed loop.

As a consequence of this statement we can specify more clearly what a grounding system is supposed to do.

A grounding system never resembles a sewer system where more and more sewage pipes converge into one main pipe with "unknown" destination (Fig. 2.2a). Instead a grounding system is a group of interlinked current loops (Fig. 2.2b).

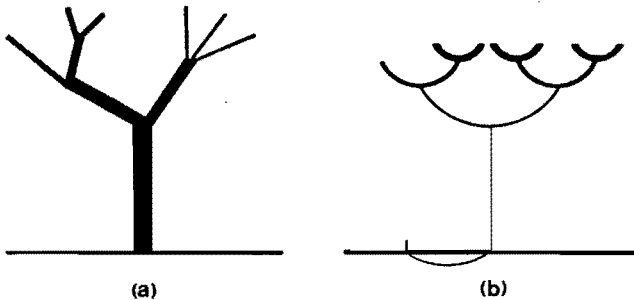


Fig.2.2: Incorrect (a) and correct (b) picture of what a grounding system is supposed to do. The thickness of the lines corresponds to the magnitude of the current.

We make three observations. First of all, Fig. 2.2b shows only the low-voltage part of all the circuits and is in that sense incomplete. Secondly the connection to the Earth in Fig. 2.2b is not unique anymore, but is only another part of a current loop. If a current flows into the Earth, this current must leave the Earth somewhere else. Therefore the connection to Earth is not essential as is demonstrated by digital watches, portable radios, airplanes and satellites.

GROUND, A POINT OF EQUAL POTENTIAL ?

This second element of standard definitions of ground implies that a connection to ground fixes the potential of the connected point of the circuit, where the potential of the ground is often taken to be zero. A first, relatively simple complication is caused by the resistivity of the conductors, in particular of the soil; we may correct for that by calculating the correct grounding resistance, which depends on shape and size of the buried grounding rod.

A more basic question is whether a highly conducting, say a metal "Earth" would form an equipotential surface. Since the size of the sphere is not important (see Section 2.2.1) we may consider any metal object, such as a ship, a screen room or an airplane (Fig. 2.3). In electrostatics such an object forms an equipotential surface. This seems also to be true according to network theory, where wires are assumed to "transport" potentials.

However, when in an airplane, struck by lightning (Fig. 2.3), we connect three voltmeters between the points A and B, we obtain different readings as a result of the distributed time-varying magnetic flux.

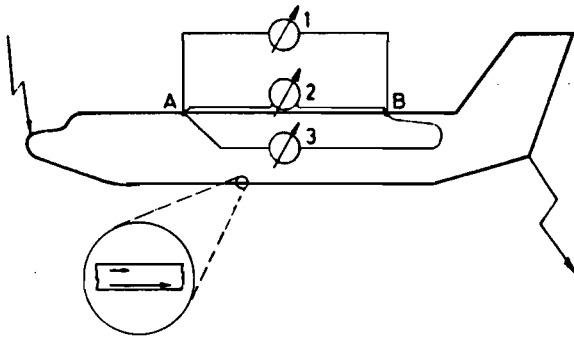


Fig.2.3: The voltage between the points A and B of an air-plane, caused by lightning current, cannot be described by a potential difference; each of the three voltmeters gives a different reading, depending on the loop enclosed by the leads.

Voltmeter 2, close to the outer surface reads $\rho l j(r_2)$, where ρ is the specific resistivity, l the length between the contacts and $j(r_2)$ the current density at the outer surface where r_2 is the outer radius of the airplane. Voltmeter 1 sees in addition to that, the voltage induced in the outside loop. When the lightning currents are evenly distributed around the tubular body the magnetic field inside the airplane is zero. Voltmeter 3 then reads only $\rho l j(r_1)$, where r_1 is the inner radius. In Fig. 2.4 the general behavior of these three voltmeter readings is shown. This picture shows first of all the strong relation

with the transfer impedance of coaxial structures and is secondly reassuring for airplane electronics since the V_3 reading drops quickly to zero at higher frequencies.

For our argument here, it is important to realize that in the loops formed by the voltmeter leads, Kirchhoff's voltage law (KVL) is not obeyed. This is also not true for the small loops in the skin (shown enlarged in Fig. 2.3) where j and E vary with depth. In these examples the simple "zero-dimensional" network theory cannot adequately describe the three-dimensional reality.

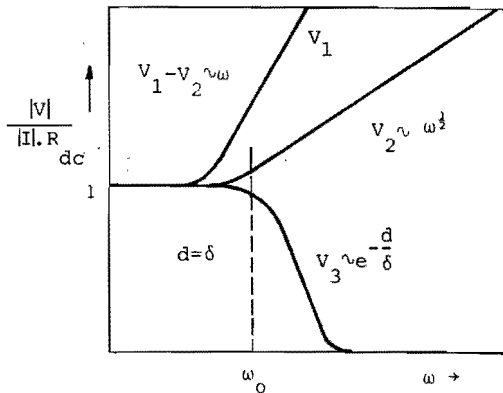


Fig. 2.4: Voltmeter readings as in Fig. 2.3 as a function of frequency. At low frequencies the dc-resistance determines the voltage; at frequencies where the skinddepth is smaller than the wall thickness d the readings V_2 and V_3 are different. For a steel hull this takes place at quite low frequencies because of the smaller skinddepth.

2.3 MISCONCEPTIONS DUE TO AN INCORRECT PHILOSOPHY

Since the analysis of grounding is commonly based on network theory and on potentials such as used in the Kirchhoff Voltage Law (KVL), many misconceptions arise, of which we mention a few.

JUMPING POTENTIALS

A lightning discharge as in Fig. 2.5a, injects a grounding current. The current flows to the Earth and returns to the cloud as a displacement current. Of this "complete current loop" we only control a small part; by a choice of diameter

and geometry and the number of lightning rods we minimize detrimental effects. This lightning current flowing through a lightning rod does not cause an unambiguous potential difference across a given length of the rod. The two voltmeters shown in Fig.2.5a illustrate that a potential in Kirchhoff sense does not exist; they enclose with their

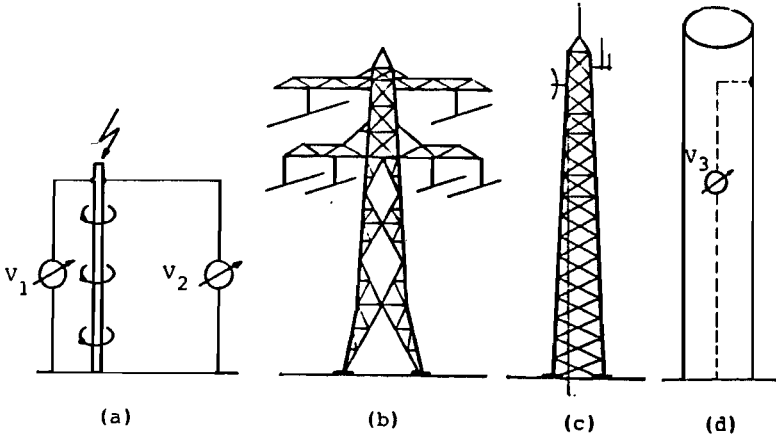


Fig. 2.5: The two voltmeters 1 and 2 (a) connected to the same points on the lightning rod show different readings. Therefore it is not correct to represent a voltage tower (b) or a communication tower (c) by a lumped network element. In the case of an metal column tower (d) voltmeter 3 shows almost zero.

leads different magnetic fluxes and show therefore different voltages. Nevertheless a high-voltage tower or a communication tower (Fig.2.5b,c) is often represented by a lumped network element, through which the lightning current flows [Van 80]. This is incorrect, because the voltage over these towers is not uniquely defined. In case the rod is a tube a voltmeter with its leads inside the tube should not show much interference voltage because no magnetic field is present in the tube (Fig.2.5d), just as voltmeter 3 in Fig.2.3.

Similarly, the diverging lightning current in the soil does not produce "step potentials", only related to the soil resistance. The "step voltage" depends also on the flux enclosed by the leads.

The same mistake is made in the modeling of lands on printed circuit boards for the purpose of predicting "ground shifts" between two points on a ground land [Pau 86]. Again this is fundamentally wrong because one cannot unambiguously localize the "lumped" inductance, or the voltage source which represents the induced loop voltage (See Sec 2.4., Eq.2.3 and remark d).

SINGLE POINT GROUNDING

In the frequently recommended single point grounding one attempts to minimize the coupling between circuits by avoiding groundloops and by having separate returns for the ground currents, at least up to the "single point" (Fig. 2.6). If all currents did flow in one direction, as in a sewer (Fig. 2.6a) this would indeed reduce coupling, although a possible large common part of the circuit beyond the single point is not considered. If the currents flow in opposite directions, as they may do when connecting leads are present (Fig. 2.6b), large loops are formed unnecessarily. Actually the defendants of single point grounding in their search for the magic zero potential, forget that current always flows in closed loops (see Sec.2.2.1).

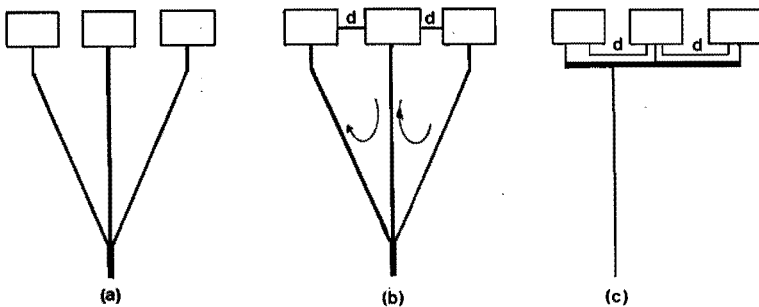


Fig. 2.6: Single-point grounding is based on the sewer idea; all currents flow to the sewer (a). In fact currents can flow in opposite directions for instance as a result of induction, when connecting cables are present (b). A more compact grounding is much better; the lower horizontal line can be a conduit (c).

A much better solution is to design these loops in a compact way (Fig. 2.6c). When the ground connection is a conduit or tube, large grounding currents can flow without coupling in voltage over critical inputs. In such case the connection to Mother Earth is only necessary as a safety ground; a long thin wire is then acceptable.

MULTIPLE GROUNDING SYSTEMS

Followers of the single point grounding concept may be concerned about the amplitude of current their grounding system can carry, and about the resulting "potential difference" over the grounding wire. This thought can lead to the installation of a number of grounding systems (Fig.2.7). Often these systems have a long connection to Mother Earth, to "transport" the desired potential zero. Unfortunately, due to the large loops formed, already a weak external magnetic field induces considerable voltages between nearby branches of two trees. In such a case,

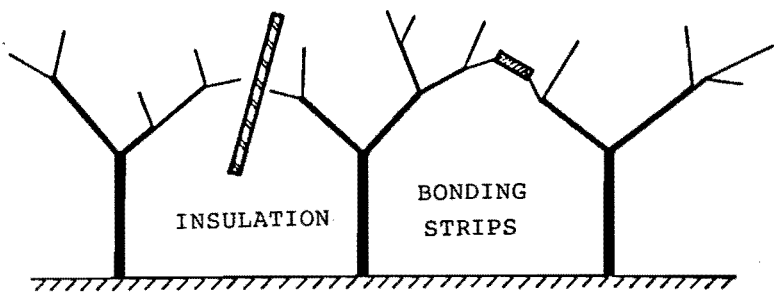


Fig. 2.7: Multiple grounding systems based on single point grounding concept.

insulation is used or surge arresters or bonding strips. Interesting is that bonding strips are supposed to "equalize ill-behaved ground potentials". In fact these bonding strips are shorting out induction voltages and provide a local closing of grounding circuits. A breakdown of insulation or a flashover in a surge arrester introduce locally new high frequency interference voltages.

THE SO CALLED CLEAN EARTH

As a special case of multiple grounding systems we mention a "clean earth" grounding system, sometimes requested for expensive equipment.

In this concept the already available ground systems in existing electrical installations are suspected. Therefore a "special" ground electrode is installed to preserve a "clean zero potential" which is kept far away from the "dirty grounds". The long separate new connection to this electrode, which is supposed to transport this "zero potential" faithfully, introduces a big loop and consequently interference voltages with respect to both the existing "dirty" Earth and metal in the building. To control these interference voltages one employs extra insulation, or (rather inconsistently) surge arresters and potential equalization strips. Clearly again nearby conducting material as in Fig.2.6c would provide a much better controlled path for the currents, and would give lower interference voltages at a lower cost.

GROUND LOOPS

Ground loops have a bad reputation because:

- They often show up in unexpected places
- They are often large in size so that the current in the loop can produce undesirable coupling effects over large distances
- A part of the ground loop is often close to a signal lead which of course causes interference.

However a current circulating in a ground loop can be less troublesome than a voltage of unknown value across an interruption introduced to break a ground loop. Capacitive currents across the interruption can give some coupling, but much worse is a breakdown at high interference voltages. The local breakdown generates steep transients which may generate serious extra interference.

Ground loops are in fact rather common. Large scale

conductors (eg. a ground plane or a screen room) could be considered as a collection of ground loops, which at high frequency lead to a different internal current distribution than at low frequency (see Fig.2.8). This redistribution can be quite useful for EMC-purposes, since it provides a lower inductance, a more localized flow of current, or a lower transfer impedance of grounding structures (see Sec.2.6).

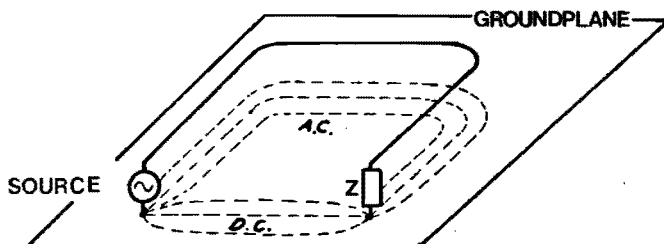


Fig. 2.8: A circuit above a plane, with two connections to the groundplane. For dc and hf the current patterns in the groundplane are different.

2.4 DISTRIBUTED INDUCTANCE AND GROUNDING

Both in electrostatics and in the network theory grounding is simple: the potential of Mother Earth is zero and a connection with the Earth fixes the potentials everywhere in our circuit. Because the network theory, with its simple Kirchhoff's laws is being used successfully everywhere in electrical engineering, we are very much accustomed to this model. In network theory all problems with E- and H-fields are hidden in the symbols for the impedances whereas around the terminals and near the connecting wires no fields are anymore present. These connecting wires shown in the diagrams are therefore zero-dimensional abstractions of the real wires in the circuit. In the diagram each wire is everywhere at the same potential and all induction effects and transit times and radiation are being neglected. Within network theory current and voltage play a dual role; we may work with either one of the two.

The simple description of grounding given by the network theory is certainly valid for electrostatics and other dc-current circuits. For the mains frequency (50 or 60 Hz) the network theory is in general correct; however, in the case of long lines, large currents and grounding, distributed fluxes cause problems. At high frequencies this is even more the case and the simple network model fails completely.

Although these problems arise because network theory is no longer adequate, we hesitate to return to the full Maxwell laws and to the resulting complicated boundary value problems. Fortunately this is seldom necessary, we already gain much insight by a study of the parasitic impedances of the relatively long ground, supply and signal wires. The parasitic resistances and capacitances can, if necessary, be represented by network elements which can be added to our circuit, without essential problems. As will be explained and was already illustrated in the previous sections, the parasitic inductance is basically much more complicated, because its effect cannot always be represented by a lumped circuit element.

Whereas in network theory the magnetic flux of an inductance is always supposed to be confined within the impedance symbol, the fluxes associated with the ground leads, the supply leads or the signal leads are essentially distributed in space. We then have to think in terms of current loops and we apply Maxwell's laws for instance to those closed contours. The induction law in its integral form is useful; we employ the customary notation.

$$\oint_C \mathbf{E} \cdot d\mathbf{l} = - \iint_S \frac{\partial \mathbf{B}}{\partial t} \cdot d\mathbf{S} = - \frac{d\phi}{dt} \quad (2.3)$$

Consequences of this equation are:

- a. Kirchhoff's voltage law (KVL) is based on this equation without enclosed flux. With enclosed time dependent flux the contour integral of \mathbf{E} is no longer zero and the KVL fails: the sum of the voltages across circuit elements in a circuit mesh is not zero.

- b. Potentials as used in the KVL, do not exist when changing magnetic fluxes are present (see also [Laa 78]).
- c. In an actual circuit there are still voltage differences, which may lead to breakdown, or to interference, or to a voltmeter reading. The voltage between points 2 and 1

$$V_{21} = -\int_1^2 \mathbf{E} \cdot d\mathbf{l} \quad (2.4)$$

depends on the actual integration path (compare Eq.2.3). The lay-out of the wiring and the lay-out of the voltmeter leads are now important; remember that this is not the case in network theory.

- d. Equation 2.3 also shows that an inductance can only be defined for an (almost) closed current loop. Since this inductance is a property of the loop as a whole, one cannot unambiguously localize the "lumped" impedance, or the voltage source which represents the induced loop voltage. A lot of confusion is caused by authors who (incorrectly) define inductances of single straight wires [Van 80, Pau 87, Ott 88]
- e. The duality of current and voltage is lost, because a potential cannot be defined (b) and voltages depend on the integration path (c). The current remains a much clearer physical quantity; its value is found from

$$\int_S (\mathbf{j} + \frac{\partial \mathbf{D}}{\partial t}) \cdot d\mathbf{S} \quad (2.5)$$

where we have to integrate over the cross section of the wire or in case $\partial \mathbf{D} / \partial t$ is important also over the area where the displacement current flows. We may describe this by saying that Kirchhoff's current law (KCL) remains valid.

- f. As a result of e) and in agreement with Ott's statement (Ott 79) we should concentrate on the currents in our analysis of grounding problems. The grounding currents circulate in a loop. Our task is to design, or to identify and if necessary modify these loops in such a way that interfering voltage differences, calculated with Eq.2.4 remain low enough at critical terminals.

2.5 DESIGN RULES FOR GROUNDING

The wish to keep interfering voltage differences across sensitive inputs or across other critical terminals low is best served when we (re)arrange the current loops and close them as compactly and locally as the circumstances allow.

To design a grounding system according to the correct picture of what a grounding system is supposed to do (see Fig.2.2b), we follow a number of steps.

- We must ignore potentials, particularly when they seem to behave wildly, according to the naive picture of network theory.
- We concentrate on the currents in our various circuits.
- We design new, or modify existing current loops such that impedances and coupling to neighboring circuits are minimized. We do this by closing the circuits as compactly and locally as the circumstances allow; this also results in a clearer design.
- We start closing the circuits for the grounding currents in the smallest subsystem. Only after we have solved the local grounding problems we move outward to the next larger system.
- The largest and final ground system (see Fig. 2.2b) is often partly formed by Mother Earth. We limit the currents to and from Mother Earth as much as possible and let her only play a role when it is absolutely necessary. In fact the connection with Mother Earth only carries current in case of lightning or -depending on the regulations- for safety grounding.
- Finally we check by means of Eq.2.4 and Eq.2.3 whether the voltages at critical inputs are indeed low enough.

This design method keeps magnetic fluxes (self and mutual) small so that we will have fewer deviations from the KVL, than a less compact design would give. Moreover the compact and local approach reduces capacitive and resistive coupling. Generally speaking we may expect the interfering voltages to be small; if not we retrace the steps outlined above.

Making grounding circuits "as compact as possible" is rather straightforward in an Integrated Circuit (IC), on a Printed Circuit Board (PCB), or inside an apparatus [Laa 86].

Good grounding connections are formed by copper ground planes, or "gridded grounds" as being used on PCB's [Ott 81, Ger 85], to offer ground currents a path with a low impedance [Ott 79]. This is especially important at the high frequencies occurring in digital circuits. Also decoupling capacitors, e.g. for digital circuits, must be mounted in close proximity to the IC in order to provide a compact path for switching currents [Dan 87]. Inside an apparatus, wherever possible, we close the current loops already within the apparatus itself, but where this is not possible (as for input, output or supply lines) short grounding connections formed by a wide metal strip (chassis or a front panel) are often excellent. Such a metal strip introduces very little extra resistance or extra flux in the current loop.

In these cases the completion of the low voltage sides can be solved locally. This is one of the reasons that so many correctly operating apparatus have been built.

More grounding problems show up in the following cases;

- large distances in a network between sub-systems,
- when a new installation, e.g. a computer network, has to be installed in an existing building with an older electrical installation,
- electrical installations, with sensitive electronics for measurements or control, which have to operate properly in the presence of intense interference, e.g. lightning events or interference due to switching events in HV-installations.

These serious problems can be solved by creating "protected regions" formed by "grounding structures" with a low "transfer impedance". The protection philosophy behind this statement, - still based on one point of view; the control of current flow to avoid interference voltages

across critical terminals-, is discussed in the next sections.

Before we start with this discussion we analyze first the problem of large distances in a network between subsystems. In this analysis we introduce at the same time terms which will be important in our protection philosophy, namely "Differential-Mode (DM)" circuit, internal and external "Common-Mode (CM)" circuit, protected region, grounding structure, and the transfer impedance.

For simplicity we consider two subsystems which have metal housings and which are connected to each other by only one cable (See Fig.2.9a).

The differential-mode circuits for DM-signal transport are usually coaxial cables or several wires in a common braid. These cables provide a correct DM-signal transport over a wide frequency band. The regular geometry and the compactness of such DM-circuits reduce not only the

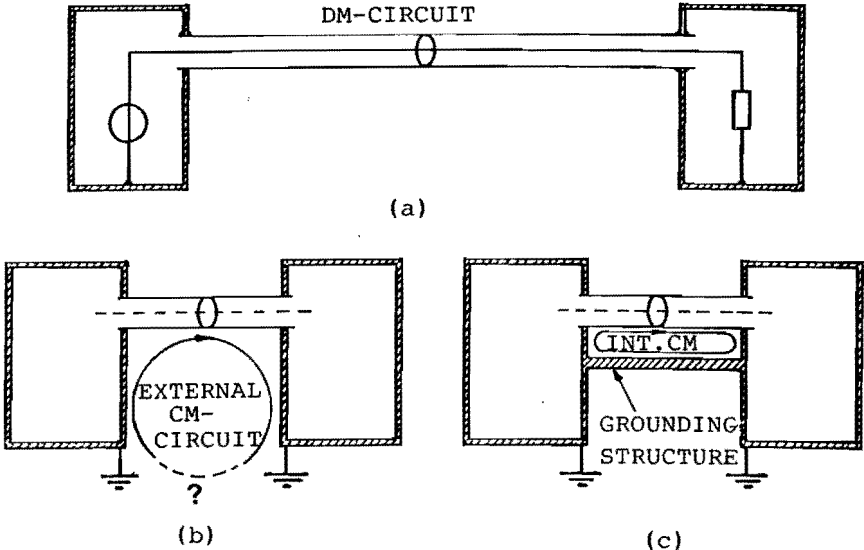


Fig. 2.9: a) A network consisting of two subsystems interlinked by a coaxial cable for DM-signal transport. b) Ground loops will be formed by external ground connections or by supply lines to the mains and c) an extra nearby ground connection creates an additional but useful ground loop.

impedance of these circuits but also the coupling to neighboring circuits.

However, Fig.2.9a is incomplete. Due to external ground connections or by supply lines, we create at the same time an irregular common-mode circuit with often unknown but usually a large loop area (see Fig.2.9b). Magnetic fluxes enclosed by this loop induce large interference currents, which because of the transfer impedance of the signal cable may introduce undesired DM-voltages.

A **grounding structure** connected between the subsystems, close to the cable creates a new well defined, regular and compact internal CM-circuit (see Fig.2.9c). When we give this grounding structure the form of a metal strip, a metal conduit or tube, we create thereby a **protected region** which can hold all leads and the fields of internal DM- and internal CM-currents (see Fig.2.10).

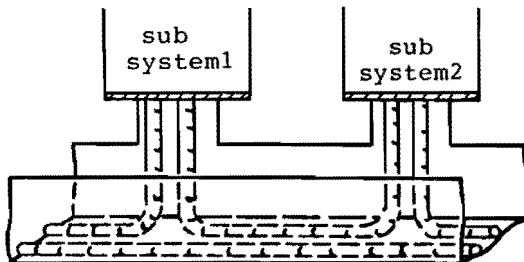


Fig. 2.10: A conduit-shaped grounding structure which connects two subsystems

On the outside is formed a new external CM-circuit, now even better closed by the grounding connection. Depending on the transfer impedance of the grounding structure the interference voltages due to the external CM-current can be calculated. With a proper designed grounding structure arbitrarily low values can be reached. In the case of a tube, especially at high frequencies, these voltages remain very small (see Fig. 2.11).

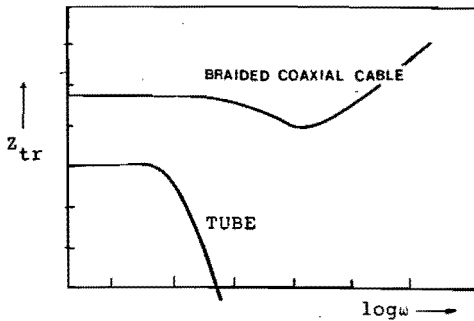


Fig.2.11:
 Typical behavior of the transfer impedance for a good coaxial cable and for a tube.

2.6 PROTECTED REGIONS FORMED BY GROUNDING STRUCTURES

Grounding structures (GS) can be used, -and for many years have been used-, in electrical engineering at several locations and in many forms. Depending on our position in electrical engineering we apply these grounding structures in complicated networks to create a local protected region, suitably sized for our "special" purpose (Fig.2.12).

For example, an experimentalist who has to use sensitive measuring equipment near intensive interference sources should use an extra suitable grounding structure (e.g. an

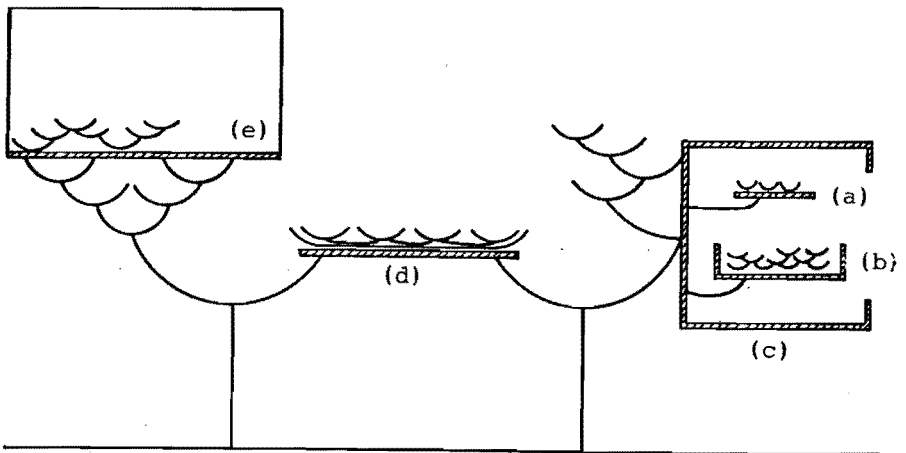


Fig 2.12: With grounding structures we decouple regions in the "grounding tree". As in Fig. 2.2, this figure shows only the low voltage part of all the circuits.

EMC-cabinet as shown in Fig.2.19). Attempts to improve the EMC-properties of the measuring instrument or of the electrical installation in the building are usually more difficult and also less certain to lead to EM-compatibility.

Examples of grounding structures at different locations in a complicated electrical system are (Fig.2.12):

- ground planes in an integrated circuit (IC) or on a printed circuit board (PCB) (a)
- a metal plate or chassis for the assembly of components, plugs and other connections (b)
- an EMC-cabinet for instruments (c)
- a conduit, for instance between EMC-cabinets (d)
- a metal floor or a completely shielded room (e).

We can also combine the protected regions, for instance those created by cabinets and a conduit (see also Fig. 2.10).

Metal, originally used for mechanical rigidity of an apparatus can often also be utilized for EMC-purposes. Already existing metal constructions, e.g. of a telecommunication tower or of a transformer housing (see Fig. 2.22b and Fig. 2.22c), can play this double role.

In this section we discuss how we, by means of GS's, create protected regions in which both sensitive signal leads and electronic equipment can operate without interference (see Fig.2.13). To utilize all benefits of these protected

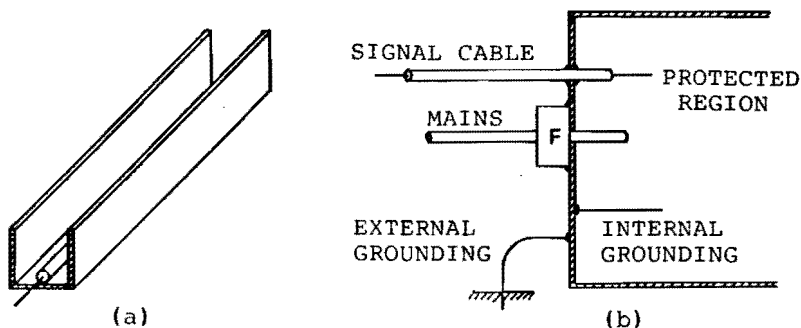


Fig. 2.13: Protected regions formed by conducting metal provide a local "climate" both for leads (a) and electronic equipment (b).

regions they should be given a correct shape and are to be properly interconnected. Also all points where leads enter the protected region should be correctly treated (see Sec. 2.6.2).

The leads that reach the protected region, such as signal cables may already carry differential mode interference superimposed on the legitimate signals. Several options are open to improve the signal to interference ratio: cables with a lower transfer impedance (see Ch.3), larger amplitude sigals or signals transported with H.F.-emphasis (see Sec. 2.6.2).

Note:

- that the creation of protected regions does not rely on the improvement of the overall "EM-environment" but instead, only provides an excellent local "climate" where it is needed.
- that the GS's not only provide protection but also give an opportunity for internal and external grounding.
- that there do not have to be conflicts between connections for safety reasons and the internal grounding facilities.

2.6.1 PROTECTED REGION FOR LEADS

Long GS's between electronic systems, in the form of metal strips, metal conduits or metal tubes, create protected regions which can hold all the leads and the fields of DM- and internal CM- currents (See Fig. 2.14). In addition the GS provides a preferred current path for external

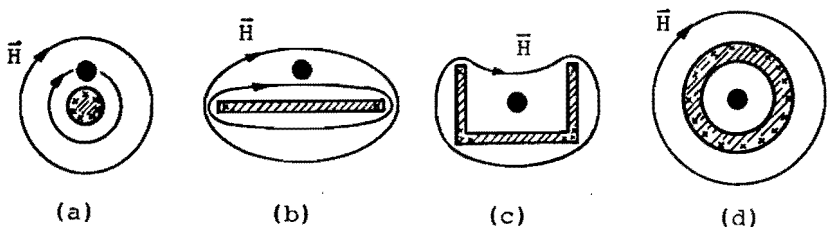


Fig. 2.14: Grounding structures (GS) for leads with their current density distribution and corresponding H-field for a CM-current carried by the GS.

CM-currents and acts as a shield against external E-fields and B-fields.

The use of metal for a GS guarantees a conducting path for external CM-currents. The E-field in the metal is very low. For dc- and low frequency currents the current density is homogeneously distributed over the cross section. At sufficiently high frequencies the CM-current is confined to the outer skin of the GS. The magnetic field lines due to this current have to go around the structure. The GS in the shape of a wide strip reduces the current density and the flux between leads and strip in the middle of the strip. Moreover the shape of a conduit, or better still that of a tube, forces the field lines away from the leads. The weakened magnetic fields then produces not much flux and reduce the induced interference voltage between DM-leads and GS.

A different way to describe this is to say that the external CM-currents in the GS couple in interference voltages via the transfer impedance (see Fig. 2.15). At high frequencies the transfer impedance of an open GS increases linearly with frequency because the magnetic field lines can penetrate between the leads and the GS. For an U-shaped GS, a larger height to width ratio helps; for a tube the transfer impedance becomes negligibly small at high frequencies. Note that even a small transfer impedance can be important because the coupling takes place over the entire length of the GS.

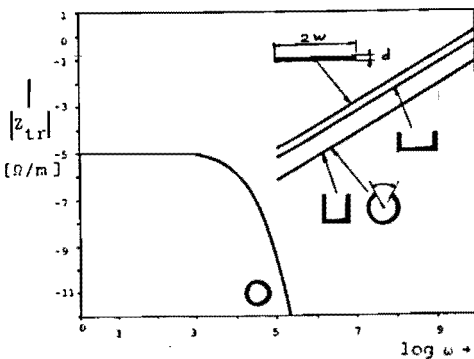


Fig.2.15:

The transfer impedance of a few grounding structures. The curves for the conduits (for $\delta \ll d$) are calculated with the model given in Chapter 3.

In most cases the transfer impedance is the most important parameter of a GS; here we also discuss the role of a GS as a shield against external E- and B-fields.

The role of the GS as a shield

a. The GS intercepts external E-lines very effectively (Fig. 2.16a,b). The current coupled in by the E-field can be carried away by a connection to ground (Fig.2.16c), and then may induce an interference voltage due to the transfer impedance, if the current has to flow along the GS over an appreciable length.

The signal leads inside the GS intercept only a few E-lines from the outside, which are responsible for the so called "transfer admittance". If the internal leads are coaxial cables with the braid connected to the GS or tubes the transfer admittance is negligibly small. Note that the region of interception of E-field lines is often limited in size in contrast to the CM-currents which couple in over the whole length of the GS.

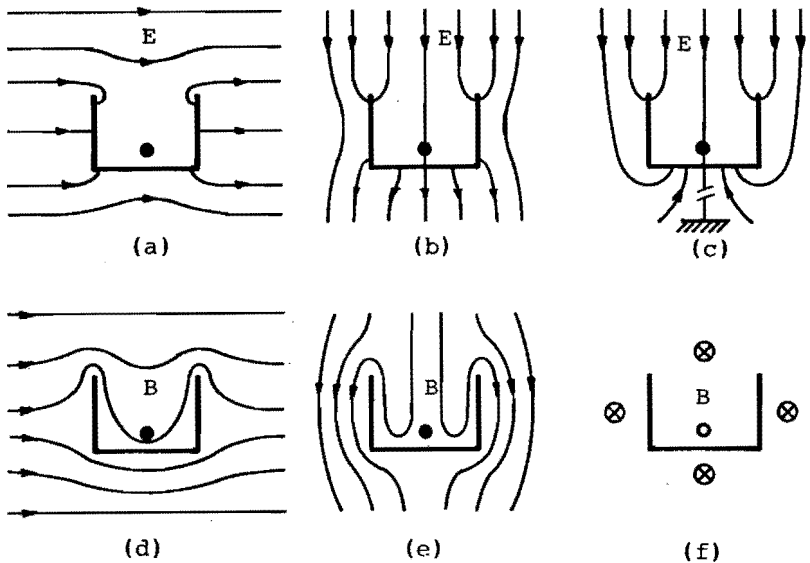


Fig. 2.16: The role of a GS as a shield. The GS intercepts E-lines (a,b,c) very effectively. The induced voltage due to a B-field perpendicular to the side walls (d) of the conduit could be of the same order as that due to the transfer impedance. B-fields perpendicular to the bottom of the GS or parallel to the GS (e,f) are not harmful.

b. The GS has a shielding effect on external magnetic fields. A B-field perpendicular to the side walls of a conduit (Fig. 2.16c) couples in some flux depending on the height to width ratio and how close the leads are to the bottom of the conduit. This coupling process could be of the same order as the transfer impedance effect (compare the fields in Fig. 2.16d and Fig. 2.14). However fairly strong sources are required to generate a perpendicular field comparable to the self field. If coils generate the perpendicular field, the effect still does act over a limited length, rather than along the entire length of the conduit, as in case of the transfer impedance.

Magnetic-fields perpendicular to the bottom of the GS or parallel to the GS (Fig. 16e,f) are not harmful; in Fig.16e the signal lead is assumed to be in the middle of the grounding structure.

2.6.2 PROTECTED REGION FOR INSTRUMENTS

Most measuring instruments have a metal housing or are installed in a metal cabinet on location and the question should be asked whether this metal housing creates a "protected region" for the electronics. Although this is true to some extent, the protection is not sufficient in situations with high interference, e.g Pulsed Power or HV-switching events. High intensity EM-waves cause undesirable interference signals in these instruments. The shielding provided by the metal housing should protect the interior, but unfortunately due to slits, paint, plug-in units and panels fastened with a few screws the shielding is poor and cannot easily be improved. A limited amount of shielding is however already adequate in case the distance from source to victim is sufficiently large. Moreover the apparatus proper is a relatively small size antenna.

More problems are caused by the leads, which carry signals or power into an electronic instrument from far away. These long leads can be efficient antennas to bring in large common mode currents (Fig. 2.17).

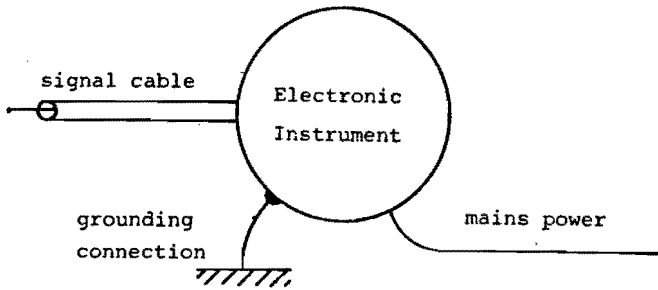


Fig. 2.17: Leads acting as large antennas. All leads carry a CM-current to or from the system. The sum of the currents is zero.

Most instrument housings cannot safely carry these currents. Interference couples in because of the poor "transfer impedance" of the instrument housing. With extra metal (a GS) we can create a protected region for the instrument, by diverting the external CM-currents away from the instrument housing. The GS works like a "current splitter"; DM-currents enter the protected region without problem while the CM-currents stay in the outside circuits formed by cable braids, the ground connections and the GS (see Fig. 2.18). The EMC cabinet, depicted in Fig.2.19 can serve this purpose. Since the currents flow mainly on the rear panel the front can often be left open.

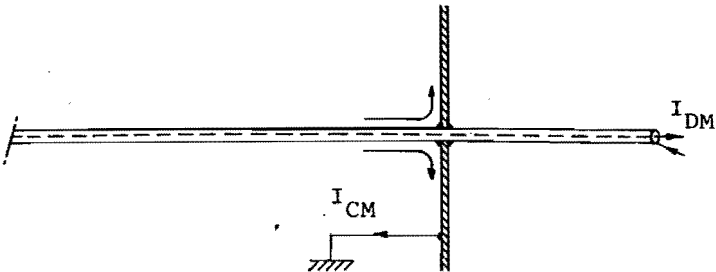


Fig. 2.18: Grounding Structure working as a "current-splitter". DM-currents can flow into the protected region while the external CM-currents are diverted by the GS.

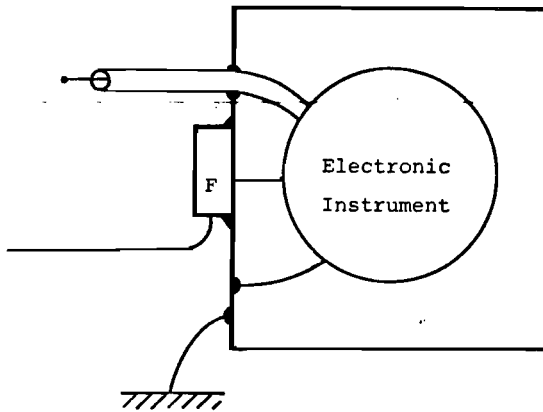


Fig. 2.19: An EMC cabinet diverts the CM-currents, and strongly reduces the combined transfer impedance of cabinet and electronic instrument (eg. an A/D converter or computer). Note that the ground does not provide a potential reference but is only a current path.

To keep the transfer impedance of the EMC-cabinet low, all cable braids are connected all around to the rear panel. A mains power filter, as well as attenuators, integrators or buffers are well bonded to the same continuous panel.

Since the cables for signal transport have sizeable transfer impedances, DM-interference signals may already leak into these cables before they enter the EMC cabinet. To improve the signal to interference ratio several options are open. We can use cables with a better braid, or transport signals with a large amplitude.

If signals of high amplitude are transported an input attenuator is required at the point of entry. This attenuator should have a flat response in the frequency band of the signal and at least a non-increasing response at the frequencies of the interference.

An alternative and attractive solution for wide band signal transport is the use of differentiated signals that are integrated again at the input of the electronic equipment. The advantage is that interference, superimposed on the differentiated signal is reduced by a factor proportional to the frequency. The integrator should have a $1/\omega$ -response

in the frequency band of the signal and at the interference frequencies a $1/\omega$ or lower response.

Note that many simple sensors, such as Rogowski coils, magnetic probes and some voltage sensors [Wol 83] give a differentiated signal.

The use of differentiated signals is comparable to the pre- and de-emphasis noise reduction system for FM-broadcast or to the RIAA correction system in record players.

Important for both options of signal transport is that passive components are used in the first section of the "receiver" (attenuator or integrator), i.e. where the interference is to be suppressed. Thus interference signals cannot reach the essentially non-linear electronics. The passive first section should be mounted in a shielded compartment next to the rear panel of the EMC-cabinet.

In cases where the integrator (or attenuator) must be connected to the front panel of the instrument directly, to maintain a correct termination, the lead can be fed in through an "inside extension" as shown in Fig.2.20a.

If the signal lead runs to the rear of the EMC cabinet close to the side panel of the EMC cabinet the CM-current in the side wall is a localized image current and interference due to external CM-currents is reduced as much as possible.

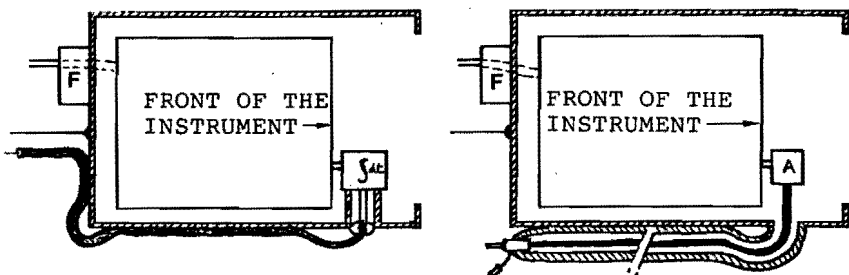


Fig. 2.20: Permitted side panel extensions:
(a) to the inside;
(b) the outside for instance for an attenuating probe.
A horizontal cross-section is shown.

An other input problem shows up with an attenuating probe such as the 1:1000 Tektronix. It is difficult, to connect the cable braid all around to the GS without damage to these special probe cables. A solution is a "flexible extension" also at the side panel as depicted in Fig.20b.

An different protection problem shows up in the case of consumer electronics, where usually only a plastic housing is present. In this case, where external CM-currents pass freely through the instrument, interference couples in via the various loops on the printed circuit boards (see Fig. 2.21a) .

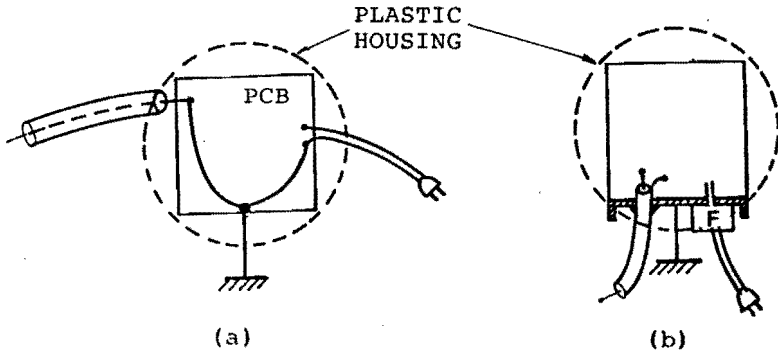


Fig. 2.21: External CM-currents have free passage through the instrument with a plastic housing (a). A simple grounding structure reroutes the CM-current out of the instrument (b).

A cheap solution to this interference is to apply the concepts of compactness during the design phase (as described in Sec.2.5). This could result in a simple grounding structure and "connector panel" where the external CM-currents are kept out of the instrument. An extra rim all around the grounding structure reduces the magnetic flux entering the protected region even more. A further reduction of the flux is obtained with a ground plane parallel to the printed circuit board.

2.7 APPLICATIONS

To illustrate the use of grounding structures to achieve correct operation of sensitive electronic equipment in situations with high interference we briefly discuss two examples:

1. A lightning protection system for a telecommunication installation [Deu 89].
2. The protection of control equipment in an open substation [Hou 89].

Both are examples of the same basic solution; namely the transport of a signal over a long cable which is locally protected against external CM-currents by a suitable GS (see Fig. 22a). In Ex.1 the external CM-current is caused by a lightning stroke, and in Ex.2 due to switching events in a primary circuit of an HV-installation.

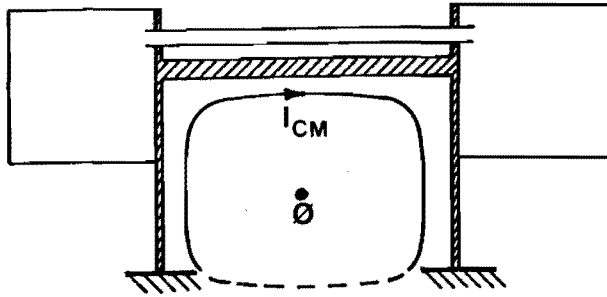
LIGHTNING PROTECTION SYSTEM

The considered telecommunication installation consists out of a tower and transmitters located in a building at some distances from the tower. The HF-signals are carried to the smaller dipole antennas by coaxial cables. Figure 2.22b shows the situation.

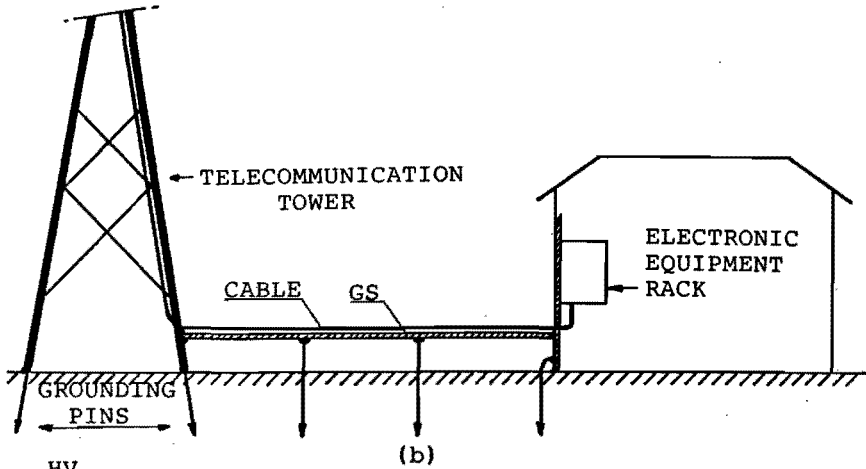
Normal lightning protection systems reduce Ohmic heating (fire-protection) and prevent local spark-over. For these purposes sufficient control of lightning current flow is provided by the metal tower and by grounding pins connected to the footing of the tower. For the more critical protection of leads and electronic equipment we must reduce the fraction of the lightning current going to the building. For this we need a grounding structure to create a protected region to keep interference low at sensitive inputs.

This protected region is formed by:

- a locally grounded EMC-cabinet for the transmitters,
- a conduit firmly connected between EMC-cabinet and the tower.
- a conduit or a special tube at the inside of tower. Also



(a)



(b)

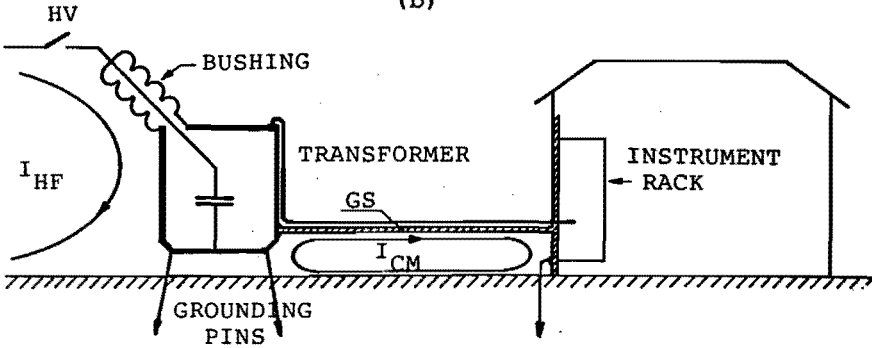


Fig. 2.22: (a) The general principle of protection by means of a GS. (b) Utilized in a lightning protection system for a telecommunication installation. (c) Utilized for the protection of control equipment in an open substation.

the inside of the angle iron leg of the tower can serve as a part of the GS.

A further control of the lightning current flow is provided by the placement of additional grounding pins. Extra pins can be connected to the footing, but also to the outside of the local grounding structure. The current is peeled off, the higher frequency part already near the tower due to the localized flux around the grounding structure.

Note that there is no need for overvoltage protectors or spark gaps. A good grounding system keeps the interference voltages low by itself.

OPEN SUBSTATION

Existing signal and control leads from a 150 kV / 10 kV transformer in an open substation were reported to show intense interference signals (a few kV) near electric circuitry in the control room of the station. Extra grounding pins installed near the transformer could not solve the problem.

Figure 2.22c explains the situation. At energization of the transformer from the 150 kV side, hf-currents in the primary circuit (1) cause a magnetic flux that couples into the secondary (signal/control) circuit (2).

To obtain substantial improvements the signal and control leads are installed in a protected region. For this situation the protected region was partly formed by the transformer housing, a conduit firmly connected between transformer and the instrument rack. In addition the instrument rack was grounded locally.

Results of many experiments show that interference can be reduced from kilovolts to less than 1 volt [Hou 89].

CHAPTER 3

THE TRANSFER IMPEDANCE OF GROUNDING STRUCTURES

An EMC-analysis for the protection of electronic systems and large scale electrical installations was given in Chapter 2 of this thesis. The present chapter considers a specific aspect of this analysis namely, the transfer impedance of grounding structures (GS).

3.1 THE TRANSFER IMPEDANCE CONCEPT

The transfer impedance is a much used concept to specify the interference properties of for instance coaxial cables and cable connectors (see Fig.3.1).

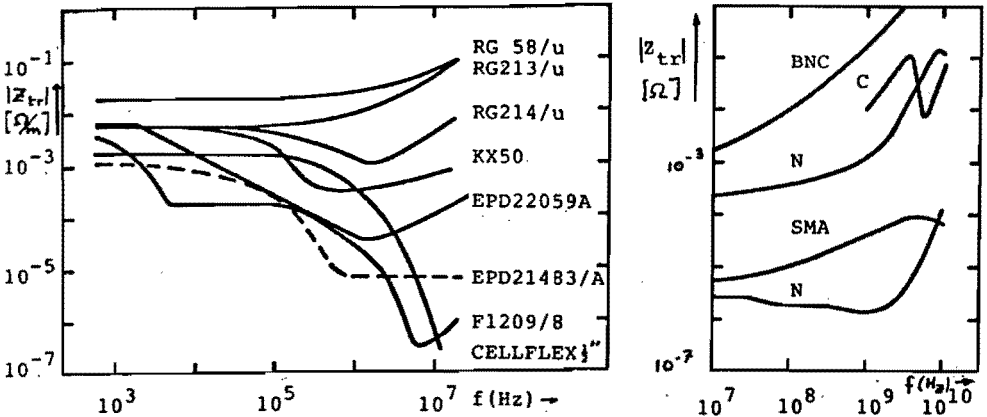


Fig.3.1: The transfer impedance of (a) coaxial cables [Sev 86] and (b) cable connectors [Eic 85].

The transfer impedance of a coaxial cable is generally defined as follows (see Fig.3.2):

if an interference current I_{CM} flows through the outer conductor of a coaxial cable and it causes a voltage difference V_{DM} at the open end of the cable which is short circuited at the other end, then the transfer impedance Z_{tr} is given by the relation

$$Z_{tr}(\omega) = \frac{V_{DM}(\omega)}{I_{CM}(\omega) l} \quad [\Omega/m], \quad l \ll \lambda/4 \quad (3.1)$$

where l is the length of the cable.

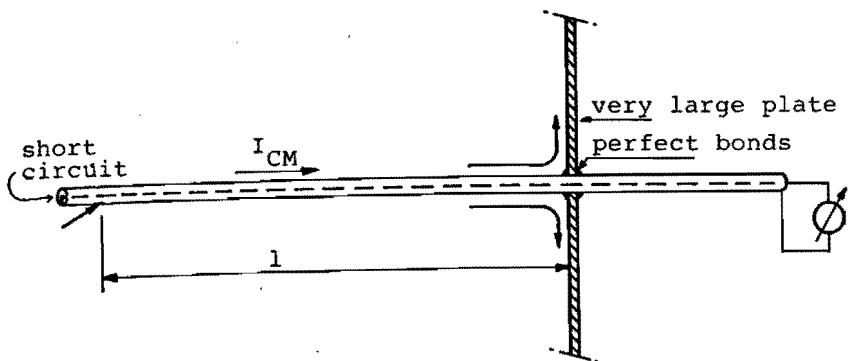


Fig.3.2: Sketch illustrating the definition of the transfer impedance of a coaxial cable.

For cables longer than a quarter wave-length the DM-voltage and DM-current due to the interference current can be calculated with a basic transmission-line model which contains per section dz an extra distributed internal series-voltage source $E(z)dz$ where $E(z)$ equals the product of the transfer impedance and the common-mode current (See Fig.3.3).

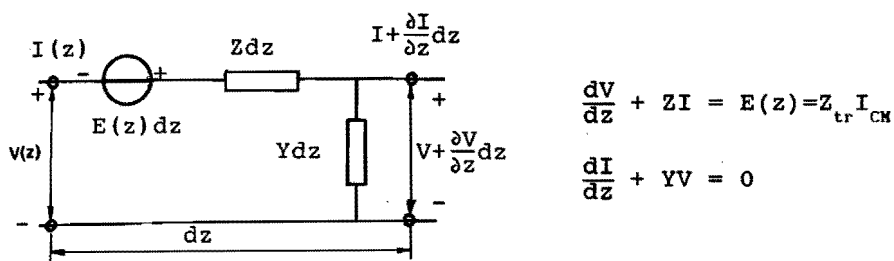


Fig.3.3: Equivalent circuit including the transfer impedance Z_{tr} , where Z is the series impedance and Y is the shunt admittance [Van 78].

Schelkunoff was the first to calculate the transfer impedance of a coaxial cable with solid outer conductor. Instead of "transfer impedance" he used the term "mutual impedance" [Sch 37].

Kaden calculated the transfer impedance of coaxial structures for various simple outer conductors. He used the term "Kopplungswiderstand" [Kad 59].

The value of Z_{tr} , both for braided coaxial cables and connectors is usually not calculable, but can be determined experimentally from a measurement of the DM-voltage caused by an injected CM-current.

The concept of transfer impedance, as defined for coaxial cables, can be used for a quantitative comparison of grounding structures, both by calculations as well as by measurements.

Clearly a properly designed grounding structure should be a structure with a low transfer impedance. Through this structure large external CM-currents may flow, and still no dangerous voltage differences are induced: the main aim of "grounding", or more general, of EMC-practice.

All grounding structures described in this thesis, fall into two categories: "Grounding Structures to protect leads" and "Grounding Structures to protect instruments" as introduced in Section 2.6. The concept of transfer impedance will be applied to both structures.

First we define the transfer impedance of a GS to protect leads:

When an interference current I_{CM} flows through an GS (see Fig.3.4), it causes a voltage difference V_{DM} between the points 1 and 2. The transfer impedance Z_{tr} of the GS is:

$$Z_{tr}(\omega) = \frac{V_{DM}(\omega)}{I_{CH}(\omega) l} \quad [\Omega/m], \quad l \ll \lambda/4 \quad (3.2)$$

where l is the length of the measuring loop.

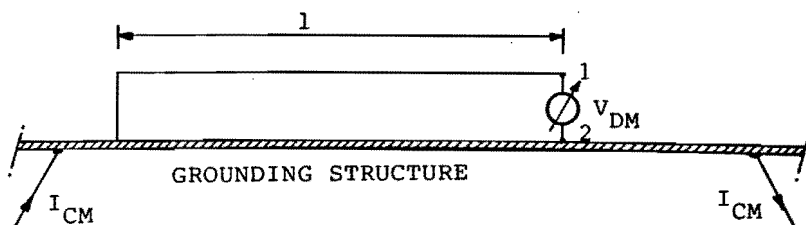


Fig.3.4: Sketch illustrating the definition of the transfer impedance Z_{tr} of a GS to protect leads.

Secondly we discuss the transfer impedance of a GS for instruments.

Due to for instance the finite size of a GS and an imperfect cable bond, CM-currents carried by leads coming from the "outside world" cause a CM-voltage in the protected region (see Fig. 3.5). The transfer impedance will be given by:

$$Z_{tr} = \frac{V_{CM}}{I_{CM}} \quad [\Omega] \quad (3.3)$$

Note that the voltage V_{CM} in Fig. 3.5 can drive a common mode current in the right hand part of the cable if its braid is grounded at the far right. In that case the behavior of the GS can also be described by a ratio of currents.

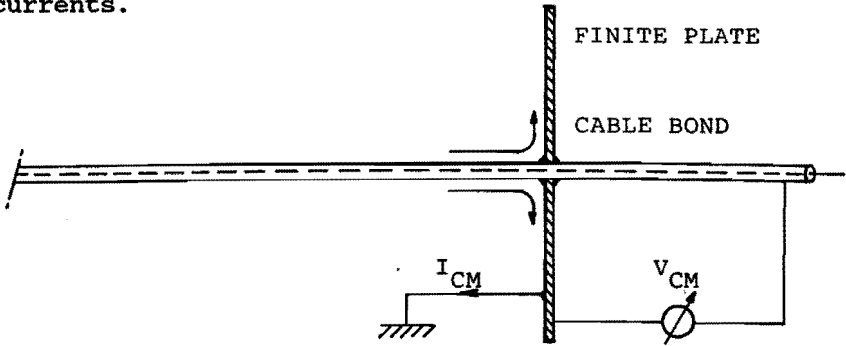


Fig.3.5: Sketch illustrating the definition of the transfer impedance of a GS to protect an instrument.

These definitions are a starting point for an evaluation of the transfer impedance of GS's. Measurements as well as calculations will be presented for the GS for leads and GS for instruments in sections 3.2 and 3.3, respectively.

The significance of the transfer impedance concept for grounding structures is that simple standard tests can provide its value and thereby a meaningful criterion for the quality of the grounding structure (including the whole "layout" of the "network"). The non-calculable overall transfer impedance of a large extended grounding structure can be determined by (CM-) current-injection test methods in which the voltage difference over critical terminals is

measured. Examples of such tests are presented in: "Measurements of Currents Around and in Large Grounded Structures" [Deu 88], and in: "Local Protection of Equipment in HV-Substations" [Deu 89]. Also Bersier's interference experiments with TV-sets presented in "Measurement of the immunity of TV-Receivers to AM, RF-fields in the 3 to 30 MHz Range, including the influence of connected cables" [Ber 81] is an example of a common-mode current-injection test.

3.2 THE TRANSFER IMPEDANCE OF GS's for leads

A GS for leads provides a controllable current path for external CM-currents and creates a protected region for leads by means of its shape.

3.2.1 AN IDEAL GS, A TUBE

The best, but in real situations not always a practical GS, is a completely closed tube (see Fig.3.6). The transfer impedance for a tube with a wall thickness d small compared to its radius r is given by [Kad 59, pg.294]:

$$Z_{tr} = \frac{k \rho}{2 \pi r \sinh kd} = \frac{k d R_0}{\sinh kd} \quad (3.4)$$

where $k = \frac{1+j}{\delta}$, $\delta = \left(\frac{2\rho}{\omega \mu_0 \mu_r} \right)^{1/2}$ is the skindepth, ρ the resistivity, $\mu_0 \mu_r$ the permeability and R_0 the DC-resistance.

The magnitude of the transfer impedance $|Z_{tr}|$ is:

$$|Z_{tr}| = \frac{2 \frac{d}{\delta} R_0}{\left(\cosh 2\frac{d}{\delta} - \cos 2\frac{d}{\delta} \right)^{1/2}} \approx \begin{cases} R_0 & d < \delta \\ 2\sqrt{2} R_0 \frac{d}{\delta} e^{-\frac{d}{\delta}} & \delta < d \end{cases} \quad (3.5)$$

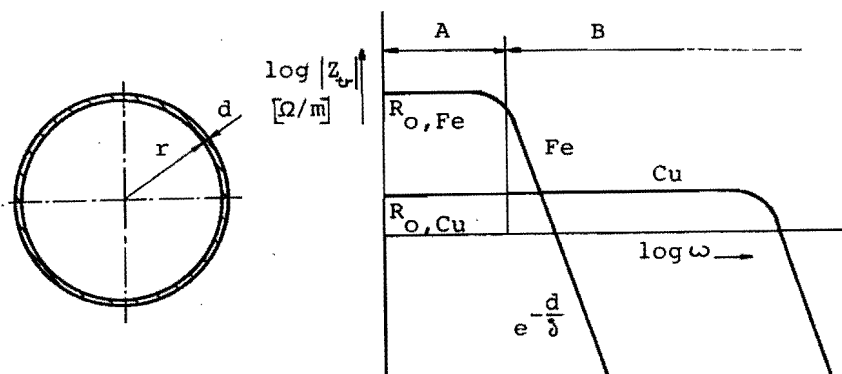


Fig. 3.6: The transfer impedance of a thin-walled tube made out of copper or iron.

We may characterize two frequency regions A and B.

- In region A, $0 < f < f_1 = \rho / (\pi \mu_0 \mu_r d^2)$, in other words where $d < \delta$, the transfer impedance remains close to R_0 .
- In region B, $f > f_1$, the transfer impedance relates the electric field which has "diffused" to the inner tube surface to the total current. For $f \gg f_1$, the Z_{tr} is almost zero in this nice, closed geometry.

The right hand part of Fig.3.6 depicts a comparison between iron and copper tubes. Although the R_0 of an iron tube is higher than that of a copper tube, the permeability of iron gives already at low frequencies a small skin depth, so that the Z_{tr} of an iron tube falls below that of a copper tube.

3.2.2 PRACTICAL GS's, PLATES OR CONDUITS

More practical GS's have the shape of a plate or a conduit. The transfer impedance of these GS's can be determined from Eq.3.2; see Fig.3.4 and Fig 3.7:

$$Z_{tr} = V_{DM} / (I_{CM} l) \quad [\Omega/m]$$

where V_{DM} is the interference voltage between the points 1 and 2, I_{CM} the interference current flowing through the grounding structure, and l is the length of the measuring loop, L (see Fig.3.7).

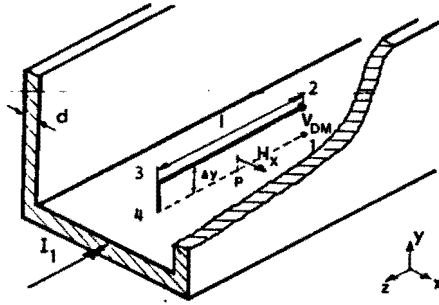


Fig. 3.7: The conduit shape of the grounding structure leads to a rearrangement of current and field and consequently to a low transfer impedance.

The voltage is given by:

$$V_{DM} = -\int_1^2 \mathbf{E} \cdot d\mathbf{l} = j\omega\mu_0 \iint_{S_2} H_x dS + \int_4^1 \mathbf{E}_s \cdot d\mathbf{l} \quad (3.6)$$

where S_2 is the area enclosed by loop L. Assumed is an $\exp(j\omega t)$ time-dependence; the E-field along the integration path 2-3-4, in the measuring wire, is zero. In this expression, the electric field \mathbf{E}_s on the inner surface ($y=0$) of the conduit as well as the magnetic field H_x in loop L, are unknown. When the skindepth δ in the conduit is less than the thickness d of the structure the electric field in the bottom of the conduit can be approximated by the expression for the electric field in a conducting half space:

$$E_z(y) = k\rho H_s e^{ky}, \quad \text{where } k = \frac{1+j}{\delta}, \quad \delta = \left(\frac{2\rho}{\omega\mu_0\mu_r} \right)^{1/2}$$

so that

$$E_s = E_z(0) = k\rho H_s \quad (3.7).$$

H_s is the magnetic field strength at point P on the inner surface of the structure. The magnetic field through surface S_2 is assumed to be constant and equal to H_s . With these simplifying assumptions the transfer impedance follows from eq.(3.6):

$$Z_{tr} = \frac{H_s}{I_{CM}} (k\rho + j\omega\mu_0\Delta y), \quad (3.8)$$

which is valid for $\delta \ll d$. The expression between brackets depends on the resistivity ρ and the permeability μ_r of the

grounding structure, the frequency and the height Δy . The ratio H_s/I_{CH} depends on the shape of the conduit.

Figure 3.8 shows the magnitude of the transfer impedance of an open GS as a function of frequency for typical conduits.

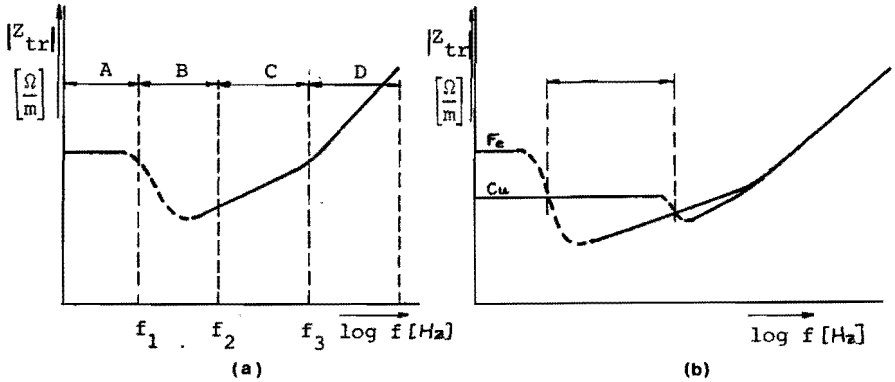


Fig.3.8: Magnitude of the transfer impedance of (a) an open GS. (b) A comparison of an iron and a copper conduit with the same dimensions.

We characterize four regions A, B, C and D (Equation 3.5 is valid for region A and gives an estimate for region B, Eq. 3.8 is valid for the regions C and D).

-Region A, $0 < f < f_1 = \frac{\rho}{\pi \mu_0 \mu_r d^2}$, in other words $d < \delta$, the transfer impedance is close to the DC-resistance R_0 .

-Region B, $f_1 < f < f_2$, where $f_2 \approx 25f_1$, which means $\delta(f_2) \approx 0.2d$. In this region two phenomena characterize the behavior of the transfer impedance. The skin effect leads to a decrease of Z_{tr} , whereas Eq.3.8 predicts an increase of Z_{tr} . Depending on the height to width ratio of the conduit, and the value of ρ and μ_r the $|Z_{tr}|$ shows a minimum or a monotonic increase.

-Region C, $f_2 < f < f_3$, $f_3 = \frac{\rho \mu_r}{2\pi \mu_0 (\Delta y)^2}$. The transfer impedance is given by $Z_{tr} \approx \frac{H}{I_{CH}} k \rho$, and $|Z_{tr}| \approx \frac{H}{I_{CH}} \sqrt{2} \frac{\rho}{\delta}$.

-Region D, $f > f_3$. The transfer impedance is given by $Z_{tr} \approx \frac{H}{I_{CH}} j \omega \mu_0 \Delta y$ and is independent of the properties ρ and μ_r of the metal of the conduit.

Figure 3.8b also compares an iron and a copper conduit with the same dimensions.

-For low frequencies this comparison is easy: the dc-resistance of the copper conduit is smaller than, that of the iron conduit.

-For the intermediate frequency region the comparison is more complicated than for a tube (Fig.3.6). The magnitude of the transfer impedance depends on material constants and geometry as explained before for the Regions B and C in Fig.3.8a.

- Finally for high frequencies, $|Z_{tr}|_{Cu} = |Z_{tr}|_{Fe}$; and is independent of material constants

Note:

(1) Due to the higher surface impedance of iron, in comparison with copper, the external CM-current might be reduced more by an iron conduit than by a copper one.

(2) For large currents iron will be saturated. For an U-shaped conduit saturation occurs where the magnetic field is high. This phenomenon results in a higher leakage of H-field into the protected region and thereby in a higher transfer impedance. Note that for a tube the fields near the inside are small, so that in the case of an iron tube saturation will not readily occur there. In the symmetric iron tube the H-field remains always zero at the inner surface.

THE SHAPE-FACTOR g.

The ratio H_s/I_{CM} in Eq.(3.8) depends only on the shape of the GS. When we bend a plate in a U-shape the field $H_s(c)$ at point P of a conduit will be considerably less than $H_s(p)$ at point P on the surface of the original plate (see Fig.3.9). This reduction can be expressed by a dimensionless shape-factor g, defined as:

$$g = \frac{H_s(c)}{H_s(p)} \quad (3.9)$$

where I_{CM} , d and $2h+2w=2b$ are kept constant.

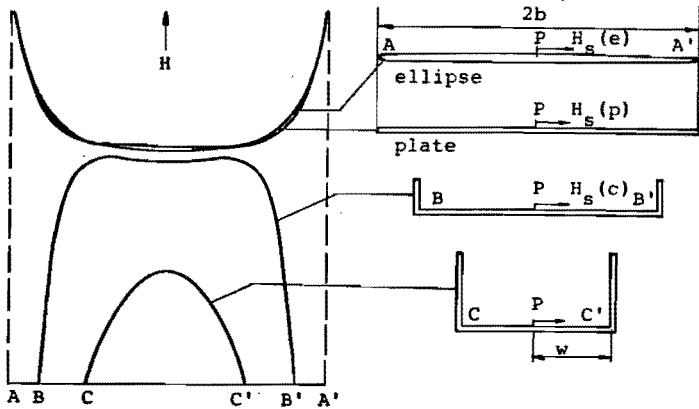


Fig.3.9: The field strength H along the horizontal surface of several GS's. Note that H is zero in an inside corner and very large at the outside corner of the plate and the ellipse.

The transfer impedance at higher frequencies becomes:

$$Z_{tr} = g \frac{H_s(p)}{I_{cm}} (k\rho + j\omega\mu_0\Delta y), \quad \delta \ll d. \quad (3.10)$$

The field $H_s(p)$ at point P on the surface of a thin plate is well approximated by the field $H_s(e)$ in point P, for a structure in the shape of an ellipse [Kad 59]:

$$H_s(e) = \frac{I_{cm}}{2\pi b}, \quad \delta \ll d. \quad (3.11)$$

The Z_{tr} of a conduit formed out of a thin plate with original width $2b$ is therefore given by the simple expression

$$Z_{tr} = g \frac{1}{2\pi b} (k\rho + j\omega\mu_0\Delta y), \quad \delta \ll d. \quad (3.12)$$

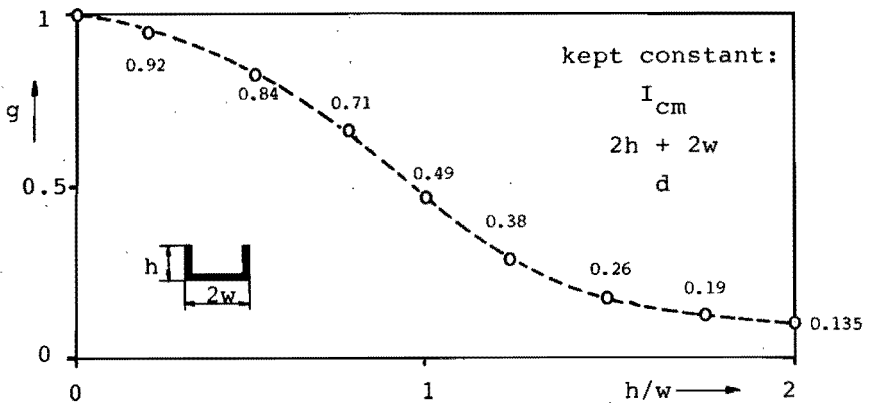


Fig.3.10: The shape factor g as a function of h/w . The \circ -dots are calculated. The return conductor for I_{cm} is supposed to be far away.

Figure 3.10 gives the calculated shape factor g , for some structures. The field strengths in points P on the surface of the U-shaped GS's were determined by means of a Boundary Element Method (BEM)-computer program [Def 90].

TRANSFER IMPEDANCE MEASUREMENTS

By means of a current-injection test we also measured the transfer impedance of a plate and two conduits, shown in Figure 3.11. The conduits were made out of a 1 mm thick aluminum plate of 270 mm width. The 4 m long conduits were placed along the axis of a metal tube with a inner diameter of 310 mm which served as the return conductor for I_{CM} .

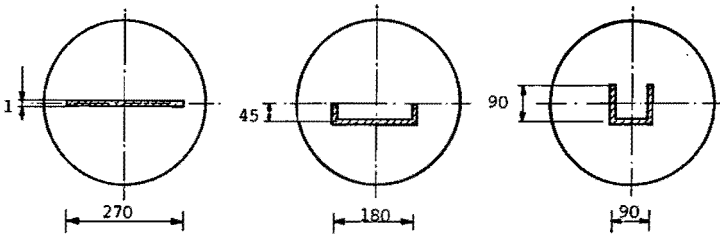


Fig. 3.11: GS's placed in a metal return cylinder for the measurement of Z_{tr} .

SETUP

Figure 3.12 shows a schematic diagram of the setup.

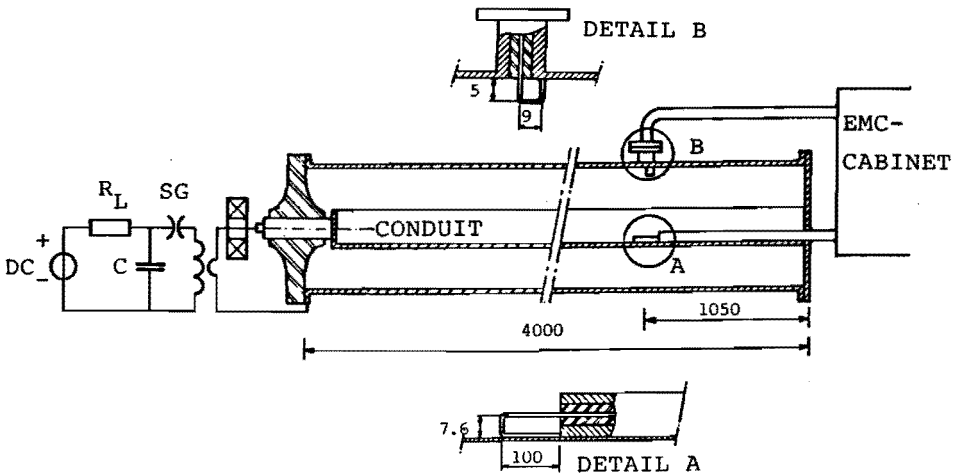


Fig.3.12: Setup for transfer impedance measurements of GS's.

To obtain a reproducible injection current a 0.5 μF , 25 kV capacitor was discharged through a spark-gap into a 3:1 pulse transformer. The secondary of the transformer was connected to the test conduit and to the outer tube, which were short circuited at the right hand end by a metal disk. The injected current $I(t)$ through the conduit, measured with a Pearson probe, is shown in Fig.3.13a. The magnetic field $H_s(c)$ was determined by measuring the change of the magnetic flux within a single turn loop (See Fig.3.12, detail A). The voltage signal $V_A(t)$ induced in this loop is shown in Fig.3.13b . The output signals were transported by RG-214 cables surrounded by copper tubes, "grounded" on both ends, and terminated with 50 Ω . The signal data were registered with a Nicolet 4094C digital oscilloscope (200 MHz max. sampling rate, 8 bit resolution), which was placed in an EMC-cabinet.

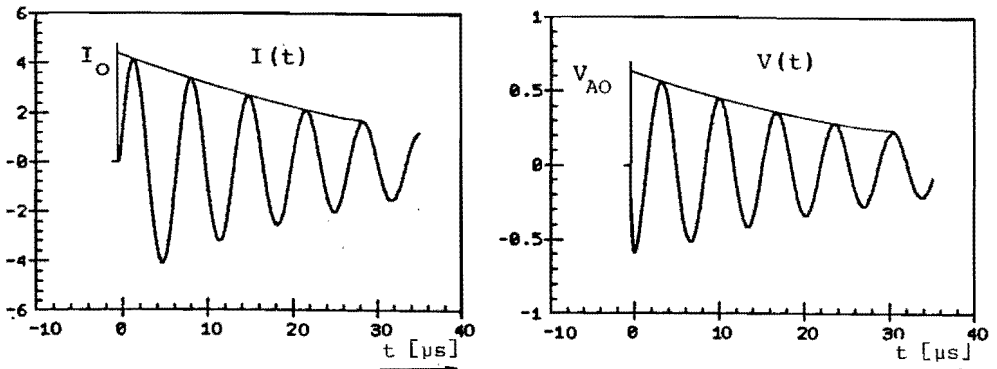


Fig. 3.13: Waveforms of the injected current $I(t)$ and the voltage $V_A(t)$ induced in a single loop.

EXPERIMENTAL RESULTS AND DISCUSSION

Table 3A gives the results of the measurements. The values of V_{AO} , I_0 , the amplitudes extrapolated to $t=0$, and ω are obtained from waveforms as in Fig.3.13a by curve fitting [Sta 87].

The magnetic field measurements are in good agreement with the calculations, under the same geometrical conditions (Table 3A, column 7).




H-FIELDS		measured				calculated		
	$\frac{h}{w}$	Return cylinder R=0.155m						R=100m
		I_o	V_{AO}	ω	$H_s = C1 \cdot \frac{V_{AO}}{O_A \cdot \mu_o \cdot I_o \cdot \omega}$	$H_{0.155}^{BEM}$	H_{100}^{BEM}	
		A	mV	rad/s	A/m for 1 Amp	A/m	A/m	
ref. case 	0	915	825	9.22×10^5	0.95	0.95	1.17	
	$\frac{1}{2}$	1012	856	9.17×10^5	0.81	0.79	0.98	
	2	824	121.7	9.21×10^5	0.156	0.153	0.158	
1	2	3	4	5	6	7	8	

TABLE 3A: Measured H-field values with loop A at point P (column 6, radius return cylinder R = 0.155 m) for a plate and two conduits (column 1). Column 7 gives H-field values obtained from BEM-calculations under the same geometrical conditions. Column 8 gives calculated H-field values but now for the situation with R = 100 m. V_{AO} and I_o , the values of the amplitudes of $V(t)$ and $I(t)$ extrapolated to $t=0$, and ω are obtained from measurements and by curve fitting. The H-fields are given for a total current of 1 Amp.

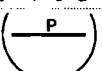
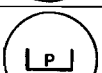

SHAPE FACTOR	return cylinder R=0.155		R= 100m
	g^M	$g_{0.155}^{BEM}$	g_{100}^{BEM}
ref. case 	1	1	1
	0.85	0.83	0.84
	0.164	0.166	0.135
1	2	3	4

TABLE 3B: Shape factors (column 2) for a plate and two conduits (column 1) calculated from measured H-field values with loop A. Columns 3 and 4 give shape factors, calculated from H-field values obtained by BEM-calculations, in the cases of return cylinder radii R = 0.155 m and R = 100 m, respectively. Note that the shape factor for the plate is kept equal to unity, both for small and large outer cylinder.

Experimental parameters such as the effective area, O_A , of the pick up loop were not very accurately known. Therefore we introduced a correction factor, C_1 , to adjust all measured H-fields; this factor (which turned out to be 0.92) is obtained from the case of the flat plate, where the calculated field should be very reliable.

Because the return cylinder of radius 0.155 m is fairly close to the central conductor, a "proximity effect" modifies the current flow in the conduit, and also the field around it. In practice conduits may be at a large distance from the return conductor. Therefore a second series of BEM-calculations (also used in Fig.3.10) was carried out for conduits with the return conductor at a larger distance (100 m in the BEM calculations). The column at the far right of Table 3A shows the resulting H-fields. As expected, we see an appreciable difference for the plate and a much smaller one for the more compact conduit with $h/w=2$.

Similar differences show up when the results are expressed as shape factors (Table 3B), where the H-fields are normalized to make them unity for the plate. Note that the shape factor for the plate is kept equal to unity, both for the smaller and the larger cylinder.

The above mentioned "proximity effect" also influences the current density distribution at the inside of the return cylinder. Calculations show the influence of the proximity effect on the current density distribution at the inner surface of the return cylinder (See Fig.3.14).

To illustrate this effect we determined the current density $j_B(t)$ by measuring the change of the magnetic flux within a single turn loop close to the cylinder surface (see Fig.3.12, detail B). The voltage signal $V_B(t)$, induced in this loop has the same damped cosine behavior as $V_A(t)$ in Fig.3.11b.

Table 3C gives the results of the measurements. The values of V_{Bo} , I_o and ω are again obtained from wave forms as in Fig. 3.13 by curve fitting [STA 87].





SURFACE CURRENT DENSITY					measured	calculated
ref. case	$\frac{h}{w}$	I_0	V_{B0}	ω	return cylinder $R=0.155m$	
					$j_B = C2 \cdot \frac{V_{B0}}{O_B \cdot \mu_0 \cdot I_0 \cdot \omega}$	
					A	A/m
	-	8.55	48.8	9.22×10^5 rad/s	1.026	1.026
	0	9.18	56.3	9.22×10^5 rad/s	0.52	0.47
	$\frac{1}{2}$	10.12	26.9	9.17×10^5 rad/s	0.434	0.429
	2	8.24	43.4	9.21×10^5 rad/s	0.94	0.88
1	2	3	4	5	6	7

TABLE 3C: Surface current density j_B , measured (column 6) for a tube, a plate and two conduits (column 1) with a return cylinder with radius $R = 0.155$ m. Column 7 gives j_B -values obtained from BEM-calculations under the same geometrical conditions. V_{A0} and I_0 , the values of the amplitudes extrapolated to $t=0$ of the induced voltage $V_A(t)$ and the injected current $I(t)$, and ω are obtained from measurements by curve fitting. The surface current is given for a total current of 1 Amp.

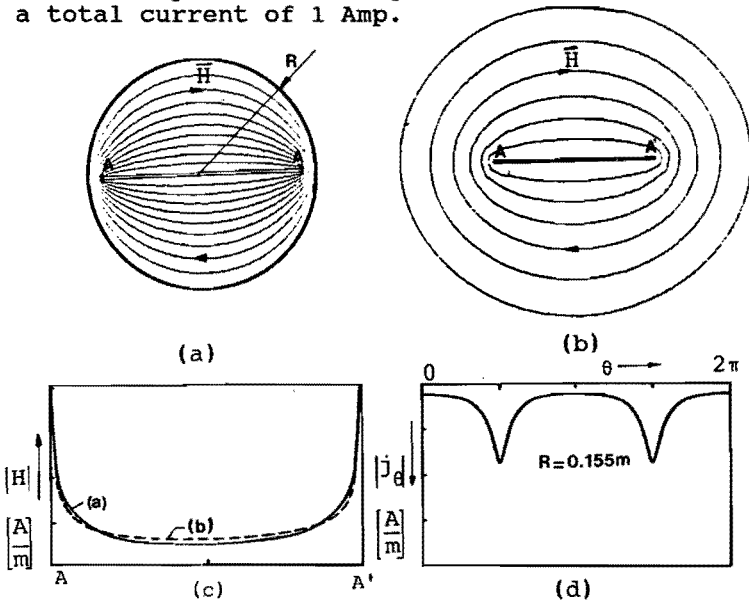


Fig.3.14: FEM plots show the H-field lines for a strip in an return cylinder with $R=0.155m$ (a) and with $R=100m$ (b). BEM-plots (c) show the H-field values at the surface of the strip for both situations. The surface current density at the inner surface of the return cylinder is shown in (d) as a function of the angle θ .

We introduced also here a correction factor to adjust all measured current densities; this factor (which turned out to be 0.94) is obtained from the case of a tube as central conductor, where the current density is homogeneous. Excentricity of the inner conductor may be the cause of the slight discrepancies found for the plate and the conduits.

3.2.3. ALMOST IDEAL GROUNDING STRUCTURES: COVERED CONDUITS

Metal plates and conduits provide an excellent conducting path for external CM- currents and create well protected regions. In situations with intense interference, the transfer impedance of these grounding structures can be further reduced by the use of non-touching metal covers of finite length in addition to the conduits, as depicted in Fig.3.15.

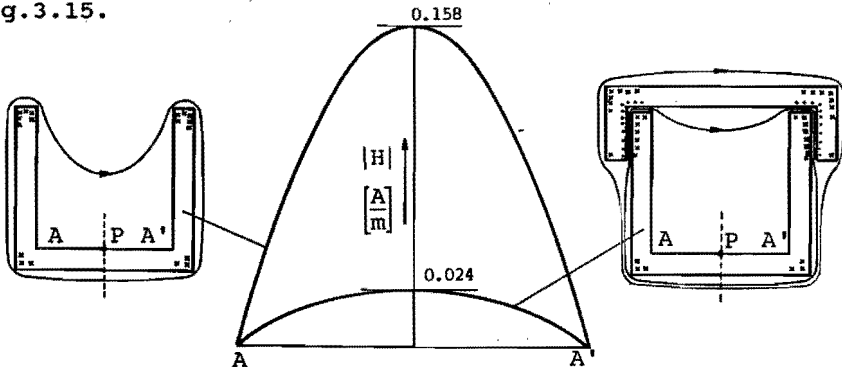


Fig. 3.15 : A conduit with $h/w=2$ with and without a cover. The graph shows the reduction of the H-field at the bottom of the conduit caused by the non-touching metal cover.

With this configuration an almost ideal GS, can be constructed, which is much more practical than a tube. At high frequencies the metal cover changes the distribution of currents and forces the already weakened magnetic field further away from the leads. Induced currents flowing at the outside surface of the cover are concentrated at the corners. These currents are parts of loops which will be closed by currents which return as current density concentrations at the overlap of cover and conduit (See Fig. 3.16).

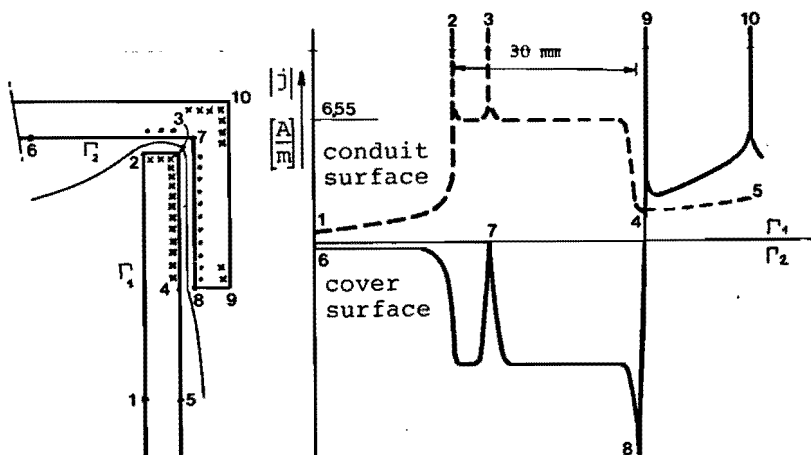


Fig. 3.16: The surface current density in the side wall of the conduit (points 1 to 5) and in the cover (points 6 to 10), normalized to a total current of 1 Amp. The concentration of the current density at the overlap of cover and conduit causes a concentration of the H-field in the overlap gap.

In the overlap-gap we get a concentration of the H-field. Since $\oint H \cdot dl$ around the cover is zero, the magnitude of the H-field in each of the two gaps, H_{gap} , is approximately:

$$H_{gap} \approx \frac{0.5}{l_{ov}} I_{ind} \quad (3.13)$$

where I_{ind} is the current induced in the outer surface of the cover and l_{ov} is the length of each overlap. The induced current is roughly equal to $0.4 \times I_{CM}$, since the cover represents about 40% of the total circumference, through which the net interference current I_{CM} is flowing. We can rewrite Eq. 3.13:

$$H_{gap} \approx \frac{0.2}{l_{ov}} I_{CM} \quad (3.14)$$

The total interference flux per meter, Φ_{int} , passing the gap can be estimated by:

$$\Phi_{int} = H_{gap} \cdot d \approx 0.2 \frac{d}{l_{ov}} I_{CM} \quad (3.15)$$

where d is the width of the gap.

According to this formula we obtain a reduction of Φ_{int}

when we use a large overlap length and a small gap width. We get also a reduction of Φ_{int} when we can reduce I_{ind} in the cover. This in fact happens when we place the cover in the conduit instead of over it. This statement can be confirmed by BEM-calculations (See Fig.3.17).

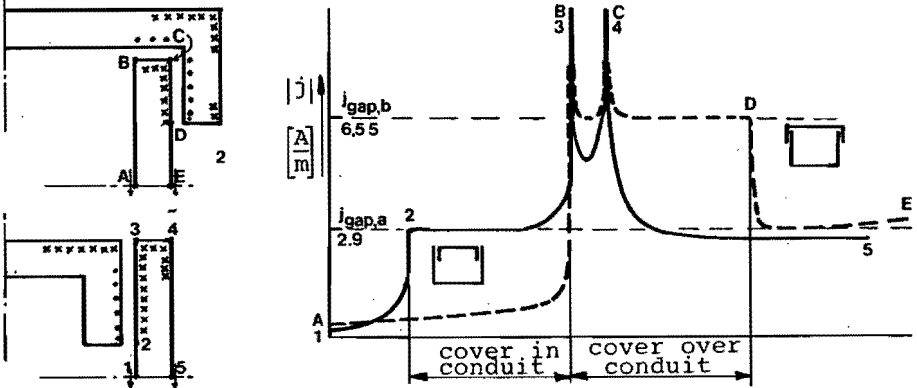


Fig.3.17: The current surface density j in the side wall of the conduit for (a) from points A to E, and for (b) from points 1 to 5, normalized to a total current of 1 Amp. The current density in the gap is lower for the "inside" cover.

Although the interference flux Φ_{int} in Fig.3.17b streams in closer to the bottom surface of the conduit than in Fig.3.17a, the magnitude of Φ_{int} is much smaller in case b. The H-field at the bottom of the conduit is therefore smaller for the inside cover. Figure 3.18 gives the fieldstrength at point P as a function of the overlap-length for a few configurations of covers placed over and in conduits.

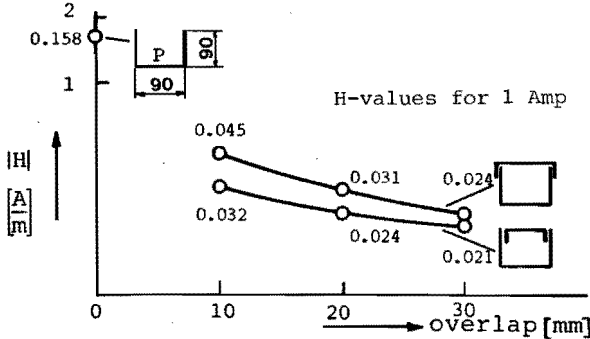


Fig. 3.18: The H-field at point P as a function of the total overlap length for both outside and inside covers.

Because of the time variation of the flux in the gap a voltage difference is induced between the non-touching cover and the conduit (See Fig.3.19). Strong time varying

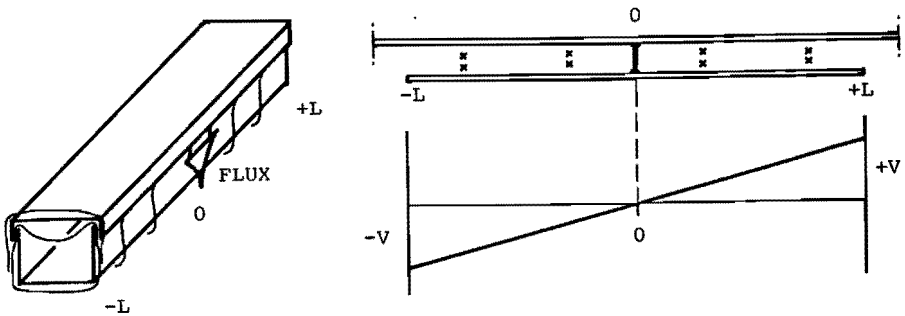


Fig. 3.19: The magnetic flux in the gap induces a voltage between cover and conduit. (b) The current through the bolt in the middle of the cover is zero for symmetry reasons.

fields may produce sparking between cover and conduit. To reduce this voltage difference and to avoid sparking and its subsequent interference two solutions can be considered.

1. We can use short segments of non-touching covers to limit the flux in the gap. To fasten the cover, one bolt in the middle at both sides of the cover is permitted. No current will flow from cover to conduit because the bolt does not change the voltage distribution between cover and conduit (See Fig.3.19b).
2. A more expensive solution is to make full metallic contact between conduit and cover over the entire length of the cover. When we use bolts we need many to reduce the resulting current density concentrations.

As a result of the above analysis we show in Fig.3.20a an example of an almost ideal grounding structure which could carry leads between "subsystems". A cover is fitted in the inside of a conduit, a bit below the top of the vertical sides of the conduit. Contact-springs allow currents to cross over the entire length of the conduit. We use round edges and more metal at places where we expect current density concentrations. The realisation of such a grounding

structure for protection of electric circuits against unwanted electric signals may be costly, but is certainly feasible. Many other configurations can be designed (See Fig. 3.20b).

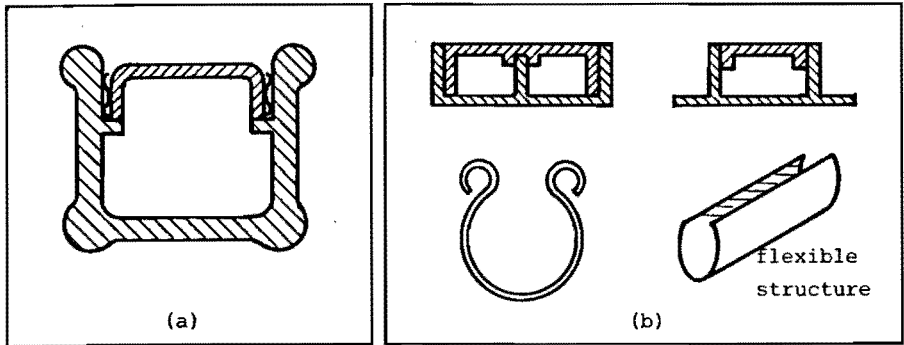


Fig. 3.20: (a) An almost ideal GS, and (b) some other possible GS's.

The combined use of a coaxial cable and a grounding structure results in a very low total transfer impedance $Z_{tr,tot}$. This $Z_{tr,tot}$ can be easily calculated (see Fig.3.21a).

The external CM-current, $I_{CM,ext}$, induces a current $I_{CM,int}$ in the internal CM-circuit equal to:

$$I_{CM,int} = (I_{CM,ext} Z_{tr,GS}) / Z_{CM,int} \quad (3.16)$$

where $Z_{tr,GS}$ is the transfer impedance of the GS and $Z_{CM,int}$ is the impedance of the internal CM-circuit.

The induced interference voltage V_{DM} in the cable becomes:

$$V_{DM} = I_{CM,int} Z_{tr,cable} \quad (3.17)$$

where $Z_{tr,cable}$ is the transfer impedance of the cable.

So the total transfer impedance becomes the expression:

$$Z_{tr,tot} = (Z_{tr,GS} / Z_{CM,int}) Z_{tr,cable} \quad (3.18)$$

For high frequencies this expression reduces to:

$$Z_{tr,tot} = (M/L) Z_{tr,cable} \quad (3.19)$$

where M is the mutual inductance between the external and internal CM-circuit, and L is the self inductance of the internal CM-circuit. When we use a proper grounding structure M is much smaller than L.

Further reduction of $Z_{tr,tot}$ is achieved when we increase $Z_{CM,int}$ by e.g. a ferromagnetic layer around the coaxial cable (see Fig. 3.21b). This layer could consist of iron tape or of ferrite rings which increase either the inductance or the resistance in the internal CM-circuit.

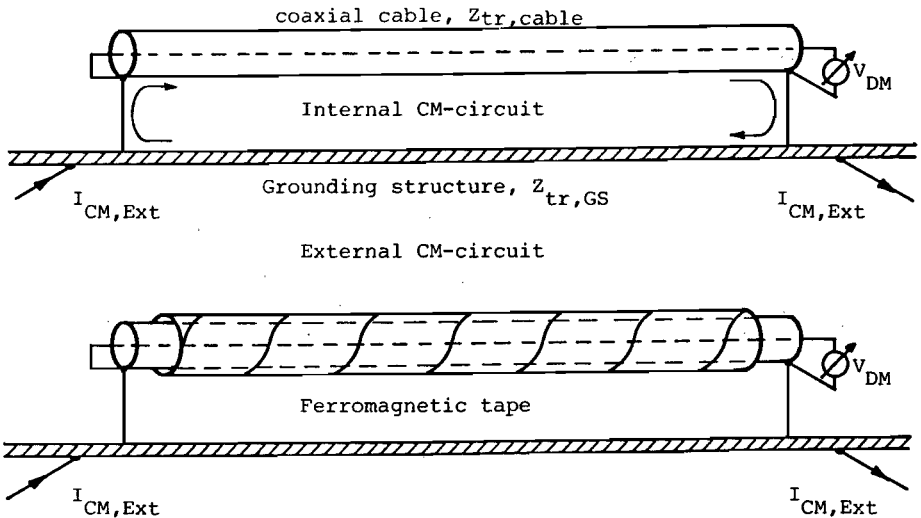


Fig. 3.21: (a) A coaxial cable in the protected region of a GS. The voltage V_{DM} due to the current $I_{CM,int}$ is very low. (b) A ferromagnetic tape wound around the cable increases the internal CM-circuit impedance.

Note:

(1) The GS's described above offer protection over a wide frequency range; in the literature protection is only judged possible over a small frequency range. A quote from (Den 74) is "neither of the four fundamental methods (isolation, single-point grounding, multiple-point grounding, or noise reduction) of minimizing the noise in the signal transfer loop will by itself provide interference-free operation over the entire range of amplitudes and frequencies encountered in many installations".

(2) For the low frequencies (e.g. 50 or 60Hz) the transfer impedance of the GS is about equal to the DC-resistance. This DC-resistance is generally low because of the bulky metal GS.

(3) An iron conduit has a number of advantages over an aluminum or copper conduit:

- The small skindepth leads to a rearrangement of the current, already at low frequencies, as shown by the drop in Fig.3.8.
- The external I_{CM} can be reduced by the extra impedance (R and L) of the thin outside skin.
- The inside V_{DM} sees a higher $Z_{CM,int}$ as a result of the extra impedance.

3.3 THE TRANSFER IMPEDANCE OF GROUNDING STRUCTURES FOR PROTECTION OF INSTRUMENTS

In Section 2.6 we mentioned that long leads, which carry signals or power towards an electronic instrument can be efficient antennas which bring in large common mode currents. Interference may couple in when these currents are not correctly treated. For this protection of instruments we need a GS through which the useful DM-currents can flow into the protected region, whereas the external CM-currents are diverted (See Sec.2.6, Fig.2.18). In situations with a high interference level where much protection is necessary an EMC-cabinet can be an efficient solution. For the protection of instruments in situations with a moderately high interference level a search for a solution with less metal (a simple GS) is meaningful. Such simple GS's are of course conceptually related to the EMC-cabinet. The transfer impedance of these simple GS's will be discussed in this section.

Note that the transfer impedance is only meaningful when primary and secondary circuit are defined. In this section we keep these circuits the same and study the influence of the size and geometry of the GS on the transfer impedance.

As a step in our analysis of the transfer impedance of simple GS's for the protection of instruments we consider a single coaxial cable with its cable braid connected all

around to the GS (A) and one additional grounding lead (B) connected to the same GS (see Fig.3.22). These leads are mounted perpendicularly to the GS, at a fixed distance of each other. For this type of GS we neglect the small "resistive" part of the transfer impedance as is reasonable at higher frequencies. We consider only the mutual inductance M between the external CM-circuit and a "testloop" placed at a fixed position in the protected region. Thus for the transfer impedance of the grounding structure we may use the expression $Z = j\omega M$.

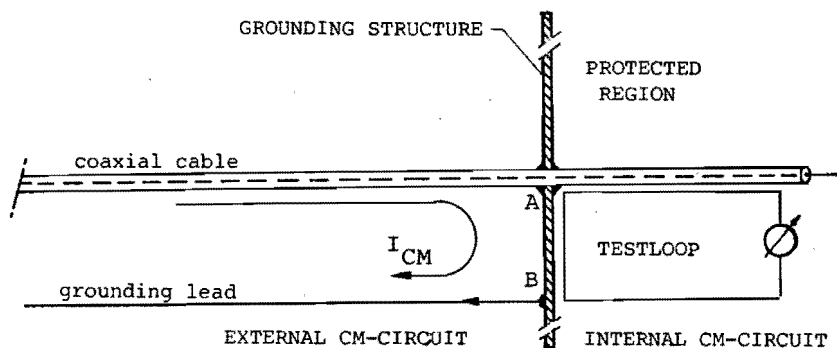


Fig. 3.22: A coaxial cable and one grounding lead mounted perpendicularly to the GS. The "testloop" is located in the protected region, in the same plane as the leads.

AN IDEAL GS FOR AN INSTRUMENT

An ideal grounding structure in this situation would be an infinitely large metal plate or a completely closed metal box. In the case of a infinitely large metal plate the external CM-current spreads over the left hand side of the plate in a "line dipole"-pattern as shown in Fig. 3.23.

The components of the current density are given by [Ram 84]:

$$J_r = \frac{I}{\pi} \frac{a(r^2 - a^2) \sin \theta}{r_+^2 \cdot r_-^2} \quad (3.20a),$$

$$J_\theta = \frac{-I}{\pi} \frac{a(r^2 + a^2) \cos \theta}{r_+^2 \cdot r_-^2} \quad (3.20b)$$

in which $r_+^2 = r^2 + a^2 - 2arsine$, $r_-^2 = r^2 + a^2 + 2arsine$; the coordinate system is given in Fig. 3.23. These results are used later as an approximation for a finite size plate. For

the infinitely large plate or the closed box the mutual inductance, between the external CM-circuit and the internal circuit, is zero just as the transfer impedance of the GS.

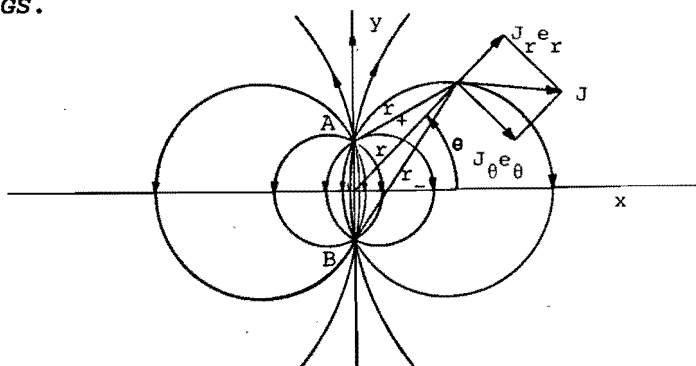


Fig. 3.23: The current density distribution for an infinitely large plate has the shape of the field lines of a line dipole.

REAL GS's FOR INSTRUMENTS

In reality only plates of finite size are used. The transfer impedance of such a GS with finite size is analyzed for the example of a circular disk as grounding structure (see Fig. 3.24). The analysis is based on measurements with the setup shown in Fig. 3.27. In addition to the measurements we derive an approximate relation between the mutual inductance, -the M between the external CM-circuit and the testloop-, and the diameter of the GS.

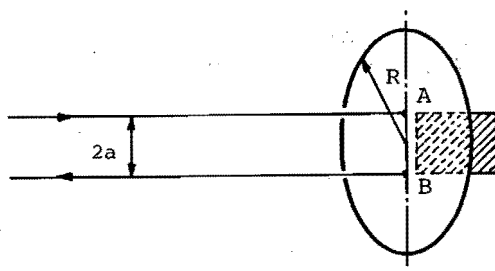


Fig. 3.24: A GS shaped as a disk. The disk serves as a simple geometry for which approximate calculations are possible. The transfer impedance depends on the radius R , the distance $2a$ between the injection wires and the location and size of the test loop at the right.

To obtain an approximate expression for the mutual inductance M , we consider a disk with radius R , where R is assumed to be large with respect to the distance $2a$ between the leads.

For the surface current density distribution, at the left side of the disk, we use -as an approximation- the solutions J_r and J_θ for the infinitely large plate in the region $r < R$ (Eqs. 3.20a,b). The values of $J_r(R)$ and $J_\theta(R)$ at the boundary of the left side are:

$$J_r^L(R) = \frac{I}{\pi} \frac{a}{R^2} \sin\theta \quad \text{and} \quad J_\theta^L(R) = \frac{I}{\pi} \frac{a}{R^2} \cos\theta \quad (3.21a,b)$$

obtained from Eqs.3.20a,b with $R \gg a$.

Continuity of $J(R)$ between left and right hand side requires:

$$J_r^L(R) = -J_r^R(R) \quad \text{and} \quad J_\theta^L(R) = J_\theta^R(R) \quad (3.22a,b)$$

A approximate solution is that the current density J at the right hand side is constant over the entire right hand surface with the value $J_y^R(x,y) = \frac{I}{\pi} \frac{a}{R^2}$ (See Fig. 3.25).

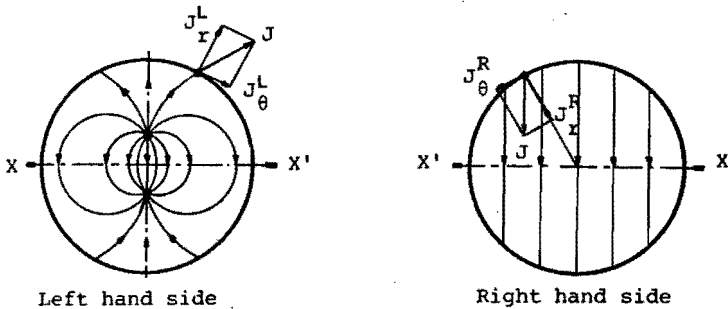


Fig. 3.25: Approximate surface current density distribution patterns for both sides of a disk.

To calculate the mutual inductance between the external CM-circuit and the testloop we assume that the field strength at the surface, H_x which is equal to J_y , is constant over the small testloop area S_{TL} .

This derivation for M leads to:

$$M = \frac{\mu_0 a}{\pi R^2} S_{TL} \quad (3.23)$$

This approximate expression shows that the mutual

inductance, -and thereby the transfer impedance-, will be reduced when we reduce the distance between the leads or enlarge the area of the disk.

We expect a further reduction of the transfer impedance when a cylinder is attached to the disk (Fig.3.26b) or when the disk is enlarged to a strip (Fig.3.26c). For the strip the question can be asked in which direction (x- or y-direction) the disk should be expanded to achieve the lowest transfer impedance. No calculations were possible for the disk with cylinder and for the strip. To answer these questions we have measured the transfer impedance of a disk, a disk with cylinder and the strip as shown in Fig.3.26; all by means of a current injection test.

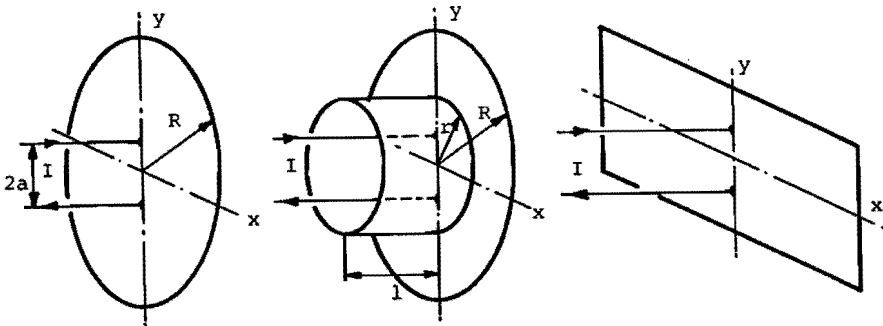


Fig. 3.26: A disk, a disk with an attached cylinder, and a strip, with injection wires in the y-direction.

TRANSFER IMPEDANCE MEASUREMENTS.

Three series of measurements have been done:

- we measured the Z_{tr} of a brass disk as a function of the disk radius ($R= 25, 50, \text{ and } 75\text{mm}$),
- we measured the Z_{tr} of the same disks now with cylinders attached; the dimensions of the cylinder were: $r= 18 \text{ mm}$ and the length was taken to be 10, 20, 30, 50 and 70 mm,
- we measured the Z_{tr} of two brass strips with dimensions 50 by 400 mm and 100 by 400 mm, both with the connections perpendicular or parallel to the long direction of the strip.

The distance between current injection wires is 16.9 mm for all measurements.

By measuring the injected current I_{inj} (See the setup shown in Fig.3.27) and the induced voltage V_{ind} in a test loop we determined the mutual inductance M between injection circuit and testloop. The mutual inductance is obtained from the relation $M = \int V_{ind} dt / I_{inj}$. The integration of V and calculation of M is carried out by means of the software package VU-point [VU- 87].

SETUP

Figure 3.27 shows a diagram of the setup.

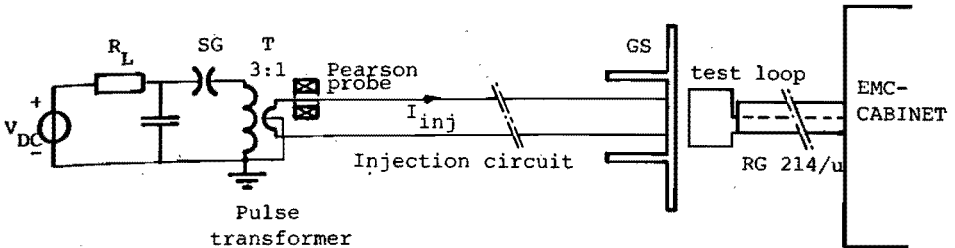


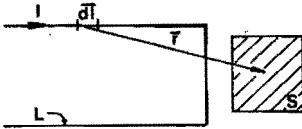
Fig. 3.27: Current injection test for transfer impedance measurements. The test section is fixed on a wooden table.

We obtained a reproducible injection current, -a 1250 A, 127 kHz, damped sine wave-, by discharging a 0.5 μ F, 25 kV capacitor through a spark-gap into a 3:1 pulse transformer. The secondary of the transformer is connected to two parallel wires, which were both connected to our test object. The length of the "Lecher"-line (1.25m) was short compared to the wave length.

The injection current was measured with a Pearson probe. Our test loop was a single turn loop placed in a fixed position as shown in Fig.3.27. The output signals were transported by RG-214 cables surrounded by an extra copper braid, connected to the RG-214 on both sides. The cables were terminated by 50 Ω and the signals were registered with a Nicolet 4094C digital oscilloscope (200 MHz max. sampling rate, 8 bit resolution) which was placed in an EMC-cabinet.

EXPERIMENTAL RESULTS AND DISCUSSION

The first tests with the setup were carried out for two simple situations, for which calculations with the formula of Biot and Savart are possible (see Fig.3.28a, "wire structure 1" and "wire structure 2") and which serve as a check on our test method. The measured mutual inductances between injection circuit and test loop of wire structure 1 and wire structure 2 are in good agreement with results obtained by the formula shown in Fig.3.29.



$$M = \frac{\mu_0}{4\pi} \int_S \int_L \left[\frac{\mathbf{r} \times d\mathbf{l}}{r^3} \right] \cdot d\mathbf{S}$$

Fig.3.29: Wire structure for which Z_{tr} follows from a Biot-Savart calculation.

These two cases show that a simple rerouting of the interference current, by a return of all leads at one side of an instrument (case2) already significantly reduces the coupling compared with the situation where interference currents flow freely into that instrument (wire structure 1, "a worst case").

Figure 3.28 shows the results of the described series of measurements for a disk and a disk with cylinder. By using a GS, - in our measurements a disk, a disk with cylinder or a strip-, we obtained large reductions of the mutual inductance. For example: a disk with a radius of 75mm as grounding structure compared with wire structure 2 gives a reduction of a factor 44. If our test loop would correspond to a loop formed by copper strips on a printed circuit board, this same reduction by a factor 44 is not easily realized by a redesign of the printed circuit board.

The magnitude of M with a disk as grounding structure, calculated with the approximate formula 3.23, deviates considerably from the measurements (see Fig.3.28a). To explain this deviation we note that the derived approximate formula is based on a two-dimensional solution for an infinite plate, while the real geometry is essentially

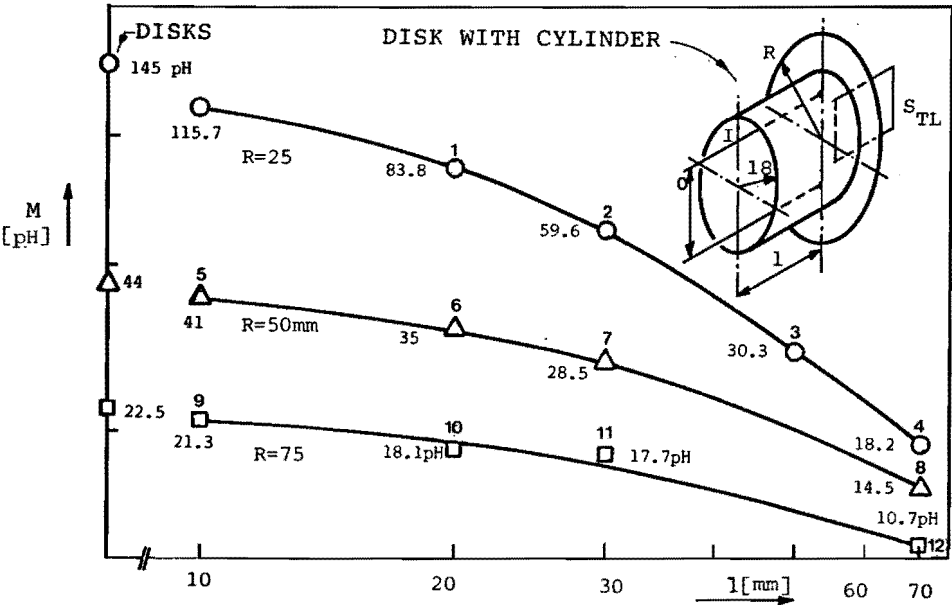
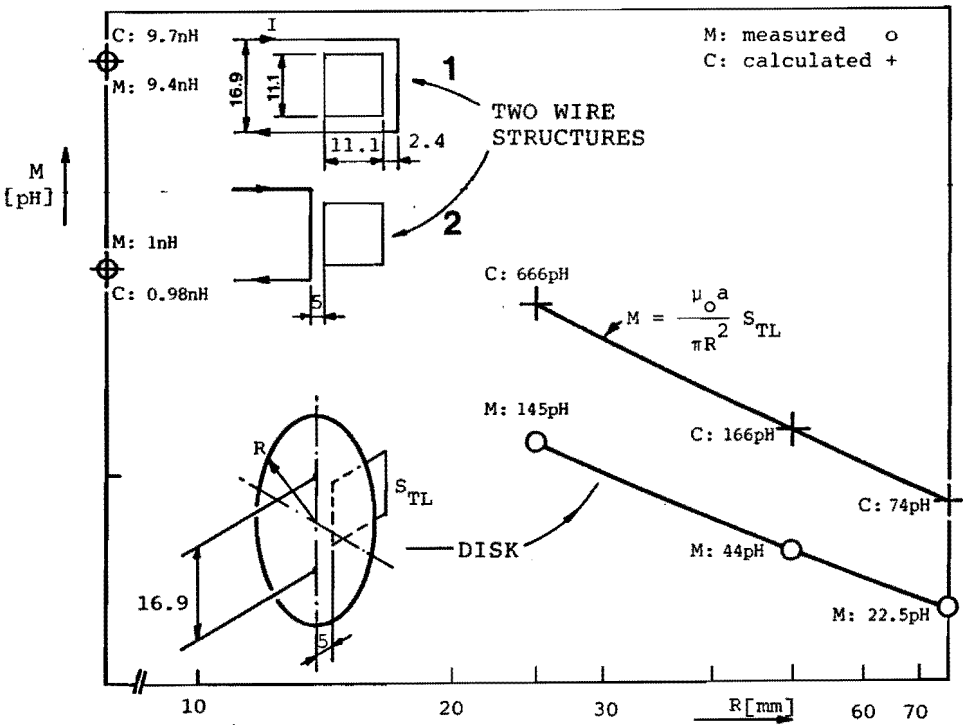


Fig. 3.28: The mutual inductance of simple grounding structures : (a) a disk, and (b) a disk with cylinder. Figure (a) also shows results for two simple wire structures (wire structure 1 and 2) where Biot-Savart calculations were possible.

three-dimensional. The bending of the H-lines around the disk implies a current density concentration at the edges of both left- and right side. This effect and the related 3D-expansion of the field lines on the right are not treated in our calculation. We expect that both will reduce the flux through the testloop (see Fig. 3.30). Clearly, Eq.3.23 is an approximation only; however it gives us a useful estimate of the dependence on the parameters.

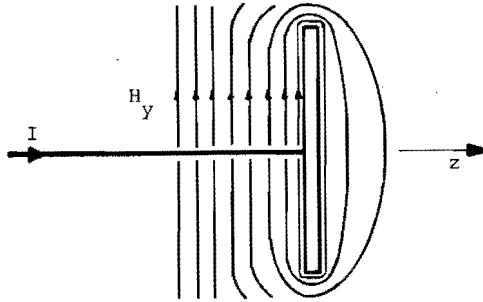


Fig. 3.30: Sketch of H-lines around a disk. The bending of the H-lines around the disk and the related 3D-expansion on the right reduce the flux through the test loop.

No analytic calculations were possible for the disk with cylinder. Figure 3.31 shows a sketch of the pattern of the current density distribution for this case. All measurements for disks with cylinder are plotted in Fig.3.32. Curve fitting of these data [Sta 87], shows an approximate $(R+1)^{-2}$ -dependence of the mutual inductance (see Fig.3.32). The effect of the cylinder can apparently be described by a virtual increase of the radius of the disk with l , the length of the cylinder.

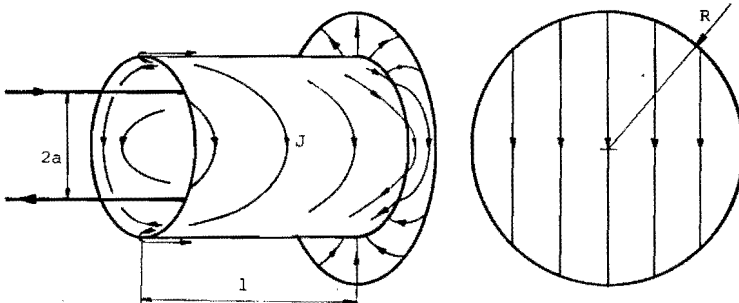


Fig. 3.31: Sketch of the current density distribution for a disk with an attached cylinder.

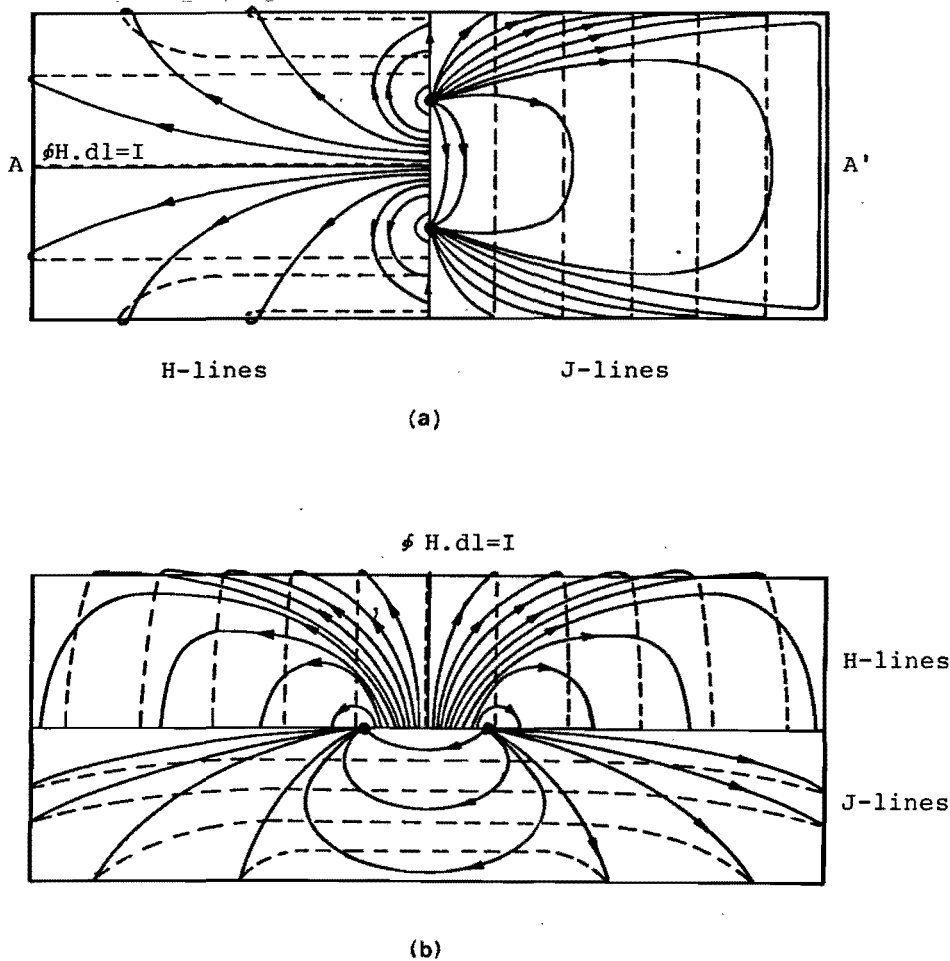


Fig 3.33: Sketch of the surface current lines and the H-field lines for a strip with (a) a vertical and (b) a horizontal connection of the injection wires. The full lines give J or H at the injection side (front); The dotted lines are at the rear.

For a disk with a radius R much larger than the distance 2a between the leads the disk itself gives already a large reduction. In this case the benefit of an attached cylinder is small. This in contrast with smaller disk ($R \approx a$); now attaching a cylinder is quite beneficial.

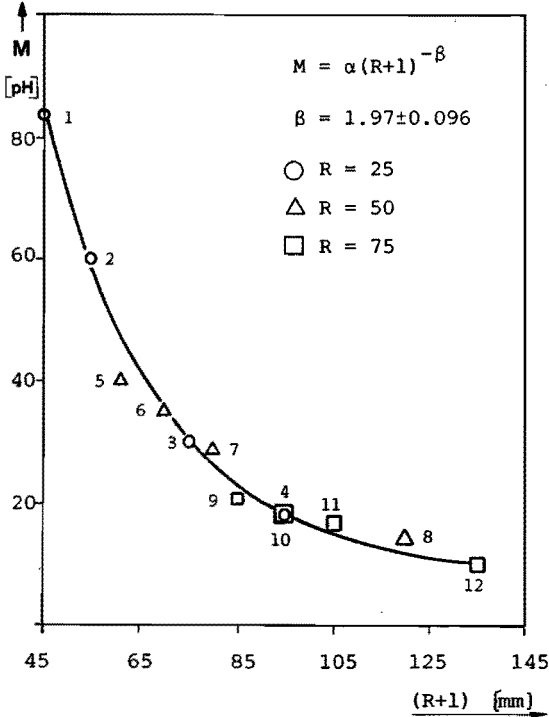


Fig.3.32: Measured mutual inductances M of all disks with a cylinder fitted to a single curve. The data points are taken from Fig.3.28 with the same numbering.

Table 3D gives the experimental results of the mutual inductance for the strips. The table also includes data for a reference disk, to illustrate the difference between the disk and a strip with a strip of the same height, for different orientations of the current injection wires. A horizontal connection of the wires gives nearly no reduction of the mutual inductance, as compared to the mutual inductance of the reference disk. Connections made vertically for the same strip give a reduction by a factor two.

No calculations have been done for these strips. Figure 3.33 gives a sketch of the current density distribution and H-lines for both cases. The sketches of the current distributions suggest two possible explanations why the

magnitude of the H-field, at the rear side, is lower for case (a) than for case (b):

1. a larger part of the total current flows at the injection side;
2. the current at the rear side flows via a wider cross-section A-A'.

Therefore the magnitude of the current density -and of the corresponding H-field- at the rear side of the wide strip is lower.

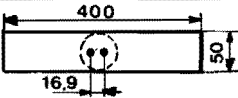



Mutual inductance measurements	strip (drawn)	disk (dashed)
	$M = \int V_{ind} dt / I_{inj}$	M
	131.15 pH	R = 25 mm M = 145 pH
	63.6 pH	
	31.7 pH	R = 50 mm M = 44 pH
	18.4 pH	

Table 3D: Column 2 gives the mutual inductance M of strips with different orientation of the current injection wires as shown in column 1. Column 3 gives the M of two comparable disks. Note that the vertically oriented wires give less coupling.

The techniques to reduce the transfer impedance of simple GS's can be applied to many practical situations on different scales e.g.:

- To a metal connector panel of an apparatus (Fig.3.32a). For protection against external CM-currents all leads which enter this panel should be correctly treated as discussed in Ch. 2, Sec. 2.6.2. Extra protection is given by a rim all around the panel, vertically oriented wires and more metal where the current density is high.
- To a central cable entry plate in a concrete floor, e.g. in a control room where many cables converge (see

Fig.3.32b). The outer cable shields which are often used for mechanical protection, should be connected all around to the entry plate. Further control of external CM-currents is achieved by an attached cylinder, by good ground connections, and by the welding of the reinforcing steel in the concrete floor together and to the central cable entry plate.

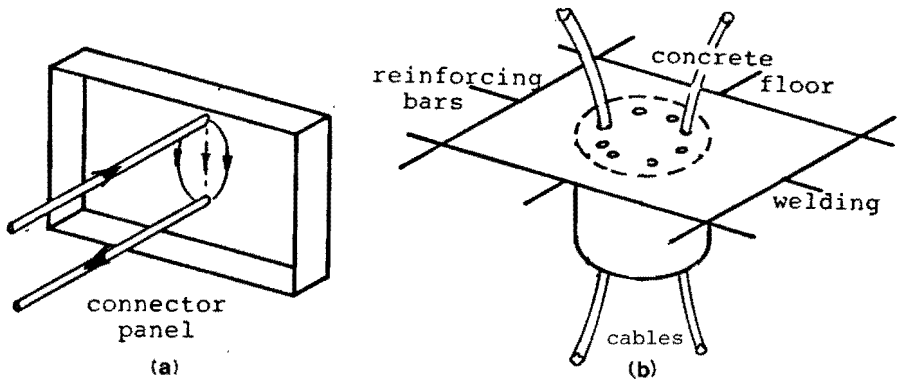


Fig. 3.32: Some GS's with a low transfer impedance: (a) a connector panel with an extra rim; (b) a central cable entry plate with cylinder for e.g. control room.

In situations with large external CM-currents and sensitive (measuring) instruments a simple GS can be extended to an EMC-cabinet as discussed in Ch.2, Sec 2.6.2. In this chapter, an EMC-cabinet was used in the two setups for measuring the transfer impedance (see Fig.3.12 and Fig.3.27). These measurements of very small quantities (picoHenries as shown in Fig. 3.28), only make sense when we measure interference-free. To obtain measurements as shown in Fig.3.13, the EMC-cabinet was highly essential. Similar EMC-cabinets, in combination with a D/I-measuring systems (Ch.4 and 5), were designed and used to measure transient voltages in HV-substations [Hee 87, Hee 89] and in H.V.-lab experiments [Zha 89].

The front of the EMC-cabinet can often stay open, if the distance between interference source and EMC-cabinet is sufficiently large, especially if the EMC-cabinet is located in a next door control room. A correct handling of

the interference currents at the points where the leads come in, is more important than the small remaining shielding currents near the open front. In these examples the useful EMC and signal transport properties of a D/I-measuring system -the possibility of signal transport over a long distance by a correctly terminated cable- are important as will be discussed in Ch.4.

In cases where the EMC-cabinet has to be located close to an intense HF-interference source (see Ch.5, Fig.5.17) the door of the EMC-cabinet must be closed to give the needed shielding against HF-interference. Examples of interference free recorded voltage waveforms are given in Ch.5, Fig.5.20 and Fig.5.21.

CHAPTER 4

ELECTROMAGNETIC COMPATIBILITY ASPECTS OF A DIFFERENTIATING/INTEGRATING MEASURING SYSTEM

As mentioned in section 2.6.2, an EMC attractive solution for wideband signal transport is the use of differentiated signals. The differentiated signal should be integrated again at the input of the electronic equipment.

This chapter deals with the design and testing of a high-voltage divider -based on the principle of consecutive differentiation and integration- for measuring fast rising high-voltage transients. An important advantage of such a system is that a long measuring cable between the high-voltage and the measuring area can be included in the system without matching difficulties [Wol 83]. Due attention will be paid to the EMC-aspects of this measuring system.

The designed D/I-system has among others been used for transient voltage measurements in a 150/10kV GIS-substation, as reported in chapter 5.

4.1 HIGH-VOLTAGE DIVIDERS

Most HV-dividers consist of two or more similar impedance elements to achieve -at least to a first approximation- a frequency independent dividing ratio. The divider can be resistive, capacitive or mixed resistive/capacitive (see Fig.4.1).

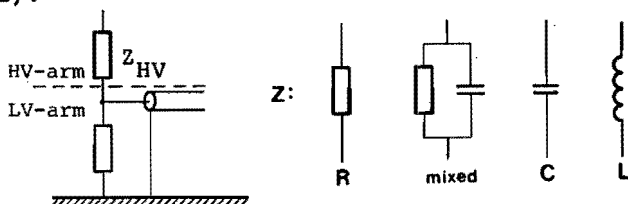


Fig. 4.1: A HV-divider; the HV-arm and the LV-arm mostly consist of two similar impedance elements. Of the three possible elements a capacitor is to be preferred because of its HF-qualities and linearity.

A HV-divider consists of a high-voltage arm and a low-voltage arm.

The ~~high-voltage arm~~ of the divider is generally large in size and therefore tends to have appreciable parasitic capacitances and inductances. When a number of HV-components is used in series the parasitic impedances make it increasingly difficult to obtain a correct frequency response. These problems are largely avoided if the HV-arm of the divider consists of one single capacitor [Wol 81] since this can result in a rather pure capacitive impedance. Such a capacitance can be a compressed gas capacitor [Sch 72] or can be formed by a sensor electrode at some distance of a HV-object [Wol 81]. Gas insulated switchgear installations (GIS, see Ch.5) have a favorable geometry for the installation of capacitive sensors inside the GIS [Hee 89].

The ~~low-voltage arm~~ of the divider can be a fairly large capacitance (see Fig.4.2a), which together with the high-voltage capacitor forms a capacitive divider.

The problems, associated with the use of undamped capacitive dividers can be summarized as follows:

(a) Natural frequencies of the low-voltage arm.

Special care has to be taken to ensure a very low inductance of the low-voltage arm. Usually special capacitors [Har 79] or a number of capacitors in parallel [Sch 71] are employed.

(b) Travelling wave oscillations on the transmission line between the high- and the low-voltage arm.

This transmission line can be long when a compressed gas capacitor is used [Sch 72].

(c) The matching of the signal cable which cannot be properly terminated with its characteristic impedance.

To prevent multiple reflections a series resistor is often employed. For long cables, the use of a buffer amplifier between divider and cable is a solution for correct signal transport to the measuring equipment; this solution is not attractive from EMC point of view.

(d) The signal to interference ratio.

To ensure a sufficient signal to interference ratio we can use a cable with a solid outer conductor, or transport signals with a large amplitude. If signals of high amplitude are transported a high-quality input attenuator is required at the receiving end (as discussed in sec.2.6.2).

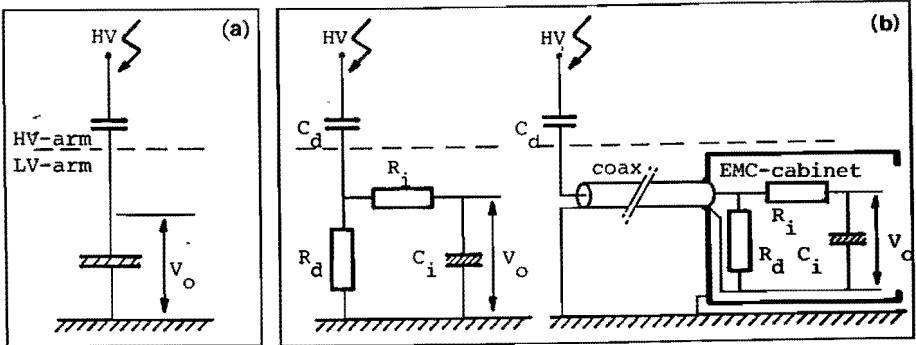


Fig. 4.2: (a) a capacitive divider and (b) A D/I-measuring system. The integrator capacitors are shaded.

An alternative design of the low-voltage arm is to use a low value resistor R_d (in fact a long characteristically terminated measuring cable) connected to a high-ohmic resistor R_i in series with a capacitor C_i (see Fig 4.2b). The output signal of the divider is the voltage across capacitor C_i . The small HV-capacitor C_d at the input of the cable and the cable impedance R_d act as a differentiator ($\tau_d = C_d R_d$) of the high-voltage. The resistor R_i in combination with C_i act as an integrator ($\tau_i = R_i C_i$). The total attenuation of the signal is given by τ_d / τ_i ; this can be adapted to the requirements by a proper choice of C_d or τ_i . This divider is called a differentiating/integrating measuring (D/I) system.

The advantages of this D/I-system are:

- (a) as explained in Ch.2 general purpose digital oscilloscopes can be used. The use of an EMC-cabinet is essential.
- (b) the components of the low-voltage arm can be of normal size as used in electronics; because no exceptionally

large or small values are needed in this arm quite pure impedances are possible. As already mentioned the differentiating R_d can be a long terminated cable. The integration capacitor C_i can be a feedthrough capacitor with excellent HF-properties.

- (c) the system presents a negligible load to the HV-source; often quite small values of C_d are possible
- (d) the system has a wide frequency response, and can also be adapted to widely different requirements.
- (e) the system is highly insensitive to interference; normal coaxial cables are suitable for signal transport. If necessary active integrators can be used.
- (f) the system is easy to install and does not require any optical fibers or isolation between "grounds" and is cheap.

The principle of consecutive differentiation and integration has been used in the past for fast pulse measurements in plasma physics experiments [Kel 64]. At the Eindhoven University of Technology (EUT), Wolzak applied this principle for DC, AC and impulse voltage measurements in HV-installations [Wol 81, Wol 83]. Further investigations have been done at the EUT by Van Heesch [Hee 87, Hee 89] and Zhang [Zha 89]. In the following two sections we describe the design of a D/I-system with a step response of less than 1ns and discuss the EMC-aspects of this measuring system.

4.2 D/I-SYSTEM FOR FAST RISING VOLTAGE TRANSIENTS

The described measuring system in combination with a Tektronix digitizer 7912AD (50 Ω plugin-unit 7A29) has an overall risetime of 0.6ns (see Fig.4.13), which corresponds to a bandwidth of 580 MHz.

In this section we deal with the design necessary to reduce the risetime and the technical realisation of the measuring system. Most step response measurements presented have been carried out by means of a mercury-wetted reed-relay pulse generator.

PRINCIPLE

A idealized circuit diagram of the measuring system is given in Fig.4.3. The high voltage capacitor is presented by C_d ; in addition a capacitance C_{ps} of the sensor to ground is shown. If $R_i \gg R_d$ the following equations can be derived:

$$V_d = R_d C_d \frac{d}{dt} V_H \quad (4.1)$$

$$V_o = \frac{1}{R_i C_i} \int_0^t V_d(\tau) d\tau = \frac{R_d C_d}{R_i C_i} V_H \quad (4.2)$$

Equations (4.1) and (4.2) are valid for the frequency range:

$$\frac{1}{R_i C_i} \ll \omega \ll \frac{1}{R_d (C_d + C_{ps})} \quad (4.3)$$

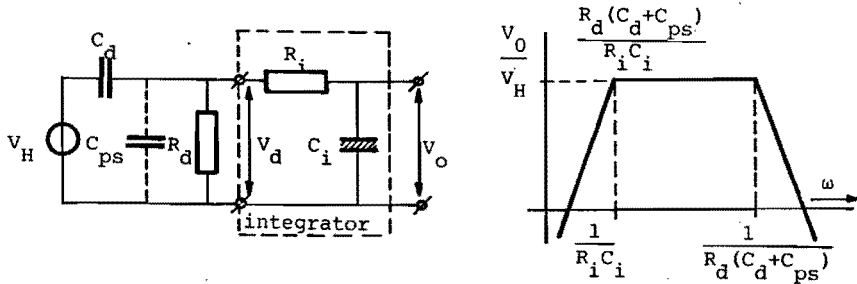


Fig. 4.3: Diagram of a D/I HV-measuring system.

HIGH FREQUENCY PROBLEMS

To measure fast rising voltage transients (FRVT) with rise times of about 1 ns correctly, imperfections of the measuring system have to be carefully checked. In Fig.4.4 a circuit diagram of the measuring system is given with relevant imperfections represented by lumped parasitic impedances.

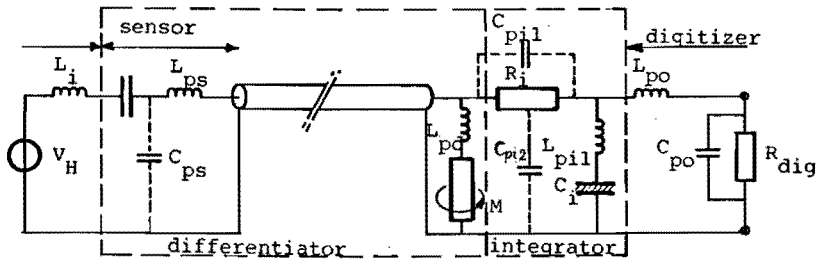


Fig. 4.4: Diagram of the D/I-measuring system including parasitic impedances important for fast measurements.

At high frequencies the response is primarily affected by:

- the capacitance C_{p11} across integrator resistor R_i
- the inductance L_{p11} in series with capacitor C_i
- the inductance L_{pd} in series with resistor R_d
- the mutual inductance M between the differentiating and integrating circuit.

At very high frequencies also the following impedances contribute to the distortion of the signal:

- the inductance L_{ps} of the sensor and its capacitance C_{ps} to ground
- the coaxial cable
- the capacitance C_{p12} between R_i and "ground"
- the connection of the measuring system to the oscilloscope represented by L_{po} and C_{po} .

The parasitic impedances C_{ps} , L_{ps} and C_{p12} represented by lumped impedances are in fact not localized but distributed.

All above contributions can be minimized or compensated by a correct choice of components and a proper layout of the measuring system. Apart from the measuring system and oscilloscope a fundamental bandwidth limitation is formed by the geometry of the input circuit. A more detailed discussion of the various effects leading to distortion is given below.

INPUT CIRCUIT

Especially in high voltage measurements, where voltmeter leads are usually long, the question: "which voltage are we measuring" shows up as a common problem which always has to be faced. To solve this problem three questions should be answered:

1. which voltage do we want to know?
2. which voltage can we measure?
3. what is the input circuit?

As an example, a typical HV-measuring problem with long voltmeter leads is shown in Fig.4.5. In this example a HV-source is situated in a metal walled HV-laboratory. A voltage of interest (e.g. interesting for flashovers to the

wall) could be the voltage V_s between the HV-electrode and the metal wall via the shortest distance ($V_s = \int_2^1 \mathbf{E} \cdot d\mathbf{l}$). This voltage can be measured with a capacitive sensor of a D/I-system. The registered voltage V_{reg} is proportional to V_s . This voltage measurement is correct because the input circuit encloses no extra magnetic flux (Fig.4.5b). But when we are interested in the voltage V_H of the HV-source ($V_H = \int_4^3 \mathbf{E} \cdot d\mathbf{l}$) and we use the same setup of Fig.4.5, we of course still register the same voltage proportional to V_s . In this situation the input circuit is very important. To obtain V_H , the time derivative of the distributed flux in the loop 1-3-4-6-1 should be taken into account.

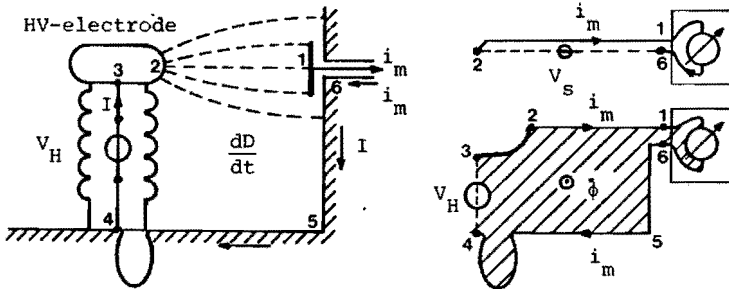


Fig. 4.5: HV-source located in a metal walled HV-lab. The input circuit of the measuring system could be extremely large especially in installations with single point grounding.

Another example is the measurement of transient voltages in a GIS-installation (Fig.4.6). Installation of a sensor in the outer conductor is easy. The registered voltage is again proportional to the local V_s , which is independent of the azimuthal angle θ (see Fig.4.6b), because there is no magnetic flux in the z-direction. In case of a radial breakdown between the central and the outer conductor the local voltage $\int_1^2 \mathbf{E} \cdot d\mathbf{r}$ is a function of θ .

A correct description of the input circuit is extremely important in physics experiments as discussed in the papers [Wet 88] and [Dan 88]. In these papers the current paths are identified and the input circuits are constructed as compactly as possible. Also in the measurements

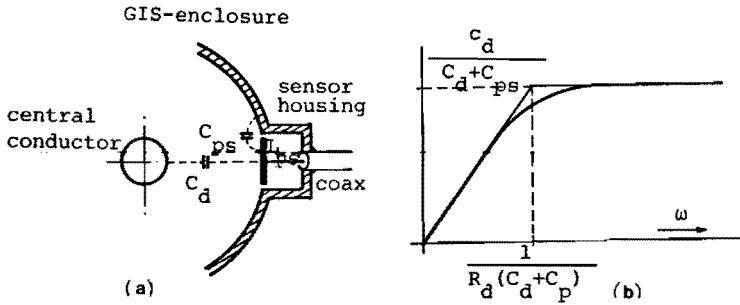


Fig. 4.7: (a) Sensor built in a GIS. For a correct step response the C_{ps} and L_{ps} are tuned. (b) The frequency characteristic.

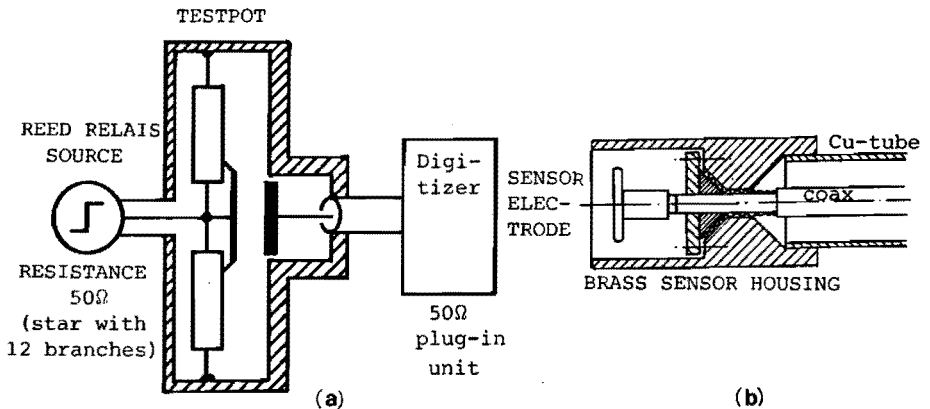


Fig. 4.8: (a) Setup for step response measurements with mercury-wetted reed-relay pulse generator. (b) Sensor as used in Ch.5.

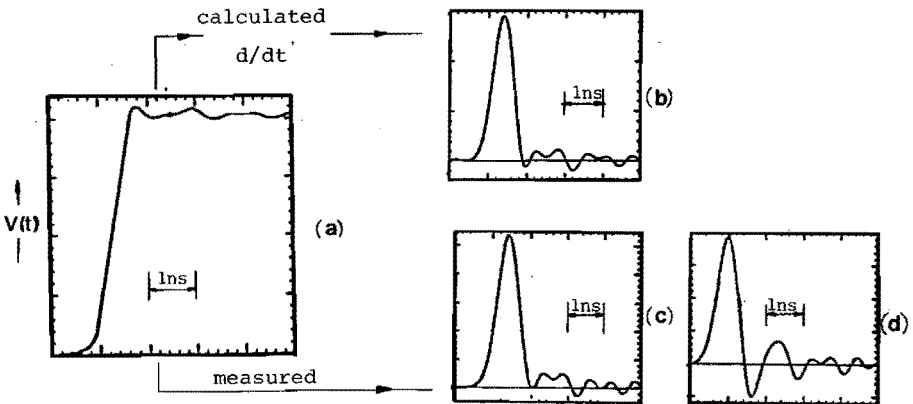


Fig. 4.9: (a) Input pulse generated by a vibrating reed relay (b) numerically differentiated signal a) (c) measured signal, L_{ps} and C_{ps} near the sensor correctly tuned (d) as c, but with a too large L .

discussed in Ch.5 (5.1.2, also Fig.5.18) the input circuit is extremely important.

Note that the inner conductor of a GIS is not an equipotential during fast transients (see also discussion in Ch.2.2).

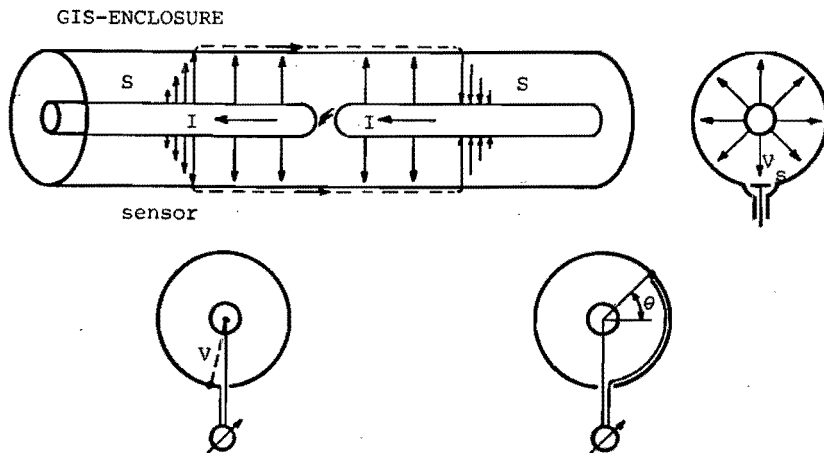


Fig.4.6: Measurement of voltage V in a GIS. The registered voltage is proportional to V_s , and is independent of θ .

SENSOR ELECTRODE

Two problems associated with the sensor electrode are:

- the coupling of the HV-circuit to the sensor which can be described by capacitors, provided the wavelength remains long compared to all dimensions;
- the transition from sensor to measuring cable.

A possible solution for the sensor to cable transition is a conical matching transition (see e.g. [Tas 86]).

An alternative approach is (see Fig.4.7):

- continue the coaxial cable -a correct TEM structure- as close as possible to the sensor electrode. The cable sheath should be circumferentially connected to the sensor housing.
- the small sensor electrode should be located in a compact housing; tuning of the stray capacitance C_{ps} and the (small) inductance L_{ps} makes it possible to obtain a linear response of the sensor up to high frequencies.

With the step response setup shown in Fig.4.8a we have tuned small sensors. Figure 4.8b shows the sensor used in a

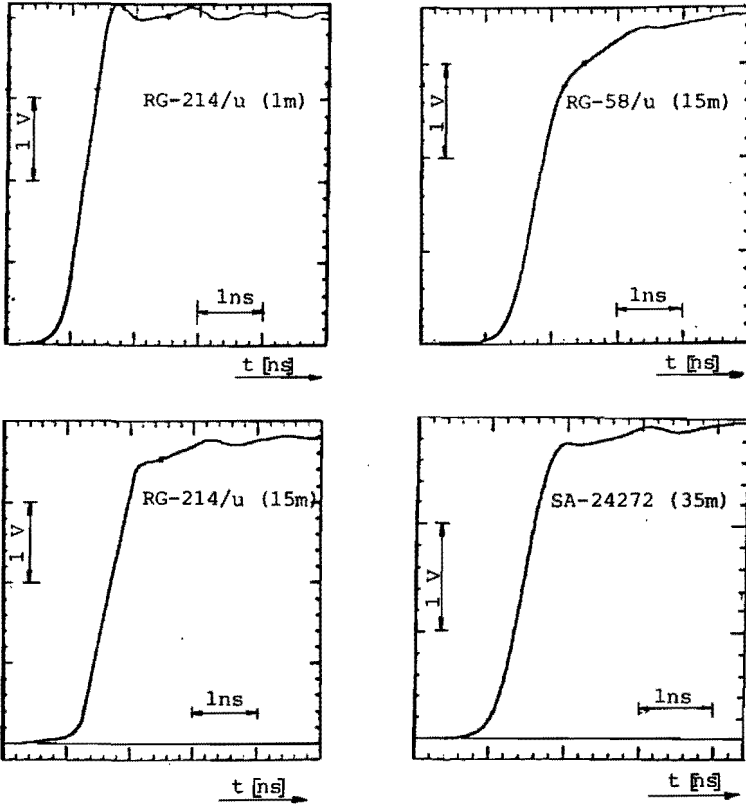


Fig. 4.10: Cable responses of the RG 58/u, the RG 214/u and the SA 24272.

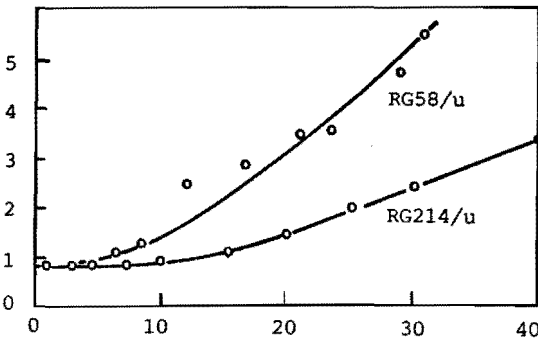


Fig. 4.11: Risetime (ns) versus cable length of the RG 58/u and the RG 214/u.

150 kV GIS-substation (Ch.5.1.2). In Fig.4.9 measured and calculated step responses are shown.

COAXIAL CABLE

To a first approximation the cable is a perfect part of the measuring system. Due to the skin effect, mainly in the central conductor, also the 50 Ω coaxial cable presents a bandwidth limitation (see for example [Nah 73]). This effect has been investigated by step response measurements for different types and different lengths of cable [Lat 88]. An increase of the rise time caused by the cable can be prevented by the choice of the type of cable, and by a reduction of the cable length. Figure 4.10 shows the step response of a number of cables and Fig.4.11 gives a graph of the 10-90% risetimes vs. cable length for two different cable types. The SA 24272 has also been used by [Mep 87]. Concerning the transfer impedance of the coaxial cable we refer to chapter 3, Fig.3.1.

FIFTY-OHM TERMINATION RESISTOR

The 50-Ohm termination resistor is designed to withstand high transients and is located in the same cylindrical housing as the integrator (Fig.4.12). We used carbon composite 2W-resistors surrounded by shrink sleeve insulation to avoid flashover across the outer resistor surface. The resistors are compactly assembled in a star configuration (three branches of 150 Ω resistors), to obtain a low self induction (loop 1-2-3-4-1) and a low mutual inductance between the differentiating circuit and the integrating circuit. The termination resistor is tested in combination with the passive integrator (see Fig.4.14).

FAST PASSIVE INTEGRATOR

The integrator is designed to recover the very fast changing signals which come out of the differentiating circuit. The fast passive integrator, built from normal sized components, should overcome two problems encountered with simple RC integrators:

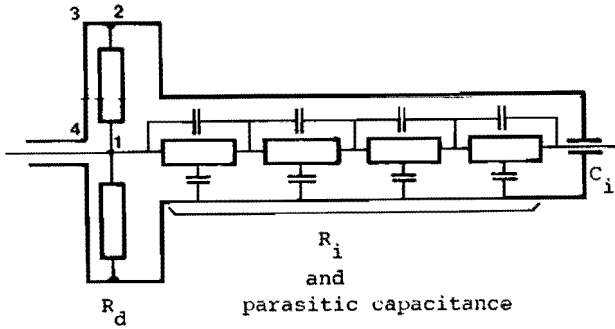


Fig 4.12: Fast passive integrator consisting of discrete components, together with the termination resistor located in a cylindrical housing.

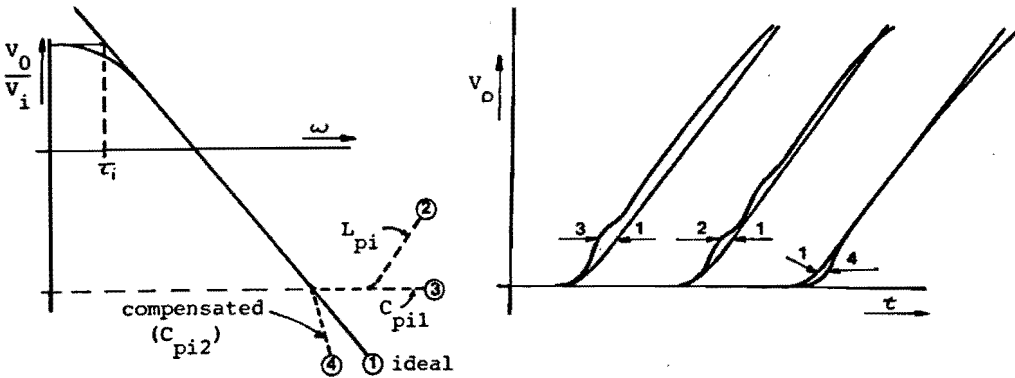


Fig. 4.13: Frequency response with possible parasitic effects and corresponding step response.

- 1: ideal slope (-1)
- 2: too much L_{pi} , a feedthrough helps
- 3: too much C_{pi1}
- 4: compensation by C_{pi2} .

The step response has been used experimentally to optimize the design.

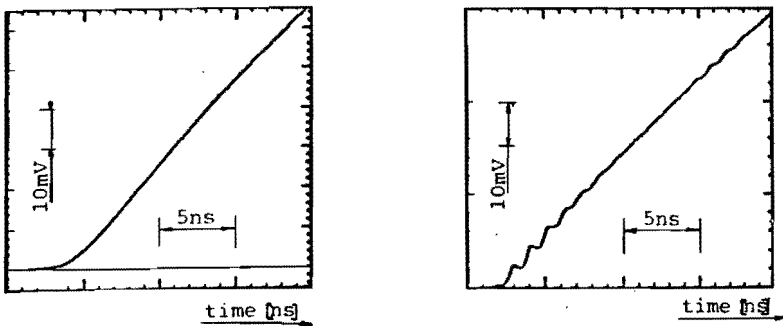


Fig. 4.14: Measured step responses.

- 1) the parasitic capacitance across the integrating resistor causes the output to overshoot for a fast rising input
- 2) the integrating capacitor may resonate because of its inductance.

A simple solution for the integrating capacitor is a feed-through capacitor. This capacitor has almost no additional inductance and has therefore good HF-qualities.

The parasitic capacitance across the integrating resistor may be minimized by the connection of several resistors in series. Experimentally we have found that a resistor R_i consisting of ten resistors in series, starting at R_d from large to small (namely: $1 \times 330\Omega$, $4 \times 100\Omega$, $4 \times 68\Omega$, and $1 \times 10\Omega$, with short interconnections) gives good results. Computations with a circuit analysis program also shows an improvement in bandwidth when R_i is built up from large to small resistors in combination with the parasitic capacitances [Lat 88].

The overshoot effect can be compensated with the stray capacitance to the cylindrical housing (copper tube). Experimentally we have found a optimal size of the tube for the desired step response of the integrator. All loops in the integrating circuit have very high resonant frequencies and are damped. In Fig.4.13 the frequency characteristic is shown as expected for various parasitic effects. Corresponding step responses are also shown in Fig.4.13.

Step response measurements have been carried out with a mercury-wetted reed-relay pulse generator and with a Tektronix 7912 AD digitizer. The 7A29 pre amp (a 50Ω plug in unit) is used to exploit the rise time capabilities (600 MHz analog bandwidth) of this pre amp. Termination of the integrator by the 50Ω input impedance results in a considerable reduction of the measuring time ($\tau=50\text{ns}$). For our purpose this is not important since we are interested in short rise time effects. Some of these step response measurements are plotted in Fig.4.14.

Notes:

-As explained in Ch.2 an EMC cabinet (Fig.2.19) is an essential part of this measuring system. The integrator should be well bonded to the rear panel. The connection between integrator and digitizer could be a coaxial cable terminated at the 50Ω plug-in unit. When a 1MΩ plug-in unit is used this connection must be as short as possible to avoid reflections. In this case the integrator may be installed in the EMC-cabinet as depicted in Fig.2.20a. Another possibility is to terminate the integrator with a buffer amplifier. The connection between buffer amplifier and digitizer can again be a coaxial cable. The buffer amplifier must be of very high HF-quality.

-An earlier publications on fast passive integrators is [Kel 64]. A more recent publication [Ral 84] gives step responses of an integrator less linear than Fig.4.14.

STEP RESPONSE OF THE MEASURING SYSTEM

The overall step response of the measuring system together with the Tektronix (7A29 pre amp) is plotted in Fig.4.15. The overall rise time obtained is 0.6 ns, which corresponds to a bandwidth of 580 MHz.

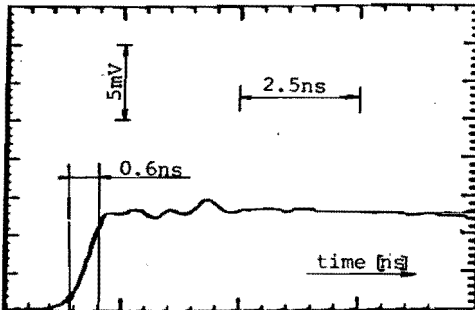


Fig.4.15: Step response of the D/I-measuring system.

After the measurement with the mercury-wetted reed-relay pulse generator, fast rising voltage transients were measured with the EHO-GIS-installation as pulse source. The advantage of this setup is that the measuring system is being tested at more realistic voltages and interference levels. A measuring setup of high EMC-quality -as applied in Ch.5.1.2 (Fig.5.16)- is necessary for this measurement.

Figure 4.16 shows the GIS installation and in Fig.4.17 a measured voltage front is plotted. This steep pulse is generated by the spontaneous breakdown of the over-volted spark gap 2 (see Fig.17) with a 4 bar SF₆ gas filing. The very large rate of voltage , 185 kV in 3 ns, was easily

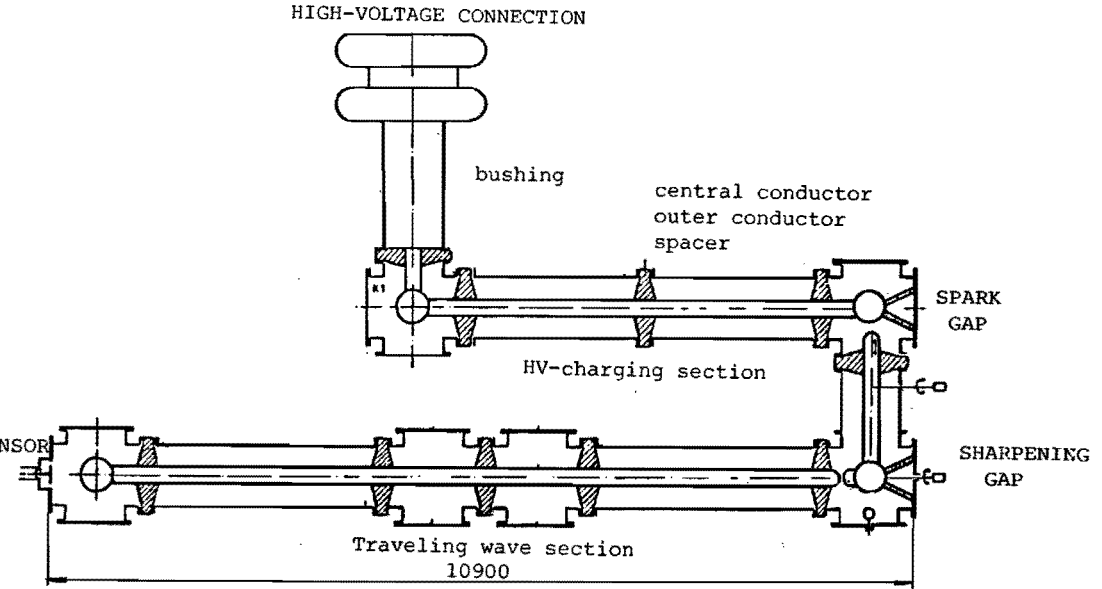


Fig.4.16: EHO-GIS-installation

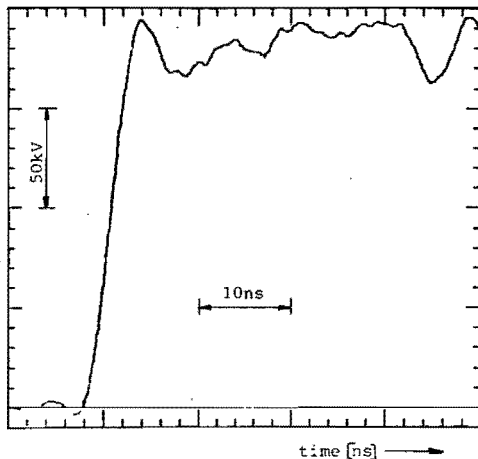


Fig. 4.17: Response measurement EHO-GIS-setup

measured with the D/I-system. Similare measurements have been done by Boggs [Bog 84], who used a special capacitive divider, and registered a rate of rise of 80 kV in 5 ns. Since we are comparing fast voltage dividing systems, the highest dV/dt which can be measured, could be considered an estimate of the quality of the system. Extra advantages of the D/I-system are: the absence of matching problems, the EMC-qualities, and the easy adaptation of the total attenuation, in case very large source voltages are to be measured.

The sensitivity of the measuring system depends on the precise capacitance between the sensor electrode and the central conductor. For this reason, calibration should be carried out on the installed sensor. In a substation the 50Hz high voltage can be used for this calibration, which is correct if the sensitivity is known to be constant for the frequency range of interest.

4.3 ADDITIONAL EMC-ASPECTS OF THE D/I-MEASURING SYSTEM

A D/I-system for measuring fast rising voltage transients, as described in Sec.4.2, is suitable for DM-signal transport without matching problems for the connecting signal cable. An EMC-cabinet creates a protected region for the registration equipment and the integrated signal, and

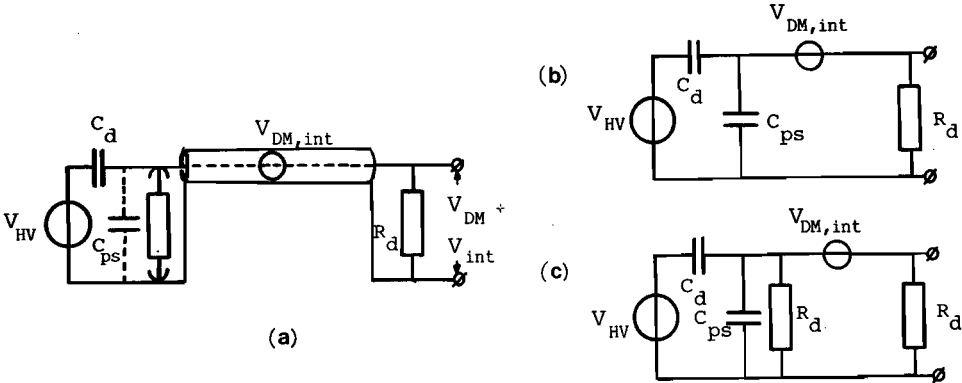


Fig.4.18: (a) The DM-interference represented by a series-voltage. (b) Equivalent diagram of the D/I-system terminated at the integrator side and (c) at both ends of the measuring cable.

gives excellent protection against the CM-currents which flow towards the EMC-cabinet. Since the cables for signal transport have sizeable transfer impedances, DM-interference may already leak into these cables before they enter the EMC-cabinet. For cables shorter than a quarter wave-length of the interference signal, the DM-interference can be represented by one lumped series voltage source $V_{DM, int}$, where $V_{DM, int}$ equals the product of the transfer impedance of the cable and the CM-current (see Fig.4.18a).

Dependent on the termination of the DM-circuit, an interference voltage V_{int} then appears at the input of the integrator. For a D/I-system, the measuring cable can be terminated only at the integrator side of the cable or at both sides of the cable without bad effects for the "legal" DM-signal. The advantage of termination at both sides of the cable is that in situations with imperfect termination resistors multiple reflections are reduced and the bandwidth is enlarged.

From an EMC-viewpoint, however, termination at both sides is disadvantageous. The signal to interference ratio at the integrator input with termination of the cable at one side and at both sides are, respectively (see Fig.18b,c):

$$\left(\frac{V_{DM}}{V_{int}} \right)_{\text{single side}} = \frac{C_d}{C_s + C_{ps}} \cdot \frac{V_{HV}}{V_{DM, int}}, \quad (4.4)$$

and

$$\left(\frac{V_{DM}}{V_{int}} \right)_{\text{both sides}} = \frac{j\omega R_d C_d}{1 + j\omega R_d (C_d + C_{ps})} \cdot \frac{V_{HV}}{V_{DM, int}} \quad (4.5)$$

For the frequency range $\omega \ll 1/R_d(C_d + C_{ps})$ -see also Eq.4.3- Eq.4.5 becomes:

$$\left(\frac{V_{DM}}{V_{int}} \right)_{\text{both sides}} = j\omega R_d C_d \cdot \frac{V_{HV}}{V_{DM, int}} \quad (4.6)$$

Comparison of Eq.4.4 with Eq.4.6 shows that the signal/interference-ratio for cables terminated at one side is $1/(\omega R_d(C_d + C_{ps}))$ times better than for a cable terminated at both ends. Since in the frequency range of interest $\omega R_d(C_d + C_{ps})$ is small compared to one, we prefer single-sided termination with a good quality termination

resistor, as discussed in Sec.4.2. Recent calculations by Van Deursen [Deu 90] give a correction to Eq.4.4; in the denominator a term $C_c/2$ has to be added to $C_d + C_{ps}$, where C_c is the capacitance of the length of cable used.

In situations with very high frequency signals or interference the Eqs.4.4-4.6 should be modified because of traveling waves on the cable and the effect of the capacitors C_d and C_{ps} . Appropriate EMC-measures are then:

In case of very high frequency interference the passive integrator can be of the compensated type (Fig.4.13) to prevent the interference to reach the active electronics.

In case both the signal and the interference contain very high frequencies the transfer impedance -and if possible the length- of the connecting cable should be reduced. High quality cables or metal conduits or cables can effectively reduce the transfer impedance (see e.g. Fig.3.21 and Fig.5.16).

CHAPTER 5

ELECTROMAGNETIC COMPATIBILITY IN GIS SUBSTATIONS

5.0 INTRODUCTION

Introduction of digital electronics in HV-substations gives access to all advantages of fast data acquisition for measurements and on-line control of substations. However, due to intense EM-interference, caused by switching at the high voltages, most of the normal digital equipment will not function properly in HV-substations, or will even be destroyed.

The HV-grid connects a (large) number of power stations and consumer areas through a meshed network. At the nodes of this network the HV-substations are situated. A HV-substation controls power flow and distributes the electric energy to the consumers. Incoming and outgoing circuits are connected to the HV-rail system via circuit-breakers, disconnect switches and transformers (the primary system).

There are two types of HV-substations:

-an open substation: The HV-rail system and the switch gear are located in the open air, installed on vertical insulating supports;

-a closed substation or GIS-substation (Gas Insulated Switch gear): The HV-rail system and switch gear, supported by insulating spacers, are housed in closed cylindrical metal vessels (see Fig.5.1). The vessels are grounded and filled with pressurized gas (e.g. SF₆-gas). Single phase as well as three-phase enclosed systems are possible.

Advantages of a GIS-substation compared to an open one are: it is compact and saves space; it protects the primary system against industrial pollution, rain, snow, and salt deposition and it is easily accessible for maintenance work.

From an EMC-viewpoint, however, a GIS-installation is a concentrated source of HF-interference for the secondary system (the system for measurement and control). The

secondary system is in many places quite close to the primary system: e.g. in current and voltage transformers; disconnect switch drives; sensors for pressure and temperature and position indicators. In this chapter we study the resulting problems, where source and victim are the primary and the secondary system.

Examples of measuring systems protected by the use of the concepts of Ch.2, are presented in [Hee 87] and [Hee 89]. These publications describe new wide-band current and voltage measuring systems tested in 150 kV and 400 kV GIS-substations. The measuring systems are based on the differentiating/integrating measuring principle (see Ch.4). Analog integrators and digital apparatus are used for signal recovery and recording, respectively.

A similar system has been used for measurements on fast rising high-voltage transients in the 150 kV GIS-substation Eindhoven-West. The system as well as the measurements are described in Sec.5.1.2 of this chapter. During many tests in substations as well as in the TUE H.V. lab, the systems have operated correctly and have shown their excellent EMC qualities.

These examples and the applications in Sec.2.8 show, that protection of electronic systems with our basic solution (see Fig.2.22a) is straightforward and generally usable whatever the interference levels are. In contrast to the "open" interference sources in Sec.2.8, -a lightning discharge and switching actions in a primary circuit of a HV-installation-, in a GIS-substation modifications are possible to contain the HF-interference.

The present chapter considers the GIS installation as a source of HF-interference. Measurements of steep transient voltages across interruptions in a GIS installation due to switching actions are presented and modifications for reduction of HF-interference are discussed.

5.1 GIS INSTALLATION AS A HF-INTERFERENCE SOURCE

A lot of locally stored capacitive energy ($\frac{1}{2}CV^2$) is present in GIS installations. During switching actions with circuit-breakers, disconnect switches and grounding switches this energy is partially converted into high power electromagnetic waves with fast rise times of less than 5 ns. These high power waves (V^2/Z_0) propagate almost loss-free in the coaxial arrangement which may have a characteristic impedance Z_0 of about 75 Ω .

No EM-waves escape from the GIS-installation when the outer conductors of the GIS enclosure and the HV-cable form one completely closed conductor (Fig.5.1). Of course it is assumed here that there are only cables connected to the GIS: a connection to an overhead line (via a high-voltage bushing) gives a quite open structure.

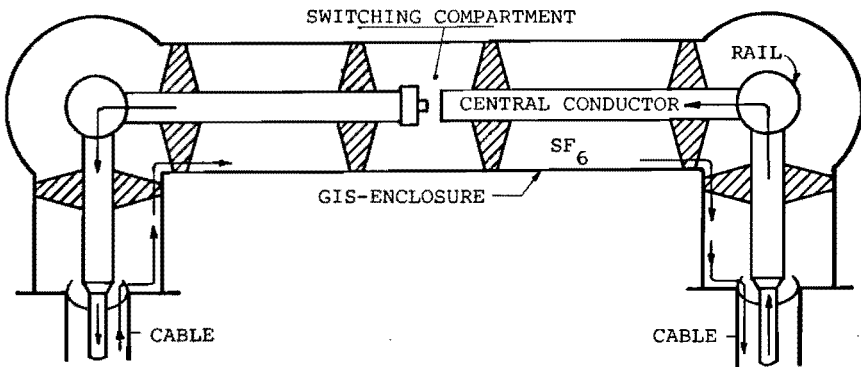


Fig. 5.1: GIS with connected cables.

Inside of a coaxial system as in Fig.5.1 the em-waves are reflected many times. The dissipation mainly takes place in the HV-cable (in Eindhoven West this cable is a cross-linked polyethylene cable with a Z_0 of about 30 Ω). The desirable reduction of the HF-waves in these HV-cables is mainly caused by semi-conducting layers on both sides of the insulation of the central conductor [Wol 83]. These semi-conducting layers are meant to smooth out local field

enhancements caused by sharp points on the metal conductors, but also serve an important EMC-purpose in suppressing high-frequency transients. If, however, there are interruptions in the GIS enclosure the HF-waves can escape freely to the outside of the installation. The resulting voltages over interruptions and between other grounded metal construction parts may lead to breakdown, sometimes within very short times, less than 1 ns (see Fig.5.20). The corresponding, very large, undesirable dV/dt 's and dI/dt 's (10^{12} - 10^{14} V/s and 10^{10} - 10^{12} A/s, resp.) can be responsible for interference in the secondary system. Moreover, the low energy HF-sparking could cause degradation of the insulation and is psychologically unacceptable for personnel in a substation.

Interruptions are present where:

- overhead transmission lines are connected to GIS terminations (bushings);
- HV-cables are connected to GIS terminations; we distinguish:
 - a) the cable sheath is isolated from the GIS enclosure by means of insulating flanges to allow cathodic protection of the cable sheath with a small DC voltage [FUJ 88].
 - b) the cable outer conductor is interrupted to permit current measurements; this situation is discussed in detail in Sec.5.1.2;
- Sections of GIS-enclosure are insulated from each other (Sec.5.1.1).

In the following we discuss proposals to improve the EMC behavior of the GIS installation, which still satisfy the other design criteria. We will distinguish between necessary and unnecessary interruptions.

5.1.1 UNNECESSARY INTERRUPTIONS IN A GIS-INSTALLATION

In some single phase enclosed GIS-installations, sections of the enclosure are electrically insulated with respect to each other and are grounded per section at one single point which is connected to the grounding mesh of the

substation (see Fig.5.2). In these installations the 50Hz HV-circuit consists of the three high-voltage central conductors; the grounding mesh carries currents during fault conditions only. It is (naively) assumed that no 50Hz-current will flow in the metal enclosure, which would mean that the enclosure does not contribute to the total dissipation of the GIS. However, even for 50Hz, induced eddy currents flow at the inside surface and, in the opposite direction, at the outside surface of the enclosure (see Fig.5.2).

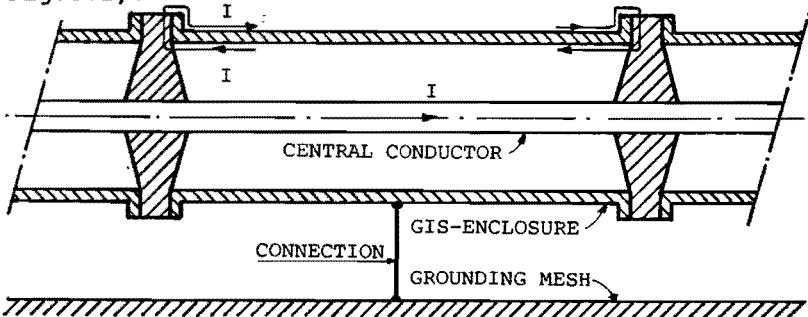


Fig. 5.2: Enclosure of a GIS grounded at a single point section. Induced 50 Hz currents flow in opposite directions at the inside and outside surfaces of the enclosure.

From an EMC point of view it is advisable to make full metallic contact all around between adjacent sections of the enclosure. In this manner, we avoid the escape of HF-waves via the transitions. The dissipation in the enclosure per single phase, because of induced 50Hz-currents, depends on the interconnection of the three single phase enclosures at the ends of the GIS (see Fig.5.3). When these connections are made with wide metal

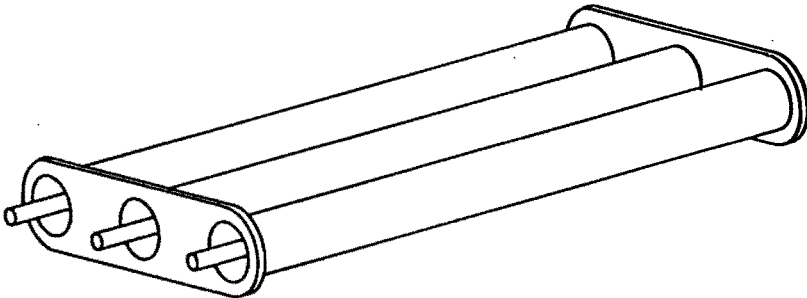


Fig. 5.3: Simplified sketch of three single phase enclosures interconnected by wide metal plates at the ends.

plates (at both ends) the magnetic fields between each pair of the enclosures are quite small, and correspondingly the 50Hz-currents in the enclosures tend to be equal and opposite to the currents in the central conductors.

The above described situations illustrate two limiting cases of current flow in the enclosures, namely:

- eddy currents flow in opposite direction at both sides of the enclosure wall (insulated enclosures grounded at one point);

- currents flow in one direction in the enclosure (continuous enclosures with the ends interconnected by wide metal plates).

To answer the question under what circumstances the dissipation is minimal, we consider both configurations.

Note that when less metal is used for the interconnection at the ends a mixture of both cases results.

INSULATED ENCLOSURES

First we determine the dissipated power in the enclosure for the case where adjacent sections are insulated from each other. Per section the enclosure is grounded at one point connected to the grounding mesh. Let I be the current in the central conductor (see Fig.5.4). The dissipated power P (W/m^2) in the enclosure is equal to the sum of the

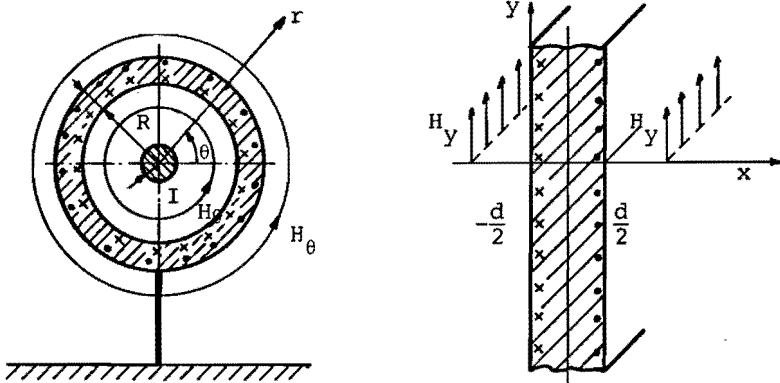


Fig. 5.4: Interrupted GIS enclosure connected to the grounding mesh at a single point (a). For $R \gg d$ the E-field in the enclosure wall is equal to the E-field in a flat large plate (b).

time average of the Poynting vectors directed into the enclosure wall. The Poynting vector S is equal to the vector product of the electric field E and the magnetic field H . We therefore have to know E and H at both sides of the enclosure wall.

To calculate the H-field we neglect the proximity effect between the enclosure and the other two enclosures in the substation. The H-field lines, at the inside as well as close to the outside of the vessel, are considered to be concentric circles around the central conductor. The H-field magnitude along these circles is given by $H_{\theta} = I/2\pi r$ (Fig.5.4).

When the radius R of the enclosure is much larger than the thickness d of the enclosure wall the E-field in the wall can be approximated by the expression for the E-field in an infinitely large plate with at both sides of the plate an H-field in the y-direction with magnitude $H_y = I/2\pi R$. The expression for the internal E-field is given by [Kad 59, pg.19]:

$$E_z = k\rho \frac{\sinh kx}{\cosh kd/2} H_y, \quad -\frac{d}{2} < x < \frac{d}{2}, \quad (5.1)$$

where $k = \frac{1+j}{\delta}$, $\delta = \left(\frac{2\rho}{\omega \mu_0 \mu_r} \right)^{1/2}$ is the skin depth, ρ is the resistivity and $\mu_0 \mu_r$ is the permeability. Assumed is an $\exp(j\omega t)$ time-dependence.

The E-field in the wall is an odd function of x , which means that the Poynting vector at the left hand side as well as at the right hand side of the enclosure wall can be directed into the material. Therefore, the power dissipation per square meter enclosure is equal to:

$$P = \frac{1}{4} \left[E_z^* H_y + E_z H_y^* \right]_{x=\frac{d}{2}} - \frac{1}{4} \left[E_z^* H_y + E_z H_y^* \right]_{x=-\frac{d}{2}} =$$

$$= \rho \hat{H}_y^2 \operatorname{Re} \left\{ k \tanh \frac{kd}{2} \right\} = \frac{\rho}{\delta} \hat{H}_y^2 \frac{\sinh \frac{d}{\delta} - \sin \frac{d}{\delta}}{\cosh \frac{d}{\delta} + \cos \frac{d}{\delta}} \quad [\text{W/m}^2], \quad (5.2)$$

CONTINUOUS ENCLOSURES

Secondly we determine the dissipated power in the enclosure for the case where neighboring enclosures are connected to each other at the ends by means of wide metal plates. The H-field lines inside the vessel are concentric circles around the central conductor with $H_{\theta} = I/2\pi r$, $r_0 \leq r \leq R$. The H-field outside the vessel is zero (see Fig.5.4a).

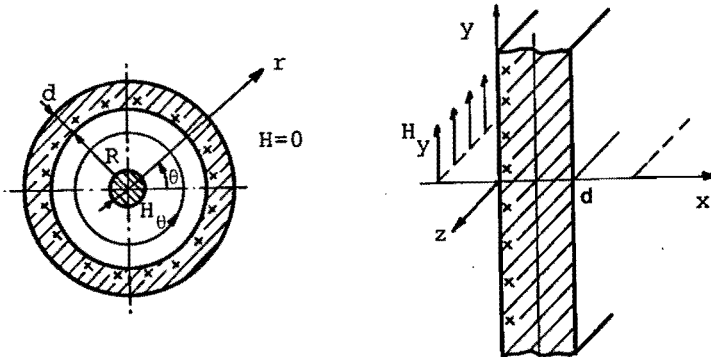


Fig. 5.5: The continuous enclosure used as current return path. The H-field at the outside of the vessel is zero (a). For $R \gg d$ the E-field in the plate can be considered to be equal to the E-field in an flat large plate with an H-field at one side only (b).

When $R \gg d$, the E-field in the wall can be approximated by the expression for the E-field in an infinitely large plate with thickness d , with at the left hand side of the plate an H-field in the y-direction with magnitude $H_y = I/2\pi R$ and no field at the right hand side (see Fig.5.4b).

The expression for E_z is given by [Ka 59, pg.139]:

$$E_z = -k\rho \frac{\cosh k(x-d)}{\sinh kd} H_y, \quad 0 < x < d \quad (5.3)$$

The Poynting vector at the left hand side of the plate is directed into the plate, therefore the dissipation per square meter is

$$\begin{aligned}
 P &= -\frac{1}{4} \left[E_z^* H_y + E_z H_y^* \right]_{x=0} = \frac{1}{2} \rho \hat{H}_y^2 \operatorname{Re} \left\{ k \coth kd \right\} = \\
 &= \frac{1}{2} \frac{\rho}{\delta} \hat{H}_y^2 \frac{\sinh \frac{2d}{\delta} + \sin \frac{2d}{\delta}}{\cosh \frac{2d}{\delta} - \cos \frac{2d}{\delta}} \quad [W/m^2] \quad (5.4)
 \end{aligned}$$

COMPARISON OF DISSIPATION IN ENCLOSURES

In this section we compare P_1 , the dissipation in an enclosure due to a current which is equal and opposite to the central conductor (Fig.5.5), with P_2 , the dissipation in an enclosure with only eddy currents (Fig.5.4). The dissipations P_1 and P_2 are given by Eq.5.4 and Eq.5.2, respectively. We are especially interested in a comparison of P_1 with P_2 at the mains frequency as a function of the enclosure thickness d for a given material (i.e.: ρ and δ are constant). Therefore, Fig.5.6 shows the graphs of P_1 and P_2 [W/m^2] as a function of d/δ .

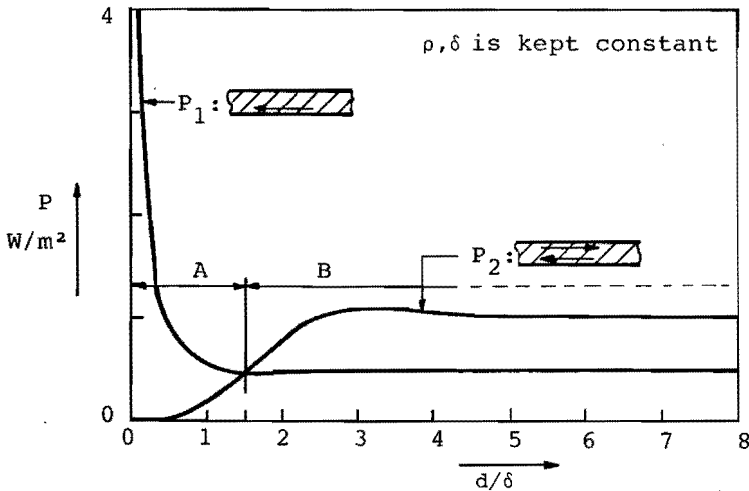


Fig.5.6: The dissipation per square meter enclosure for an enclosure with at one side an H-field (a) and at both sides an H-field (b) as a function of the wall thickness.

We may characterize two regions A and B, on either side of the point $d=1.5\delta$ where $P_1 = P_2$.

-In Region A, $0 < d < 1.5\delta$, P_1 is larger than P_2 .

For $d \rightarrow 0$, P_1 is very large and P_2 is almost zero.

-In Region B, $d > 1.5\delta$, P_1 is smaller than P_2 .

For $d > 4\delta$, P_2 is almost equal to $2 \times P_1$

We apply this comparison to a GIS enclosure made of iron or aluminum; to the lead sheath of a single phase HV-cable and to an Isolated-Phase Bussystem [Sen 83].

GIS enclosures

Some GIS enclosures are made of iron. The thickness of the enclosure wall (chosen also to safely contain the pressurized insulating gas) varies between 6 and 8mm. The skin depth δ_{Fe} at 50Hz is on the order of 1mm. In Fig.5.6, we are clearly in Region B ($d > 3 \times \delta_{Fe}$) which means that P_1 is smaller than P_2 . In this case, both for 50Hz-dissipation as well as for HF-EMC arguments, a continuous enclosure with at one side an H-field is advisable. Of course less dissipation occurs in an aluminum enclosure.

Most GIS-installations have aluminum enclosures. The thickness of the enclosure wall varies between 8mm and 15mm. The skin depth for aluminum δ_{Al} at 50Hz is about equal to 12.3mm. Now we are in Region A (left of $d < 1.5\delta$). In this case the dissipation is less for an non-continuous enclosure. However, a continuous GIS-enclosure may be still advisable, because:

- the dissipation in the enclosure is only a fraction of the total dissipation in the GIS-installation;
- P_1 could still be considerably less than the sum of P_2 and dissipation by eddy currents in nearby structural steel caused by the H-field outside the interrupted enclosure.

Note: When the ends of the GIS are interconnected by narrow strips and not by wide metal plates, an H-field is present outside the continuous enclosure. In this situation the dissipated power in the enclosure is between P_1 and P_2 over the entire region (A+B, see Fig.5.6).

HV-cables with a lead sheath

For HV-cables it is important to keep the power dissipation in the lead sheath low to limit the temperature rise in the dielectric. The skin depth of lead δ_{Pb} for 50Hz is about 36.3mm. Therefore the variable d/δ_{Pb} is in Region A, close to zero. To avoid large net currents in the HV-cable sheaths of a three phase system, "cross-bonding" techniques (see Fig.5.7) are applied. By means of this technique, normally used for long lengths of cable, the induced currents in the HV-cable sheaths are zero because the

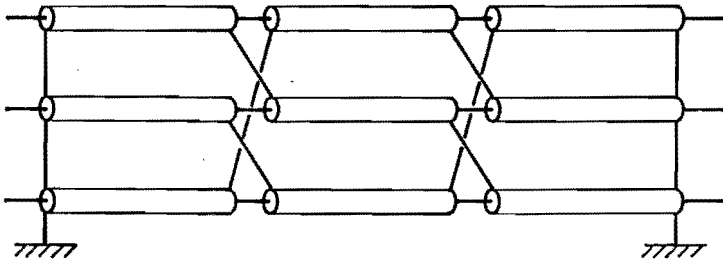


Fig.5.7: Cross-bonding of lead sheaths of HV-cables.

overall induced flux in every closed loop formed by the sheaths is zero. The left and right far ends of the cables are interconnected and grounded to carry away capacitive currents during abnormal conditions.

Note:

(1) The interconnections at the end of the cables in Fig.5.7. can coincide with the interconnections at the ends of the GIS in Fig.5.3.

(2) When the HV-cables ends in a GIS-installation and the cable sheaths are connected all around to the GIS-enclosure we are in the EMC-ideal situation which is described in Sec.5.1.

Isolated-phase bussystems [Sen 83]

Isolated-phase bussystems are used in power stations to connect the generator to the main transformer (Fig.5.8). Each of the three-phase conductors is completely shielded by an aluminum enclosure against dust, moisture and

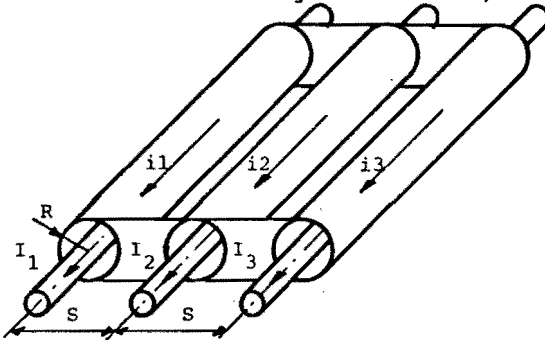


Fig. 5.8: A sketch of the basic layout of an isolated-phase bussystem.

accidental contact. The wall thickness is about equal to 7mm. In this case we are in Fig.5.6 to the left of point $d=1.5\delta$ ($\delta_{A1}(50\text{Hz})=12.3\text{mm}$). Although P_1 is larger than P_2 , nevertheless the enclosure ends are interconnected with wide metal plates. These plates allow net enclosure currents to flow, which largely cancel the magnetic fields outside the enclosure. Consequently, the electromagnetic forces between the enclosures and between the conductors remain low even for dangerously large currents for instance during faults. An additional advantage is that eddy current losses in structural steel in the vicinity remain very small.

5.1.2 NECESSARY INTERRUPTIONS IN A GIS-INSTALLATION

In our attempt to contain HF-waves inside the GIS-enclosure it is obvious that interruptions are to be avoided as much as possible. Unavoidable interruptions, however, remain at the transition from a HV-line to a GIS and in some situations at the transition HV-cable to GIS. This section deals with the control of HF-waves escaping via these necessary interruptions. We briefly discuss a HV-line/GIS transition and a HV-cable/GIS transition if cathodic protection of the cable sheath is used. We discuss in detail a HV-line/GIS transition where HV-cable sheaths are interrupted to permit current measurements.

GIS/HV-LINE TRANSITION

A connection of an overhead line to a GIS-installation via a high-voltage bushing gives a quite open structure (see Fig.5.9). During switching actions HF-waves escape via this transition. The escaped hf-waves propagate partly via the HV-line circuit to the outside world and partly via the transmission line formed by GIS-enclosure and ground in the direction of the GIS-building. Reflected waves returning along the HV-line partly reflect again at the transition, a small part turns back into the GIS-installation and a larger part travels between GIS-enclosure and ground to the GIS-building.

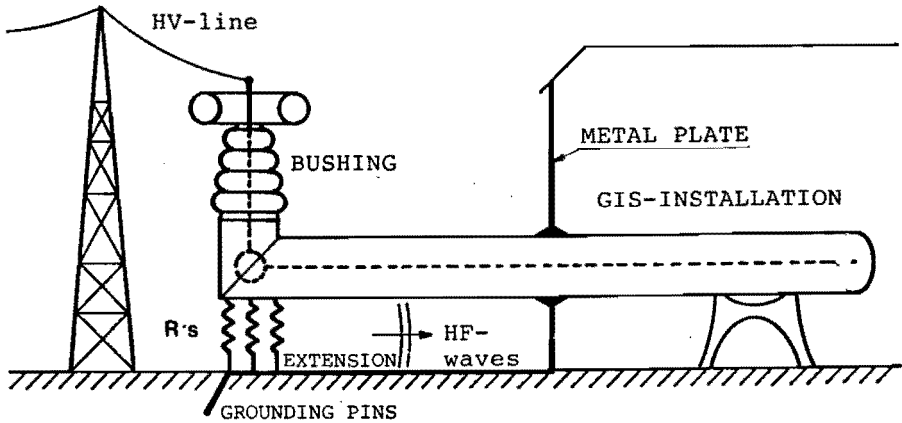


Fig.5.9: GIS/HV-line termination with protective measures.

To avoid large currents inside the GIS building, we create a protected region with a metal plate (analogous to a simple grounding structure, see Sec.3.3). The GIS-enclosure should be connected all around to the grounding structure (GS). To achieve a better control of the external HF-currents this metal plate is horizontally extended in the direction of the HV-lines (Fig.5.9). Further control is achieved by the installation of grounding pins (also adequate for low frequency currents, e.g. in the event of a short circuit) and by the connection of the GS to structural steel in the building. Useful HF-losses can be obtained with strings of carbon composite resistors ($\approx 500\Omega$) connected between the GIS-enclosure and the extension of the GS.

HV-CABLE/GIS TRANSITION; CATHODIC PROTECTION

To allow cathodic protection of the cable sheath with a small DC-voltage the cable sheath can be isolated from the GIS enclosure (Fig.5.10). Traveling wave transients, due to switching actions in the GIS-installation, often cause sparking across the insulating flanges at the cable/GIS transition. Fujimoto [Fuj 88] investigated the use of capacitors, metal-oxide varistors (MOVs) and spark gaps, as a means of protecting the insulating flange, both for new installations as well as for existing installations as retrofits.

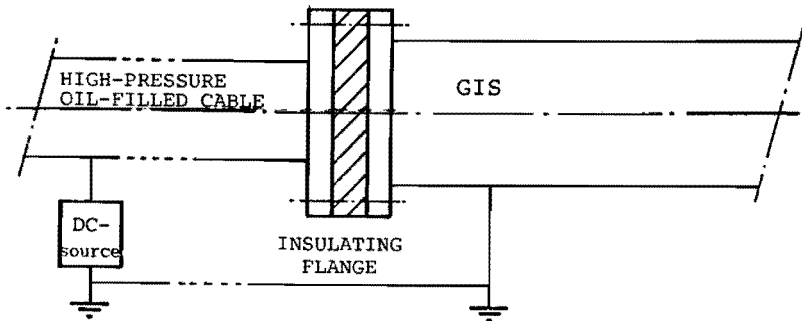


Fig.5.10: Basic cable/GIS transition, insulated to allow cathodic protection [Fuj 88].

The results of this investigation were: a) spark gaps installed circumferentially around the insulating flange are not a suitable "quick fix" solution for existing installations; b) it is better to use MOVs or capacitors to provide a HF-current path, if the components are carefully installed. The connection leads must be kept as short as possible, and several components, perhaps one at each bolt hole, are necessary to reduce the inductance.

In this context we remark that feedthrough capacitors have excellent HF properties. Carbon composite resistors, surrounded by shrink sleeve, and in series with the capacitors give extra HF-losses (see Fig.5.11). Several series-connected capacitors and resistors should be installed circumferentially around the insulating flange. A compact arrangement as shown in Fig.5.11 should keep the inductance low.

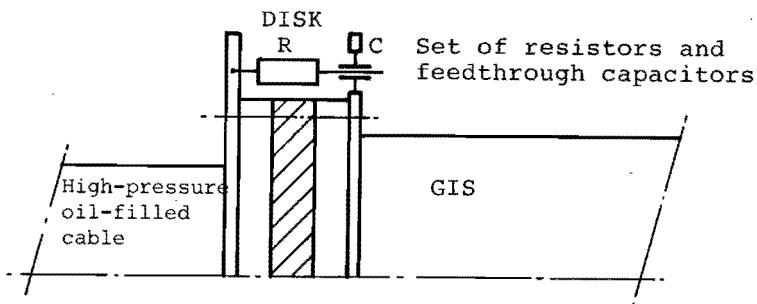


Fig.5.11: Feedthrough capacitor in series with a carbon composite resistor provide a compact HF-current path and attenuates the transient.

GIS/HV-CABLE TRANSITION; CURRENT TRANSFORMER ARRANGEMENT

Similar problems as above occur at a GIS/cable transition if a current-transformer is used. In this case cable sheaths are interrupted to permit current measurements. Induced HF-voltages over these interruptions may lead to breakdown. The low energy HF-sparking could cause degradation of the insulation near the transition. We have investigated this problem in the 150/10kV GIS-substation Eindhoven-West of the PNEM (Power Company Province Noord-Brabant). Fast rising high-voltage transients across the interruption are measured and possible solutions to avoid HF-sparking are tested.

The substation Eindhoven-West is linked with the substations Eindhoven-Noord and Eindhoven-Zuid via two three-phase connections, each consisting of three 150kV XLPE-cables. It supplies electric energy to the consumers via two 150/10kV transformers. Figure 5.12 and Fig.5.13 depict the three-phase enclosed GIS-installation and show a diagram of the substation, respectively. The dashed contour in Fig.5.13 encloses the GIS part of the installation.

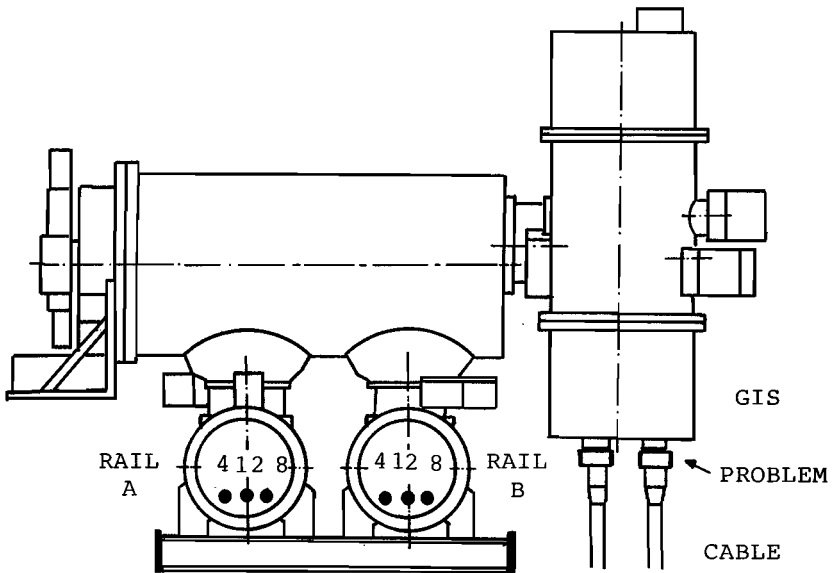


Fig. 5.12: Three-phase GIS-substation Eindhoven-West

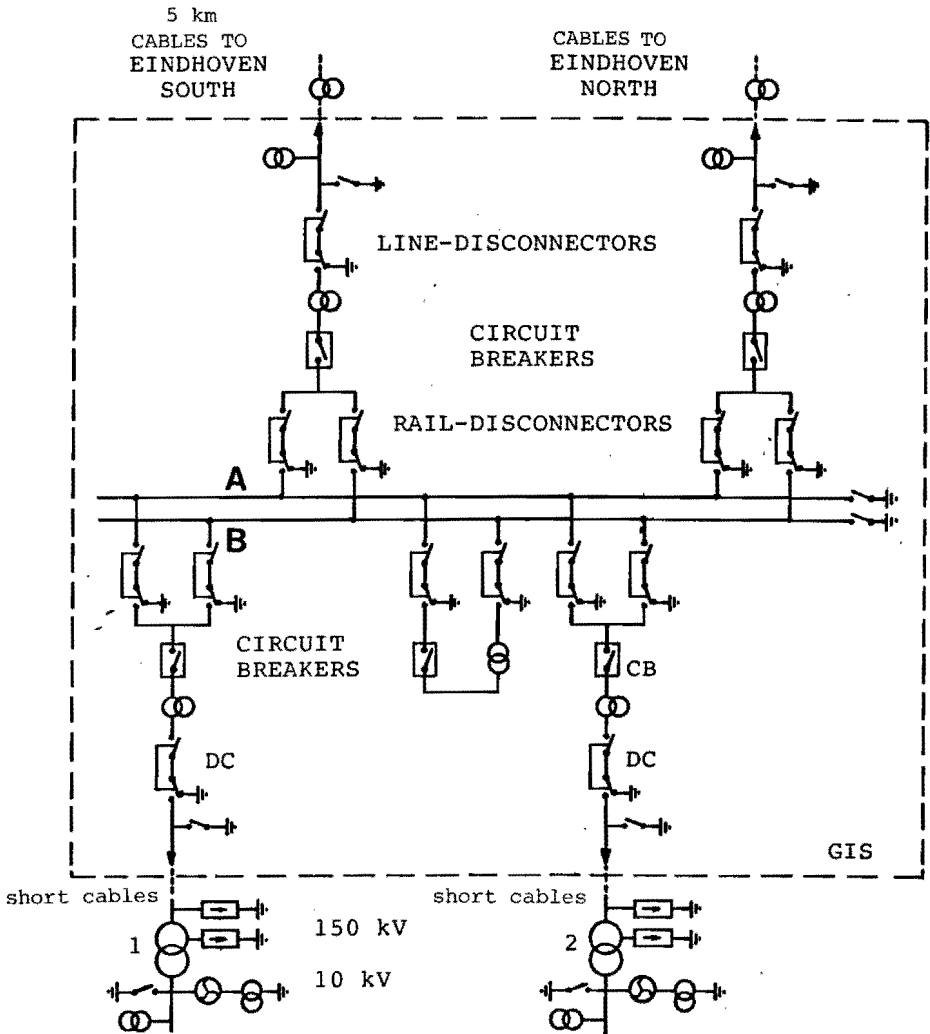


Fig. 5.13: Configuration substation Eindhoven-West.

The GIS contains: two rail systems (A and B); five three-phase circuit-breakers, two for each 150kV connection (CB-North and CB-South), two for the 150/10kV transformers (CB-trafo-1 and CB-trafo-2) and one between rails A and B; the necessary disconnectors (for rail, cable, and transformer) and grounding switches.

The GIS-installation has four three-phase terminations, two for the 150kV cables to substations North and South and two for the 150kV cables to the transformers. At the ends of the GIS, around each cable (total twelve), a current transformer is placed outside the GIS-enclosure as depicted in Fig.5.14. The lead sheath of the cable is interrupted to permit current measurement. An insulating collar also serves as a pressure-seal. With a grounding strip, outside the current-transformer, the 50Hz-circuit is completed.

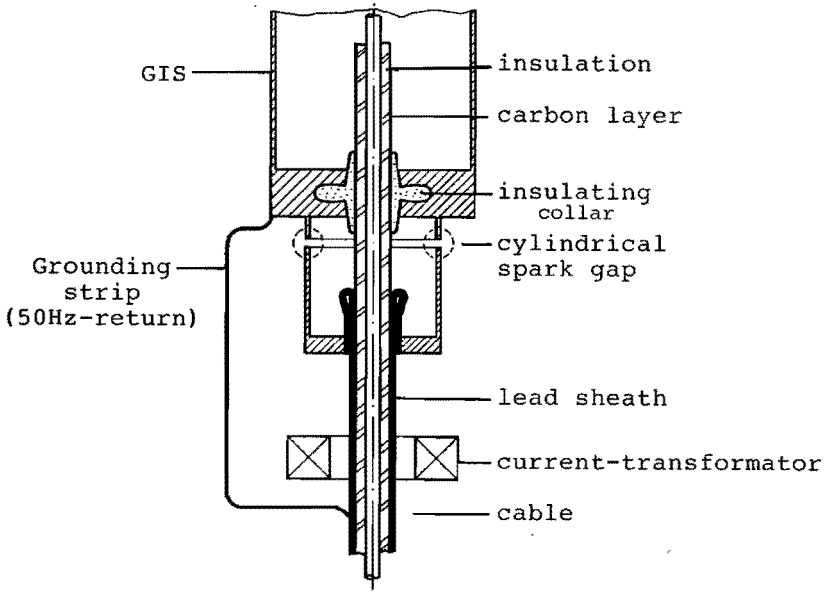


Fig. 5.14: Simplified sketch of the GIS/cable-transition with current-transformer arrangement. Only one of the three cables is shown.

To avoid degradation of the insulating collar and the cable insulation, voltage limiting "cylindrical spark gaps" are installed (see Fig.5.14). The sparking of these gaps -and at many other places- during switching actions indicates

the escape of HF-waves. In an attempt to reduce hf-sparking the power company had prepared a brass cylinder which could be installed around the three-phase current-transformer arrangement (Fig.5.15a) to provide a closed low-inductance return path for the HF-current. The cylinder has a length of 115cm and a radius of 50cm. Another modification, a proposal of our group, is to install a ring of resistors, with a total resistance of about 30Ω across each cylindrical spark gap (Fig.5.15b). In this manner an even more compact and dissipative circuit for the HF-currents is formed. The 50Hz-currents still flow via the grounding strip around the current-transformer. Each resistor ring is composed of 24 parallel branches each with two resistors in series. We used carbon composite 2W-resistors with shrink sleeve insulation and a resistance.

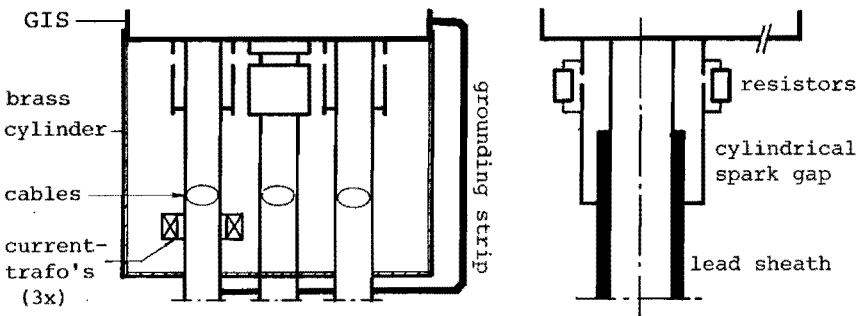


Fig. 5.15: A GIS-transition with (a) a brass cylinder around the current-transformer arrangement and (b) with a ring of resistors across each spark gap.

To study the effect of these two modifications the next measurements have been done:

- we measured the voltage V_G across the cylindrical spark gap as a function of the gap distance ($d=2, 5, 10$ and 20mm)
- we measured V_G when the brass cylinder is installed around the current-transformer arrangement ($d= 10\text{mm}$), and
- we measured V_G when resistor rings are installed across the cylindrical spark gap ($d= 10\text{mm}$).

These measurements have been done during circuitbreaker as well as disconnecter switching actions.

SETUP

Experiments have been done at the transition of termination South (see Fig.5.16). A Tektronix 7912 AD digitizer (600MHz analog bandwidth, 50Ω plug-in unit) was used to register the first 50ns of the voltage across the spark gap of phase 8. With two multi-channel Nicolet 4094C digital oscilloscopes (200MHz max. sampling rate, 8 bit resolution) we had determined beforehand that the given circuit breaker often showed its first breakdown at phase 8. The time-window of the Nicolets during these measurements was 1250ns (1MΩ input). The applied measuring systems were based on the D/I-measuring principle. The rise time of the step response of the measuring system in combination with the Tektronix was 0.6ns (Sec.4.2).

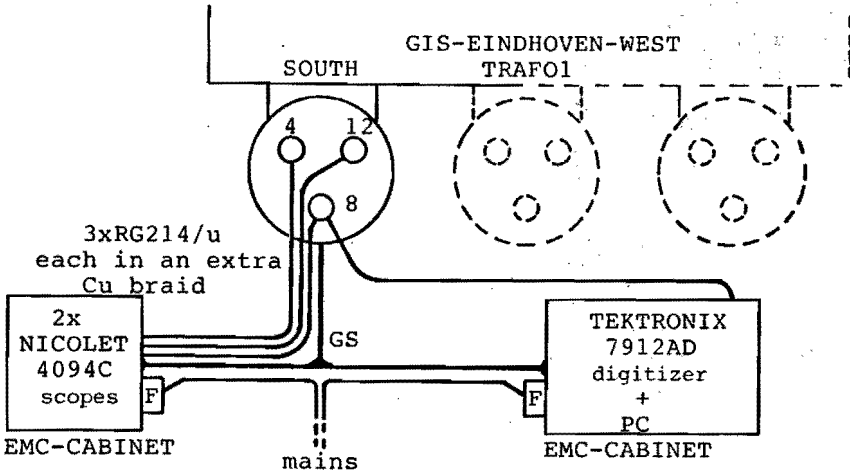


Fig. 5.16: Setup for voltage measurements across the sparkgaps of termination South.

The Tektronix, together with a PC for data-handling, and the two Nicolets were placed in two EMC-cabinets. These EMC-cabinets and the GIS-installation were firmly interconnected by means of a grounding structure. The three signal cables (type RG-214/u) of the measuring systems for the Nicolets were each surrounded by an extra copper braid and tied to the grounding structure. To achieve optimal wide band signal transport to the Tektronix a short

(4 meter, see also Fig.4.11) RG-214 cable was used. The cable was fed in through an "inside extension" (see Ch.2, Fig.2.20). Inside the EMC-cabinet the cable was terminated by its characteristic impedance. To be absolutely safe the cable was surrounded by a copper tube which was connected both to GIS and to the EMC cabinet. The EMC-cabinets were located close to the intense HF-interference source (see Fig.5.17). Therefore, the EMC-cabinets had to be closed during measurements to give the required shielding against HF-interference.

Note that for this setup a lot of "plumbing" was necessary. Under less critical circumstances, we may omit the extra copper around the D/I measuring cable, and we may leave the door of the EMC-cabinet open.



Fig. 5.17: EMC-cabinet with Tektronix digitizer and PC for data handling located close to the GIS at the left.

The measurements were carried out with the D/I-system described in Ch.4. The signal registered with the Tektronix is proportional ($A \approx 10 \text{ mV/kV}$, $\tau_1 \approx 70\text{ns}$) to the voltage V_{ss} between the sensor and the sparkgap cylinder ($V_{ss} = \int_1^2 E \cdot dl$, see Fig.5.18).

Concerning the input circuit of the measuring system we distinguish two situations:

- (a) there is no arc between the two cylinders of the spark gap,
- (b) there is an arc.

In situation (a) the voltage V_{ss} is equal to the voltage V_G across the gap when the measuring circuit 1-2-3-4 is compact (see Fig.5.18a), i.e:

- the induced voltage in this loop, due to the current I , is small compared to V_G ;
- the measuring loop contains 50Ω , the capacitance of the sensor, and an inductance. To keep the inductance low the connection 3-4 is shaped as a short wide metal bracket.

In situation (b) the voltage V_{ss} is the sum of the arc voltage V_{arc} ($\int E \cdot dl$ through the arc) and the voltage V_{ind} induced in loop 1-2-3-4-5-6 (see Fig.18b). The voltage V_{ind} is far from small compared with V_{arc} . Moreover the voltage V_{ss} depends on the arc position in the spark gap.

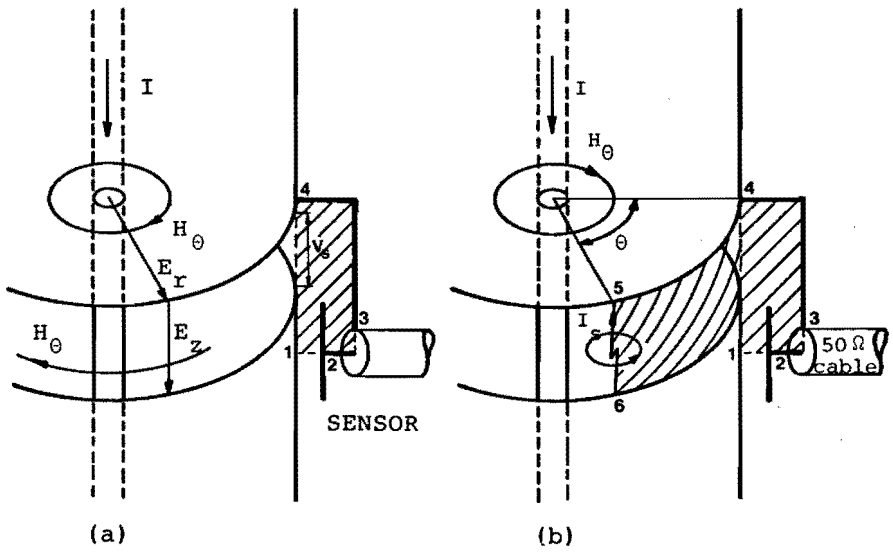


Fig. 5.18: The input circuit of the measuring system without an arc (a) and with an arc between the gap (b).

EXPERIMENTAL RESULTS AND DISCUSSION

The proposed experiments were mainly carried out during switching actions with circuit-breaker South (CB-South) and rail-disconnector North (DC-North) in substation Eindhoven-West. Because in real substations the number of switching actions should be limited and the exact switching time with regard to the 50Hz voltage is unknown, there is a certain spread in the results. Preparations in our own laboratory with a GIS-setup which generated a much more reproducible transient, were therefore very useful.

The initial state of the Eindhoven-West installation was:

(a) in advance of the closure of CB-South: rail A was fed via HV-cable North; CB-North, rail- and cable-DCs North and South were closed; HV-cable South was open at the far end (see Fig.5.19a);

(b) in advance of the closure with rail-DC North: rail A was fed in via HV-cable South; CB-South, rail- and cable-DC South were closed; CB-North and cable-DC North were open (see Fig.5.19b).

During both actions a) and b) sparks were audible and clearly visible across the spark gaps of termination South. In contrast to a DC-action, which is always accompanied by a long train of sparks, a CB-action is accompanied by one

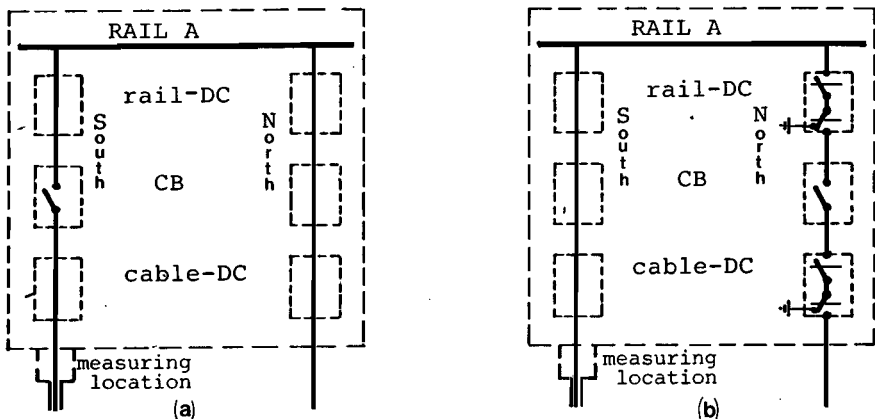


Fig. 5.19: Simplified diagrams of substation Eindhoven-West. The diagram at the left hand shows the initial state for switching actions with CB-South and at the right hand for switching actions with rail-DC North.

audible spark. Only the experimental results obtained during CB-actions are discussed here, because they provided clearer and more reproducible signals.

The purpose of the experiments was to study the effect on the sparking: of a brass cylinder installed around the current-transformer arrangement, and of resistor rings installed across the cylindrical spark gaps. Therefore we have measured the voltage across the spark gap in both situations. As a reference we have measured the voltage across the gap as a function of the gap distance in case there is neither a brass cylinder nor resistor rings. These measurements have been done at termination South during actions with CB-South.

Original situation: cylindrical spark gaps only

The first series of measurements were the voltage measurements across the spark gap of phase 8 at termination South with different gap distances during switching actions with CB-South.

Table 5A gives the results of the measurements. The values of the maximal top voltage and the average top voltage are obtained from waveforms as in Fig.5.20.

Figure 5.20 shows the recordings of voltage waveforms with four different spark gap distances. The recordings show a considerable change in waveforms due to the variation of the gap distances between 2 and 10mm. For distances between 10 and 20mm the waveforms are identical.

For gap distances 2 and 5mm the recordings show a steep voltage drop, corresponding with breakdown across the spark gap. Although this breakdown limits the magnitude of the voltages, the fast voltage drop corresponds with very large dV/dt 's and dI/dt 's. These rapid changes can be responsible for interference in the secondary system. Noticeable is:

- the 0.6ns voltage drop in air because of an overstressed spark gap ($d= 2mm$);
- after a breakdown of the spark gap there is still a considerable voltage (a few kV's) because of the large

CB-South				
spark gap distance (mm)	maximum top-voltage (kV)	average top-voltage (kV)	deviation	number of measurements
2	21.9	16.1	30%	4
5	33.0	31.4 *	*	2
10-20	39.7	29.0	40%	6

*)not enough measurements

TABLE 5A: Amplitude as function of spark gap distance.

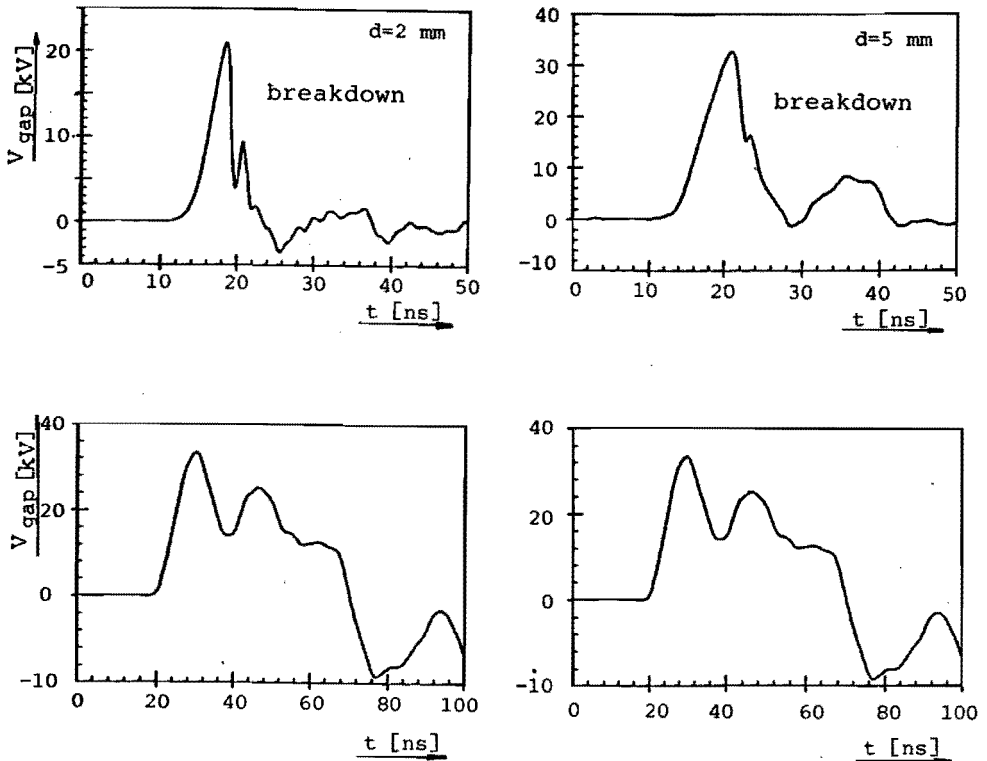


Fig. 5.20: Voltage across the cylindrical spark gap measured with Tektronix digitizer for different gap distances; original position, without a brass cylinder or resistor rings; measured at termination South during switching actions with CB-South.

measuring loop in combination with the large dI/dt (about 300 A/ns), already discussed in Fig.5.18. Calculations with a 2D-model on this problem have been done. Uncertain in this model are however: the unknown arc radius; the limited validity of the 2D-model since the field lines escaping through the gap expand in 3D.

For gap distances larger than 10mm the waveforms were not affected by the spark gap during the first 100ns. Although the waveform reached its top in this time interval no breakdown occurred. On a longer time scale breakdown always occurred. The time necessary to initiate a breakdown increases with the gap distance and inversely with the voltage. Therefore, for transients breakdown can occur a certain time after the first top of the voltage.

Brass cylinder and resistor rings

The second series of measurements were the voltage measurements across the same spark gap during switching actions with CB-south in the case that termination South was equipped with:

- spark gaps only;
- spark gaps combined with a brass cylinder;
- spark gaps combined with resistor rings.

To make a comparison possible between these three tests the gap distance was chosen 10mm so that no breakdown occurred during the first 100ns.

Table 5B gives the results of the measurements. The values of the maximum top voltage and the average voltage are obtained from waveforms as in Fig.5.21. Figure 5.21 shows recordings of the Tektronix digitizer.

A brass cylinder around the current-transformer arrangement, gives in comparison with only spark gaps, little or no reduction of the voltage. Although the HF-circuit is more compact, it is still too large for the fast transients to avoid sparking (1.15m corresponds with a back and forth transit time of 6.9ns).

DESIGN	maximum top-voltage (kV)	average top-voltage (kV)	deviation	number of measurements
spark gap	39.7	29.0	30%	6
-with cylinder	29.6	24.6	20%	3
-with resistors	15.9	13.3	25%	3

TABLE 5B: Amplitude of the voltage across the spark gap.

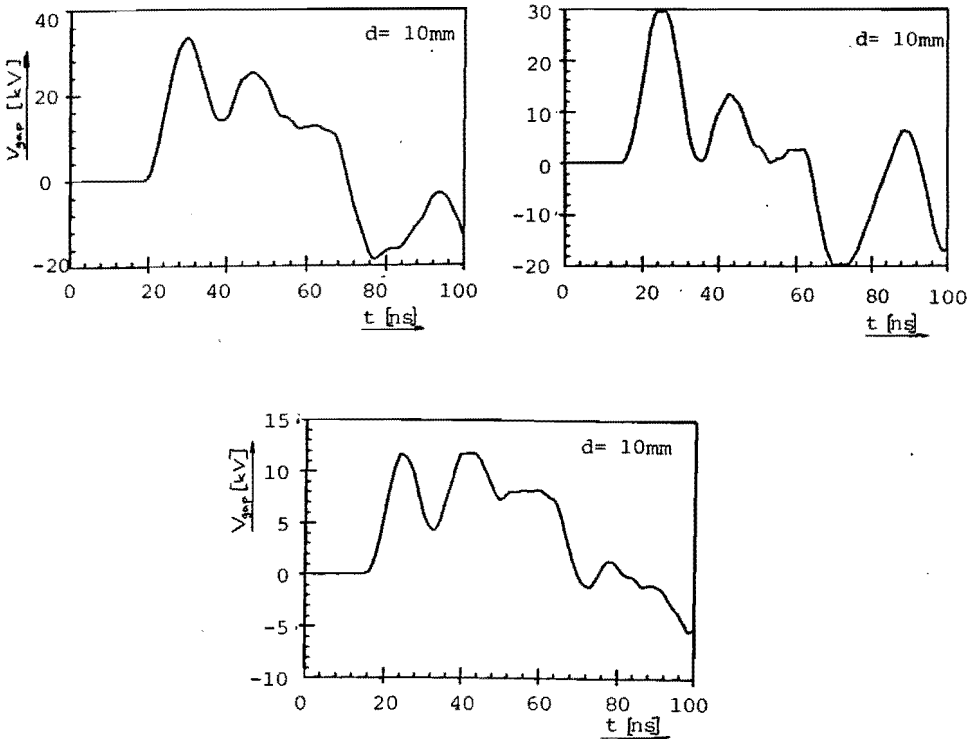


Fig. 5.21: Voltage across the spark gap during switching actions with CB-South. Left: only spark gaps; right: spark gaps with brass cylinder; below: spark gaps with resistor rings.

Resistor rings across the spark gaps reduced the voltages across the gaps significantly. In contrast to the two other test situations no sparking occurred irrespective of the switching action (CB- or DC-action). Because the spark gap is the weakest link the risk to the insulating collar is even more reduced.

The 50Hz-current measurements are not affected by the resistor rings ($R \approx 30\Omega$). The induced current in the loop formed by resistor rings and grounding strip outside the current transformer (see Fig.5.14) is only a few milliamps (measured by PNEM: 2-3mA while the total primary current is 400A). Also for a sheath current there are no problems because the impedance of the grounding strip ($\approx 1.5m\Omega$ at 50Hz) is much smaller than the 30Ω of the resistor rings. Dissipation is not a limiting factor in the choice of the resistors. A resistor ring is composed of 24 parallel branches each with two resistors in series. When we approximate the waveform of the voltage during a CB-action (see Fig.5.22) as an exponential curve with a maximum voltage of 13.3 kV and an $1/e$ -time of 200 ns the peak dissipated power is about 5.9 MW, i.e. about 122 kW per resistor. The corresponding energy is however only 12.3 mJ per resistor because of the short pulse duration. Even when

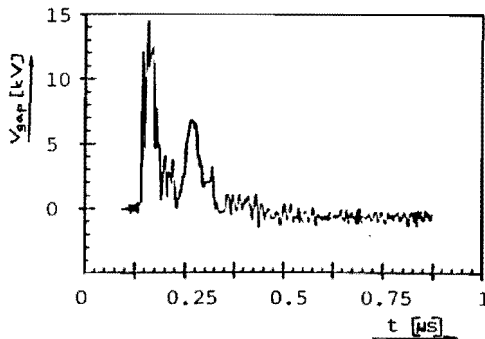


Fig. 5.22: The transient voltage across the spark gap equipped with a resistor ring falls off in about 200ns (deviation 20%). This is obtained from 5 measurements (recordings of the Nicolet) such as shown in this figure. For the average top-voltage the value given in Table 5B is used.

we take into account the repetitive behavior of the breakdowns during DC-actions the energy still remains low. The power and energy per (single) waveform during a DC-action is about 33 kW and 3.3 mJ per resistor, respectively. The total dissipated energy is about $(500/10) \times 3.3 \text{ mJ} = 165 \text{ mJ}$ when during 500ms every half-period a breakdown occurs.

A more important question is whether the resistors can withstand the high pulse voltages (about 8kV per resistor during 200ns). Therefore we used carbon composite 2W-resistors with shrink sleeve insulation to avoid flash over across the outer resistor surface. Moreover the resistors must be carefully installed to reduce the inductance. The connection leads must be kept as short as possible, and several series-connected resistors should be installed circumferentially around the cylindrical spark gap. A properly distributed resistor keeps the transient B-fields inside the coaxial structure, but of course still acts as an E-field antenna with respect to the outside world.

CHAPTER 6

CONCLUSIONS

GENERAL CONCLUSIONS

- General, linear and basic design methods can be developed, for the protection of electronics and (large) interconnected electrical systems against interference. Such an approach early in the design phase of apparatus or experimental setups saves production costs for the manufacturer and research time for the experimentalist.
- The design methods described in this thesis concentrate on the reduction of dangerous voltages between critical points. This reduction can be achieved by the choice of a correct layout, even under conditions of intense disturbances. In the emphasis on dangerous voltages and in the possibility to create a safe local climate, we are critical of the more vaguely formulated IEC definition of Electro-Magnetic-Compatibility which is quoted here for completeness: "The ability of a device, equipment or system to function satisfactorily in its electromagnetic environment without introducing intolerable electromagnetic disturbances to anything in that environment".

From the results of chapter 2 through 5 the following conclusions can be drawn.

ELECTROMAGNETIC COMPATIBILITY AND GROUNDING

- The activity "grounding" should, and can indeed, reduce dangerous voltage differences between critical points to safe values.
- A grounding system is always a part of a number of interlinked current loops. Design of a grounding system involves an analysis based on the concept of closed current paths.
- The circuits for ground currents should be designed as compactly and locally as the circumstances allow; this also results in a clearer design.
- A properly designed grounding structure is a structure with a low transfer impedance. Through this structure large external CM-currents may flow and still no dangerous voltage differences are induced. In many electrical installations grounding problems can be solved locally by creating protected regions formed by grounding structures.
- The creation of a protected region does not rely on the improvement of the overall "EM-environment" but instead, provides an excellent local "climate" where it is needed.
- Our design method keeps fluxes (self and mutual) small so that we will have fewer deviation from the Kirchhoff's Voltage Law than a less compact design would give. Moreover the compact and local approach reduces capacitive and resistive coupling.

TRANSFER IMPEDANCE OF GROUNDING STRUCTURES

-The significance of the transfer impedance concept for grounding structures is that simple measurements can provide its value and thereby a meaningful criterion for the quality of the grounding structure (including the entire "layout" of the "network").

-The transfer impedance is only meaningful when primary and secondary circuit are fully defined.

Grounding structures can be divided into two categories: "grounding structures to protect leads" and "grounding structures to protect instruments".

Grounding structures to protect leads

-A GS for leads provides a controlled current path for external CM-currents and creates a protected region for the leads by means of its shape.

-The transfer impedance of a tube drops rapidly to zero at higher frequencies because of its symmetric geometry.

-Although the dc-resistance of an iron tube is higher than that of a copper tube, the permeability of iron gives a small skindepth, so that already at low frequencies the transfer impedance of an iron tube falls below that of a copper tube.

-Practical GS's with a low transfer impedance can also be shaped as a plate or a conduit.

-In situations with intense interference, the transfer impedance of conduits can be further reduced with metal covers.

-Due to the higher surface impedance of iron, in comparison to copper, the external CM-current is reduced more by an iron conduit than by a copper one.

Grounding structures to protect instruments

-For the protection of instruments we use GS's around or near the instruments. The useful DM-currents can enter the protected region, whereas the external CM-currents are diverted.

-In situations with a moderate level of disturbance, simple GS's -as described in this thesis- can be installed in many practical situations, on different scales. Simple techniques as orientation of the cable connections and more metal at strategical places (e.g. plates, disks or cylinders) can give significant reductions of the transfer impedance of these GS's.

-In situations where much protection is necessary an EMC-cabinet is an efficient solution. The front of the EMC-cabinet can often stay open, if the interference source is at some distance. A correct handling of the interference currents at the points where the leads come in, is more important than the lack of shielding near the open front. In cases where the EMC-cabinet has to be located close to an intense HF-interference source the

door of the EMC-cabinet must be closed to also give the required shielding.

DIFFERENTIATING/INTEGRATING MEASURING SYSTEM

- A D/I measuring system has been developed with a overall risetime of 0.6ns, corresponding to a bandwidth of 580MHz.
- The advantages of a D/I-system are:
 - i) The benefits of a single capacitor as the high-voltage arm in a impulse voltage divider are fully exploited when this capacitor forms a part of a D/I-measuring system: no traveling wave between high and low voltage arm and an easy matching of the measuring cable.
 - ii) The components of the low-voltage arm can be of normal size as used in electronics. The differentiating resistor can be a long terminated cable. The integrator capacitor can be a feedthrough capacitor.
- The advantage of a feedthrough capacitor as integrator capacitor is that its symmetric configuration reduces the mutual inductance to the output to zero.
- The type and length of a coaxial cable should be carefully selected when nanosecond risetime measurements have to be made.
- Differentiating sensors combined with appropriate cabinets allow EMC-correct measurements in high-interference surroundings, in high-voltage engineering, in lightning research and in pulsed power.

ELECTROMAGNETIC COMPATIBILITY IN GIS-SUBSTATIONS

- A GIS-installation is an intense and concentrated source of HF-interference. During switching actions locally stored electrical energy is partially converted into high power EM-waves with fast rise times of less than 5 ns.
- At interruptions in GIS-enclosures HF-waves can freely escape to the outside of the installation. Resulting voltages over interruptions and between other grounded metal construction parts may lead to breakdown, sometimes within very short times, less than 1 ns.
- A GIS-installation with only cables connected to the GIS is an EMC-ideal installation when the outer conductors of the GIS enclosure and of the HV-cables form one completely closed conductor.
- In situations with necessary interruptions in a GIS-enclosure (eg. GIS/HV-line transitions and in some situations at GIS/HV-cable transitions) reduction of HF-waves escaping via these interruption is possible. Carbon composite resistors, surrounded by shrink sleeve, across GIS/HV-cable interruptions reduce the voltages across these interruptions and avoid sparking. Useful HF-losses are caused by the resistors.

REFERENCES

- [Ber 81] Bersier, R.
 MEASUREMENTS OF THE IMMUNITY OF TV-RECEIVERS IN THE 3 TO 30MHz RANGE
 Proc. 4th Int. Symp. on EMC, Zürich (1981) p.289
- [Ber 83] Bersier, R. and B. Sentkutti
 RATIONALE AND EXPERPERIMENTAL EVIDENCE ON THE ADEQUACY OF CONDUCTED INSTEAD OF RADIATED SUSCEPTIBILITY TESTS
 Proc. 5th Int. Symp. on EMC, Zürich (1983) p.257.
- [Bog 84] Boggs, S.A. and N. Fujimoto
 TECHNIQUES AND INSTRUMENTATION FOR MEASUREMENT OF TRANSIENTS IN GAS-INSULATED SWITCHGEAR
 IEEE Trans. on Electrical Insulation Vol. EI-19 No.2, 1984
- [Dan 85] Danker, B.
 NEW MEASURES TO DECREASE RADIATION FROM PRINTED CIRCUIT BOARDS
 Proc. 6th Int. Symp. on EMC Zürich (1985), p. 115.
- [Dan 88] Danikas, M.G. and P.C.T. Van der Laan
 FAST MEASUREMENTS OF PARTIAL DISCHARGE CURRENTS IN SOLID DIELECTRIC SAMPLES CONTAINING VOIDS
 IEEE Int. Symp. on Electrical Insulation, 1988, Boston, pp. 250-252
- [Def 90] Defourny, M.M., M.A. Van Houten, T.F. Buss and E.J.M. Van Heesch
 ELECTRICAL FIELD COMPUTATION. DESCRIPTION AND EXAMPLES WITH EXPERIMENTAL COMPARISON
 Int. ELECTROSOFT Conf., 21-23 aug. 1990, Lowell, Massachusetts, USA, (to be published).
- [Den 74] Denny, H.W. and J.A. Woody
 CONSIDERATIONS IN THE DESIGN OF A GROUNDING SYSTEM FOR A COMPLEX ELECTRONIC FACILITY
 IEEE Symp. on EMC (1974) San Francisco, p. 85.
- [Deu 88] Van Deursen, A.P.J., M.A. Van Houten, E.W.L. Van Engelen, P.F.M Gulickx, P.C.T. Van der Laan, E. Zwennes, A.J. Van Dongen.
 MEASUREMENTS OF CURRENTS AROUND AND IN LARGE GROUNDED STRUCTURES
 Proc. 19th Int. Conf. on Lightning Protection (ICLP, 1988), Graz, Austria 3.1. p.143-147.
- [Deu 89] Van Deursen A.P.J., M.A. Van Houten, P.F.M. Gulickx, P.C.T. Van der Laan, E. Zwennes, A.J. Van Dongen.
 REROUTING LIGHTNING CURRENTS IN A COMMUNICATION TOWER
 Proc. 8th Int. Symp. on EMC Zürich (1989), p. 267.
- [Deu 89] Van Deursen, A.P.J., J.M. Wetzer, P.C.T. Van der Laan
 LOCAL PROTECTION OF EQUIPMENT IN HIGH VOLTAGE SUBSTATIONS
 Proc. 6th Int. Symp. on HV Eng., 1989 New Orleans, USA, paper 31.03, 4p.
- [Deu 90] Van Deursen A.P.J.: (private communication).

- [Eic 85] Eichert, B. and C. Staeger
EXTREMELY BROADBAND RF-CONNECTOR AND CABLE SCREENING
MEASUREMENTS (UP TO 150 dB SCREENING ATTENUATION) FOR
FREQUENCIES OF 1 kHz TO 10 GHz
IEC technical paper, committee 46A (1985).
- [Fuj 88] Fujimoto, N., S.J. Croall and S.M. Foty
TECHNIQUES FOR THE PROTECTION OF GAS-INSULATED SUBSTATIONS TO
CABLE INTERFACES
IEEE Trans. on Power Delivery, Vol.3, No.4, 1988
- [Ger 85] German, R.F.
USE OF A GROUND GRID TO REDUCE PRINTED CIRCUIT BOARD
RADIATION
Proc. 6th Int. Symp. on EMC Zürich (1985), p. 123.
- [Gun 86] Gunn, R.
A COMMON APPROACH TO SIGNAL SEPARATION
EMC Technology 5 no.4 (1986) p. 53.
- [Har 79] Harada, T. and Y. Aoshima
DEVELOPMENT OF HIGH PERFORMANCE LOW VOLTAGE ARMS FOR
CAPACITIVE VOLTAGE DIVIDERS
Proc. 3rd Int. Symp. on High Voltage Engineering, Milan, Italy,
1979, paper 42.14.
- [Hee 87] Van Heesch, E.J.M., J.N.A.M. Van Rooij, R.G. Noij, P.C.T. Van
der Laan.
A NEW CURRENT AND VOLTAGE MEASURING SYSTEM; TESTED IN A 150kV
AND 400kV GIS
Proc. 5th Int. Symp. on High-Voltage Eng., Vol.3, 73.06,
Braunschweig (1987), 4p.
- [Hee 89] Van Heesch, E.J.M., A.P.J. Van Deursen, M.A. Van Houten, G.
Jacobs, J. Kersten, P.C.T. Van der Laan.
FIELD TESTS AND RESPONSE OF THE D/I H.V. MEASURING SYSTEM
Proc. 6th Int. Symp. on High Voltage Engineering, New Orleans
(1989), paper 42.23, 4p.
- [Her 72] Herring, T.H.
A DESIGN PROBLEM FOR THE GROUNDING SESSION
IEEE 1972. CHO638-7EMC
- [Hou 89] Van Houten, M.A., E.J.M. Van Heesch, A.P.J. Van Deursen,
J.N.A.M. Van Rooij, R.G. Noij, P.C.T. Van der Laan
GENERAL METHODS FOR PROTECTION OF ELECTRONICS AGAINST
INTERFERENCE, TESTED IN HIGH-VOLTAGE SUBSTATIONS
Proc. 8th Int. Symp. on EMC Zürich (1989), 84N2.
- [Jon 80] Jones, J.W.E. and M.A. Bridgwood
THE USE OF MAGNETIC CORES IN CONTROLLING EARTH LOOP CURRENTS
IERE Conf. Proc. No.47 on EMC 1980, p.387.
- [Jon 83] Jones, J.W.E.
THE CONCEPTUAL PROBLEMS OF GROUND-PLANES
Proc. 5th Int. Symp. on EMC Zürich (1983), p. 363.
- [Kad 59] Kaden, H.
WIRBELSTRÖME UND SCHIRMUNG IN DER NACHRICHTEN TECHNIK
Springer Berlin 1959 2. Auflage.

- [Kel 64] Keller, R.
WIDEBAND HIGH VOLTAGE PROBE.
Rev. Sci. Instrum., Vol.35 (1964), pp.1057-1060.
- [Laa 78] Van der Laan, P.C.T.
VOLTAGES IN TOROIDAL PINCH EXPERIMENTS
Los Alamos Reports LA-7335-MS, 1978.
- [Laa 86] Van der Laan, P.C.T. and M.A. van Houten
DESIGN PHILOSOPHY FOR GROUNDING
Proc. 5th Int. Symp. on EMC, York (1986), p. 267.
- [Laa 87] Van der Laan, P.C.T., M.A. Van Houten, A.P.J. Van Deursen
GROUNDING PHILOSOPHY
Proc. 7th Int. Symp. on EMC, Zürich (1987), p. 567.
- [Lat 88] Lathouwers, A.G.A.
ONTWERP VAN EEN D/I-MEETSISTEEM VOOR HET METEN VAN SNELLE
TRANSIENTE SPANNINGEN IN GIS
Master thesis TU-Eindhoven, EH.88.A.97
- [Mar 86] Marsman, H.G.
BEVEILIGING VAN HOOGSPANNINGSNETTEN: TREND OF KEERPUNT
PATO Hfd.7: Stoorspanningen, (1986).
- [Mep 87] Meppelink, J., and P. Hofer
DESIGN AND CALIBRATION OF A HIGH VOLTAGE DIVIDER FOR
MEASUREMENTS OF VERY FAST TRANSIENTS IN GIS
Proc. 5th Int. Symp. on High-Voltage Eng., Vol.3, 71.08,
Braunschweig (1987).
- [Mer 72] Mertel, H.K.
EXPLICIT GROUNDING ALLUSIONS
Proc. Int. EMC Symp. Chicago, Illinois (1976) pp.302-304.
- [Nah 73] Nahman, N.S.
A NOTE ON THE TRANSMISSION (RISE)TIME VERSUS LINE LENGTH IN
COAXIAL CABLES
IEEE Trans. on circuit theory (1973), p. 165.
- [Oer 89] Oerlemans, A.J.W.A
HOOGFREQUENTE SPANNINGSMETINGEN
Master thesis TU-Eindhoven, EH.89.A.103
- [Ott 76] Ott, H.W.
NOISE REDUCTION TECHNIQUES IN ELECTRONIC SYSTEMS
Wiley Newyork 1976, 1st edition
- [Ott 79] Ott, H.W.
GROUND -A PATH FOR CURRENT FLOW
IEEE Proc. Int. Symp. on EMC, (1979) 167
- [Ott 81] Ott, H.W.
DIGITAL CIRCUIT GROUNDING AND INTERCONNECTION
Proc. 4th Int. Symp. on EMC, Zürich (1981), p. 292.
- [Pau 86] Paul, C.R.
MODELLING AND PREDICTION OF GROUND SHIFT ON PRINTED CIRCUITS
BOARDS
Fifth Int. Conf. on EMC, York, 1986, p.37

- [Ott 88] Ott, H.W.
NOISE REDUCTION TECHNIQUES IN ELECTRONIC SYSTEMS
Wiley Newyork 1989, 2e edition.
- [Pea 62] Pearlston, C.B.
CASE AND CABLE SHIELDING, BONDING, AND GROUNDING
CONSIDERATIONS IN ELECTROMAGNETIC INTERFERENCE
IRE Transaction on RFI. Vol. RFI-4 no.3 (1962) pp.1-16
(supplements).
- [Ral 84] Raleigh, M, and R. Pechacek
FAST PASSIVE INTEGRATOR
Rev. Sci. Instrum., Vol.55 (1984), pp. 2023-2026
- [Ram 84] Ramo, S., J.R. Whinnery and T. Van Duzer
FIELDS AND WAVES IN COMMUNICATION ELECTRONICS
John Wiley & Sons, Second Edition, 1984
- [Rie 88] Van Riet, M.J.M.
AARDING GESLOTEN SCHAKEL INSTALLATIES
Electrotechniek, 66, Vol.1 (1988), p. 33.
- [Sch 34] Schelkunoff, S.A.
THE ELECTROMAGNETIC THEORY OF COAXIAL TRANSMISSION LINES AND
CYLINDRICAL SHIELDS
Bell Syst. Tech. J. 13 (1984) p.532-579.
- [Sch 71] Schwab, A.J.
HIGH VOLTAGE MEASUREMENT TECHNIQUES
MIT Press, Cambridge, 1971.
- [Sch 72] Schwab, A.J. and J.E. Pagel
PRECISION CAPACITIVE VOLTAGE DIVIDER FOR IMPULSE VOLTAGES
IEEE Transactions vol. PAS 91 (1972) pp. 2376-2382.
- [Sen 83] Senff, J.J., P.C.T. Van der Laan, H. Antonides and L.M.L.F
Hosselet
SHIELDING PROPERTIES OF ISOLATED-PHASE BUSSYSTEMS
IEEE Trans. on Power App. and Systems, Vol. PAS-102 (1983),
2231-2238
- [Sev 86] Sevat, P.A.A.
CONSTRUCTIE ELEMENTEN VOOR ONDERDRUKKEN VAN STORINGEN
PT Electrotechniek 39 (1984) p.36.
- [Tas 86] Lange, K. and K.H. Löcherer
TASCHENBUCH DER HOCHFREQUENZTECHNIK
Berlin: Springer, 1986, p. L11-L12.
- [Van 80] Vance, F.E.
ELECTROMAGNETIC-INTERFERENCE CONTROL
IEEE Transaction on EMC, Vol. EMC-22 (1980), pp.319-328.
- [Van 87] Vance, E.F.
COUPLING TO SHIELDED CABLES
RE Krieger Publishing Company, Malabar, Florida 1987
- [VDE 86] Werkgroep Stoorspanningen in Gesloten Schakelinstallaties
concept: STOORSpanningen in ONDERSTATIONS EN MAATREGELEN TER
BESTRIJDING; deel III GESLOTEN SCHAKELINSTALLATIES
VDEN, 0067-HFL/WTGS 86-3965 Arnhem, mei 1986

- [Vol 82] Volland, H.
HANDBOOK OF ATMOSPHERICS
Vol.1, CRC Press, Boca Raton USA 1982
- [Wig 57] Wigington, R.L. and N.S. Nahman
TRANSIENT ANALYSIS OF COAXIAL CABLES CONSIDERING SKIN EFFECT
Proc. IRE, 45 (1957). p. 166.
- [Wil 75] Wikinson, W.S.
A SURVEY OF PAST, PRESENT AND POSSIBLE FUTURE SYSTEMS FOR THE
TRANSMISSION OF SIGNALS FROM THE EMC VIEWPOINT
Proc. 1st. Int. Symp. on EMC, Montreux, 1975.
- [Wet 88] Wetzer, J.M., C. Wen and P.C.T. Van der Laan
BANDWIDTH LIMITATIONS OF GAP CURRENT MEASUREMENTS
Proc. IEEE Int. Symp. on Electrical Insulation, 1988, Boston,
p.355-358.
- [Wol 81] Wolzak, G.G., J.A.G. Bekkers, P.C.T. Van der Laan
CAPACITIVE MEASUREMENT OF HIGH DC VOLTAGES
Rev. Sci. Instrum., Vol.52 (1981) pp. 1572-1574.
- [Wol 83] Wolzak, G.G.
THE DEVELOPMENT OF HIGH-VOLTAGE MEASURING TECHNIQUES
Ph.D. Thesis Eindhoven University of Technology, 1983.
- [Zha 89] Zhang, W.Y., A.P.J. Van Deursen, P.C.T. Van der Laan
DIGITAL MEASUREMENTS ON HIGH VOLTAGE SURGE GENERATORS
Sixth Int.Symp. on High-Voltage Engineering, New Orleans,
1989, 50.04, 4p.

User software programs:

- [ANS 89] ANSOFT: A Finite Element Method field calculation program.
ANSOFT Corporation, University Technology Development
Center/4516 Henry street Pittsburg, PA 15213 412-683-4846
ENGINEERING SOFTWARE, January, 1989.
- [STA 87] STATGRAPHICS: Statistical graphics system by statistical
graphics corporation. 1987 STSC. INC.
- [VU- 87] VU-POINT: A digital data processing system for IBM
PC/XT/AT and compatible personal computers.
Version 1.2, oct.1987, SSS-IR-87-8347

SAMENVATTING

Het vakgebied Electromagnetic Compatibility (EMC) binnen de elektrotechniek heeft tot doel elektronische apparaten en elektrische systemen storingsvrij in elkaars nabijheid te laten functioneren.

Dit proefschrift behandelt nieuwe EMC-concepten die leiden tot een doelgerichte en consistente aanpak van praktische storingsproblemen. Analyse dient methodes op te leveren om storingen te verhelpen en liefst te voorkomen. De ontwikkelde concepten worden in dit proefschrift voornamelijk toegepast in hoogspanningsinstallaties. Integratie van moderne elektronica in dit soort installaties stelt hoge EMC-eisen. Electromagnetic Compatibility wordt in deze gevallen bereikt door een correcte layout toe te passen en door leidingen en extra metaal op strategische plaatsen te installeren. Overigens zijn de ontwikkelde concepten in aangepaste vorm toepasbaar binnen de gehele elektrotechniek.

Het proefschrift begint met een kritische analyse van het begrip "aarde", een onderwerp van fundamenteel belang binnen de EMC. Tengevolge van een onjuiste voorstelling van de werking van een aardingsstelsel is een verwarrende praktijk ontstaan rond het zelfstandig naamwoord "aarde". Deze foute voorstelling is gekoppeld aan twee basiselementen die in de gangbare definities van "aarde" te vinden zijn, nl.:

- Een "aarde" kan stroom opnemen of afgeven zonder daardoor in spanning te veranderen
- Een "aarde" is een punt of vlak van gelijke potentiaal dat kan dienen als referentie voor onze schakeling.

Door ons nadrukkelijk te distantieëren van het potentiaalconcept en ons te concentreren op de fysisch zinvolle stromen, op de circuits waarin deze stromen lopen en op de magnetische fluxen, hebben we een algemene beschermingsfilosofie ontwikkeld. Centraal hierin staat het begrip transferimpedantie van aardingsstructuren (AS-en). Met behulp van AS-en creëren we beschermende gebieden waarin

gevoelige elektronica probleemloos kan werken. We maken onderscheid tussen AS-en voor leidingen en apparaten. In deze zin vormt de geleidende buitenmantel van een coaxiale kabel als simpele AS ook reeds een beschermd gebied. Voor de bescherming van gevoelige instrumenten is een "EMC-kast" een onmisbaar deel van de AS.

De transferimpedantie van een AS is een belangrijk begrip omdat het een zinvol criterium oplevert voor de kwaliteit van een AS (samen met de hele "layout" van het "netwerk"). De vaak niet berekenbare transferimpedantie van een uitgebreide AS kan experimenteel worden bepaald met "current injection test methods" waarbij de veroorzaakte spanningsverschillen tussen kritische klemmen worden gemeten. Zowel modellen voor als metingen van de transferimpedantie van AS-en voor leidingen en AS-en voor instrumenten worden behandeld.

Voor het meten van hoge spanningen in hoogspanningsinstallaties is het transporteren van gedifferentieerde meetsignalen gunstig voor EMC. Naast het belangrijke voordeel dat de meetkabel karakteristiek kan worden afgesloten is een tweede EMC-voordeel dat het eerste deel van de integrator passief kan worden uitgevoerd. Onderdrukking van snelle transiënten kan dan plaats vinden voordat deze de kwetsbare actieve elektronica bereiken. Een belangrijke rol is hier weggelegd voor de EMC-kast die zowel de meetapparatuur als het geïntegreerde meetsignaal moet beschermen. Beschreven wordt het ontwerp van een Differentiërend/Integrerend (D/I)-systeem voor het meten van snelle spanningstransiënten. Het D/I-systeem is onder andere gebruikt voor het meten van spanningstransiënten in het "Gas Insulated Switchgear" onderstation Eindhoven-West. Een GIS-installatie is een hoogfrequente stoorbron van hoog electromagnetisch vermogen. Middelen om deze stoorbron gedeeltelijk te temmen zijn voorhanden en worden besproken.

DANKWOORD

Het in dit proefschrift beschreven onderzoek is uitgevoerd in de vakgroep "Hoogspanningstechniek" van de Technische Universiteit Eindhoven. In dit onderzoek trachten we een balans te vinden tussen theorie en praktijk. In het zoeken van deze balans hebben velen een zinvolle bijdrage geleverd. Hen wil ik daarvoor danken.

Prof. dr. ir P.C.T. van der Laan ben ik zeer erkentelijk voor de vele discussies over en stimulering van het onderzoek.

Prof. dr. M.P.H. Weenink dank ik voor het kritisch doornemen van dit proefschrift en voor de aanvullende opmerkingen.

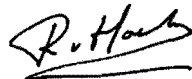
Dr. A.P.J. van Deursen, dr.ir. E.J.H. van Heesch en dr.ir. J.M. Wetzler, wil ik danken voor de vele vruchtbare discussies en collegiale samenwerking in de diverse projecten en meetexpedities.

De technische staf van het hoogspanningslaboratorium wil ik danken voor de steun bij de experimentele realisatie van het onderzoek. Met name wil ik vermelden ing. F.M. van Gompel met wie ik plezierig heb samen gewerkt en die tevens het tekenwerk verzorgde.

Een nuttige bijdrage aan het onderzoek werd geleverd door de afstudeerders ir. A.G.A Lathouwers en ir. A.J.W.A. Oerlemans en meerdere stagiaires.

Verder werd belangrijke medewerking verleend door de PNEM en Holec Distributie Systemen te Amersfoort.

Hiervoor ben ik allen zeer erkentelijk.



M.A. van Houten.

CURRICULUM VITAE

Rinus van Houten werd op 16 december 1950 geboren te Breda. In 1957 ging hij naar de Openbare Lagere School "Middellaan" met als hoofd de Heer Viergever. Daarna volgde hij achtereenvolgens:

- 1964-1968 Lagere Technische School "Gemeentelijke Technische School Breda".
Afdeling: Electrotechniek.
- 1968-1971 Middelbare Technische School "Albertus Magnus" Breda.
Afdeling: Electrotechniek.
- 1971-1976 Hogere Technische School "St.Virgilius", Breda
Afdeling: Electrotechniek.
Afstudeerrichting: Informatietechniek.
- 1976-1980 Technische Hogeschool Eindhoven.
- 1982-1985 Afdeling: Electrotechniek.
Afstudeervakgroep: Theoretische Electrotechniek.
Afstudeeronderwerp: "Stabiliteitsonderzoek van M.H.D. Plasma".
Afstudeerhoogleraar: Prof.dr. M.P.H. Weenink.
Afstudeerdatum: 23 mei 1985

Vervolgens werkte hij van 1985 tot 1989 in het Hoogspanningslaboratorium van de Technische Universiteit te Eindhoven als wetenschappelijk assistent. Zijn werk, onder leiding van Prof.dr.ir. P.C.T. van der Laan, leidde tot dit proefschrift.

STELLINGEN
behorende bij het proefschrift

ELECTROMAGNETIC COMPATIBILITY
in
HIGH-VOLTAGE ENGINEERING

van

M.A. van Houten

Eindhoven, 23 oktober 1990.

I

Vance is van mening dat zelfs de beste aardingspraktijk de grote veranderingen in potentiaal van een centraal aardpunt in een gebouw, ontstaan ten gevolge van een bliksem of EMP, niet kan voorkomen. Hij verklaart dit met de spanningsval $Ri + L \frac{di}{dt}$ over de aardingsimpedantie. Tot nu toe treffen we deze onjuiste mening en verklaring aan in vrijwel elk EMC-boek.

Edward F. Vance, "Electromagnetic-Interference Control", IEEE Trans. on EMC, -Vol. EMC-22, No.4, 1980

II

Classificering van aardingsystemen op grond van potentialen leidt tot een veelvoud van aardingsystemen en tot een inconsistente aardingspraktijk. Die inconsistentie blijkt ook uit de kunstgrepen, zoals het toepassen van vonkbruggen en potentiaalvereffeningsstrips, waarmee men achteraf de toch optredende spanningsverschillen tussen de afzonderlijk gearde structuren tracht weg te werken.

John D.M. Osburn and Donald R.J.White, "Grounding a Recommendation for the Future", IEEE Int. Symp. on EMC Atlanta (1987), pp.155-160.

III

Ott's alternatieve definitie van aarde - een pad van (hopelijk) lage impedantie voor stromen terug naar de bron - is een stap in de goede richting. In feite mag die impedantie echter hoog zijn; vereist is een lage transferimpedantie naar het te beschermen circuit.

-Henry W. Ott, "Ground -A Path For Current Flow", IEEE Proc. Int. Symp. on EMC, (1979) pp. 167-170

-Henry W. Ott, "Noise Reduction Techniques In Electronic Systems" Wiley New York 1988, 2nd edition.

IV

Het belang van het transferimpedantie concept voor aardingsstructuren is dat de werking van aardingsstructuren aanschouwelijk wordt. Daarom kan dan ook vaak met eenvoudige metingen de kwaliteit van de aardingsstructuur bepaald worden. In principe is de transferimpedantie niet alleen afhankelijk van de aardingsstructuur, maar ook van de gehele layout van het netwerk. In de praktijk geeft een royaal uitgevoerde aardingsstructuur (b.v. een EMC-kast) aanzienlijke vrijheid bij de layout van de schakeling.

Dit proefschrift, hoofdstuk 3.

V

De differentiërende/integrerende meetmethode (o.a. beschreven door Wolzak) in combinatie met een EMC-kast levert een flexibel meetsysteem op, dat bruikbaar is in allerlei situaties met intense elektromagnetische storingsbronnen zoals in hoogspanningstechnieken, in bliksemonderzoek en in "Pulsed Power".

-Gerard G. Wolzak, "The Development of High-Voltage Measuring Techniques", proefschrift TUE (1983)

-Dit proefschrift, hoofdstuk 4.

VI

Een Gas Insulated Switchgear (GIS)-installatie in combinatie met uitsluitend hoogspanningskabels is vanuit het gezichtspunt van EMC een ideale installatie, indien de GIS-omhulling en de aardschermen van de kabels metallisch een volledig gesloten geheel vormen.

Dit proefschrift, hoofdstuk 5.

VII

Het nieuwe vakgebied EMC - de kwalificatie nieuw is nog steeds van toepassing - is ontstaan dankzij bijdragen uit diverse gevestigde vakgebieden die alle op hun wijze iets met elektromagnetische storingen te maken hebben. Deze verwarrende situatie is inherent aan de aanloopfase; een groei naar conceptuele helderheid en consistentie is echter noodzakelijk. Aan deze groei kan de universiteit een belangrijke bijdrage leveren.

VIII

Na een periode van overaccentuering in het onderwijs van de vakken economie en informatica zou nu meer aandacht voor de niet direct nuttige vakken zoals muziek en sterrenkunde een meer ontspannen leefklimaat ten goede kunnen komen.

IX

In vlakke landen moet een fietser vooral de wrijvingskracht overwinnen en nauwelijks de zwaartekracht. In bergachtige streken is de situatie net andersom. Dit maakt fietsen in Nederland tot een niet-conservatieve activiteit, doch in Peru hoofdzakelijk tot een conservatieve.

X

Op de ambtsketen van de rector magnificus en op de ingenieurs- en doctorsbullen van de Technische Universiteit Eindhoven staat de ark van Noach als een symbool voor "goede techniek". Het zou aanbeveling verdienen dat de voorzitters van examencommissies hieraan enige woorden zouden wijden tijdens de buluitreiking.